

STATUS OF THESIS

Title of Thesis

Flux and Rejection Characteristics of Amine Wastewater Using Membrane Separation Processes

I, BINYAM SEYOUM WOLDEHAWARIAT

hereby allow my thesis to be placed at the Information Resources Center (IRC) of Universiti Teknologi PETRONAS (UTP) with the following conditions:

1. The thesis becomes the property of UTP.
2. The IRC of UTP may make copies of the thesis for academic purposes only.
3. This thesis is classified as

Confidential

Non – confidential

If this thesis is confidential, please state the reason:

The contents of this thesis will remain confidential for _____ years.

Remarks on disclosure:

Endorsed by

Signature of Author

Permanent : Bahirdar University
Address : Engineering Faculty
Bahirdar, Ethiopia

Date: _____

Signature of Supervisor

Name of Supervisor
Assoc. Prof. Dr. Hilmi Mukhtar

Date: _____

UNIVERSITI TEKNOLOGI PETRONAS

FLUX AND REJECTION CHARACTERISTICS OF AMINE WASTEWATER USING
MEMBRANE SEPARATION PROCESSES

by

BINYAM SEYOUM WOLDEHAWARIAT

The undersigned certify that they have read, and recommended to the Postgraduate Studies Programme for acceptance this thesis for the fulfillment of the requirements for the degree of Master of Science in Chemical Engineering.

Signature: _____

Main Supervisor: Assoc. Prof. Dr. Hilmi Mukhtar

Signature: _____

Co-Supervisor: Dr. Lau Kok Keong

Signature: _____

Head of Department: Dr. Shuhaimi Mahathir

Date: _____

FLUX AND REJECTION CHARACTERISTICS OF AMINE WASTEWATER USING
MEMBRANE SEPARATION PROCESSES

by

BINYAM SEYOUM WOLDEHAWARIAT

A Thesis

Submitted to the postgraduate studies programme

as a Requirement for the Degree of

MASTER OF SCIENCE

CHEMICAL ENGINEERING DEPARTMENT

UNIVERSITI TEKNOLOGI PETRONAS

BANDAR SERI ISKANDAR,

PERAK

JULY 2010

DECLARATION OF THESIS

Title of thesis

Flux and Rejection Characteristics of Amine Wastewater Using
Membrane Separation Processes

I, BINYAM SEYOUM WOLDEHAWARIAT

hereby declare that the thesis is based on my original work except for quotations and citations which have been duly acknowledged. I also declare that it has not been previously or concurrently submitted for any other degree at UTP or other institutions.

Witnessed by

Signature of Author

Signature of Supervisor

Permanent: Bahirdar University
Address: Engineering Faculty
Bahirdar, Ethiopia

Name of Supervisor
Assoc. Prof. Dr. Hilmi Mukhtar

Date: _____

Date: _____

ACKNOWLEDGEMENT

I would like to thank Associate Professor Dr. Hilmi Mukhtar for his professional guidance, support and patience throughout this study and beyond. I am indebted for his helpful suggestions during the course of my research. His advice and expertise were invaluable and are well woven into the final form of this thesis. I am also thankful to Dr. Lau Kok Keong for his valuable comments, time and effort in guiding me throughout my study.

I would like to acknowledge Universiti Teknologi PETRONAS for material and financial support on this research. I am also thankful to Chemical Engineering Department staffs and technologists, especially Mr. Affendy and Mr. Yusup for their technical support.

Finally, I would like to thank and give special tribute to my mother, brother and friends whose constant moral and emotional support has guided me to reach this stage of my career.

DEDICATION

To My Mother and Brother

ABSTRACT

Sour natural gas must be purified by removing various impurities, including acid gases particularly carbon dioxide and hydrogen sulfide before it can be utilized. Various amine solutions such as monoethanolamine (MEA), methyldiethanolamine (MDEA) and diethanolamine (DEA) are used for the absorption of these gases. During the absorption-desorption process, a small amount of amines carry-over and discharged to the effluent stream. Treatment of this wastewater which contains high COD content using existing biological treatment is not suitable since the wastewater can endanger the activated sludge.

Thus, the main objective of this study is to investigate the removal of amines, namely MEA, MDEA and DEA from artificial wastewater using membrane separation processes. The experimental studies were conducted to evaluate the permeate flux and observed rejection of artificial amines wastewaters using AFC99, AFC40 and CA202 membranes by varying the operating pressure, cross-flow velocity, feed concentration and pH. Two membrane transport models, namely combined film theory–solution diffusion (CFSD) and combined film theory–Spiegler Kedem (CFSK) models were used in order to estimate the membrane transport parameters and predict their rejection performances.

The experimental study shows that the permeate flux is linearly increased with operating pressure. The percentage of rejection was found to be depending on the type of amines used as well as the operating conditions selected. Results showed that the observed rejection was found to be increasing with the increase in operating pressure and cross-flow velocity, whereas was found to be decreasing with the increases in feed concentration. In addition, the observed rejection was also found to be increasing as the pH of the feed decreases from 8 to 3. The findings also showed that AFC99 membrane exhibited the best rejection efficiency in all amines solutions followed by AFC40 and CA202 membranes. AFC99 membrane was able to reject more than 96% for all amines

under the present study. On the other hand, the AFC40 and CA202 membranes were able to reject MEA up to 70% and 30 %, respectively, and for MDEA up to 94 % and 38%, respectively.

The estimated transport parameters obtained from CFSD and CFSK models, including the solute transport parameter, reflection coefficient and mass transfer coefficients were found to be depending on the feed concentration and cross-flow velocity. For both models, the solute transport parameter was found to be increasing with cross-flow velocity and feed concentration. Similarly, the mass transfer coefficient and reflection coefficients also increased with cross-flow velocity, but both were found to be decreasing with the increase in feed concentration. All trends obtained from this work are consistent with the cited literatures. The validation study shows that the CFSD and CFSK models predictions are in excellent agreement with the experimental results.

In conclusion, membrane processes particularly reverse osmosis (with the application of AFC99 membrane in the present study) can be effectively used to remove various types of amines present in the wastewater using a single process. Similarly, nanofiltration and ultrafiltration membranes such as AFC40 and CA202 can also be selected for the same purpose but both are more suitable to be employed for complementing the existing biological treatment.

ABSTRAK

Gas asli masam perlu dituliskan daripada pelbagai komponen bendasing termasuk gas-gas asid seperti karbon dioksida dan hidrogen sulfida sebelum ia boleh digunakan. Pelbagai larutan amina seperti monoethanolamina (MEA), metildiethanolamina (MDEA) dan diethanolamina (DEA) boleh digunakan untuk penyerapan gas-gas asid tersebut. Dalam proses penyerapan - penyahserapan, sebahagian kecil daripada larutan amina akan terkeluar daripada saluran proses di mana ia akan dinyahkan ke saluran kumbahan. Disebabkan air kumbahan tersebut mengandungi tahap keperluan oksigen kimia (COD) yang tinggi, penggunaan rawatan biologi adalah tidak sesuai kerana air kumbahan ini akan membahayakan enapcemar teraktif yang terkandung dalam proses rawatan tersebut.

Oleh sebab itu, objektif utama kajian ini adalah untuk mengkaji tentang penyingkiran amina buatan bernama MEA, MDEA and DEA dalam air kumbahan dengan menggunakan proses pemisahan membran. Kajian eksperimen telah dijalankan untuk menilai fluks penelapan dan penolakan pemerhatian untuk air kumbahan buatan amina dengan menggunakan membran AFC90, AFC40 dan CA202. Tekanan operasi, halaju aliran silang, kepekatan suapan dan pH telah diubah dalam kajian tersebut. Dua model pengangkutan termasuk pengabungan teori film-larutan resapan (CFSD) dan pengabungan teori film-Spiegler Kedem (CFSK) telah digunakan untuk menganggar sifat pengangkutan membran dan prestasi penolakan.

Kajian eksperimen menunjukkan bahawa fluks penelapan meningkat secara linear dengan tekanan operasi. Peratus penyingkiran telah didapati bergantung kepada jenis amina yang digunakan dan juga pemilihan keadaan operasi. Keputusan eksperimen menunjukkan bahawa penyingkiran pemerhatian meningkat dengan tekanan dan halaju aliran silang, sementara menurun dengan peningkatan kepekatan suapan. Selain daripada itu, penyingkiran pemerhatian didapati meningkat apabila pH suapan diturunkan daripada 8 ke 3. Keputusan tersebut juga telah memaparkan bahawa membran AFC99 memberi

penyingkiran berkesan yang terbaik untuk semua larutan amina diikuti dengan membran AFC 40 dan membran CA202 secara berurutan. Membran AFC99 didapati menyingkir lebih daripada 96% untuk semua amina dalam kajian ini. Tetapi sebaliknya, membran AFC40 didapati boleh menyingkir MEA dan MDEA sebanyak 70% dan 94% sementara membran CA202 berjaya menyingkir MEA dan MDEA sebanyak 30% dan 38.

Anggaran parameter pengangkutan membran yang diperolehi daripada model CFSD dan CFSK, termasuk parameter pengangkutan zat terlarut, pekali pemantulan dan pekali pemindahan jisim, adalah bergantung kepada kepekatan suapan dan halaju aliran silang. Untuk kedua-dua model, parameter pengangkutan zat terlarut didapati meningkat dengan halaju aliran silang dan kepekatan suapan. Pekali pemindahan jisim dan pekali pemantulan didapati meningkat dengan halaju aliran silang tetapi menurun dengan kepekatan suapan. Semua arah alir keputusan daripada kajian ini adalah konsisten dengan bahan-bahan rujukan. Kajian pengesahan mendapati bahawa model anggaran CFSD dan CFSK telah memberi keputusan cemerlang selaras dengan keputusan- keputusan eksperimen.

Sebagai kesimpulannya, proses membran terutamanya osmosis berbalik (dengan menggunakan membran AFC99 dalam kajian ini) dapat menyingkirkan pelbagai jenis amina yang terdapat dalam air kumbahan secara berkesan dengan menggunakan satu proses. Selain itu, membran penapisan nano dan penapisan ultra seperti AFC40 dan CA202 boleh juga digunakan untuk tujuan yang sama tetapi kedua-duanya sesuai digunakan bersama-sama dengan rawatan biologi yang sedia ada.

In compliance with the terms of the Copyright Act 1987 and the IP Policy of the university, the copyright of this thesis has been reassigned by the author to the legal entity of the university,

Institute of Technology PETRONAS Sdn Bhd.

Due acknowledgement shall always be made of the use of any material contained in, or derived from, this thesis.

© Binyam Seyoum, 2010
Institute of Technology PETRONAS Sdn Bhd
All rights reserved.

TABLE OF CONTENTS

STATUS OF THESIS	i
APPROVAL PAGE	ii
TITLE PAGE	iii
DECLARATION OF THESIS	iv
ACKNOWLEDGEMENT	v
DEDICATION	vi
ABSTRACT	vii
ABSTRAK	ix
COPYRIGHT PAGE	xi
TABLE OF CONTENTS	xii
LIST OF TABLES	xvi
LIST OF FIGURES	xvii
NOMENCLATURES	xxi
ABREVIATIONS	xxiii
CHAPTER 1: INTRODUCTION	1
1.1 Overview of Natural Gas	1
1.2 Natural Gas Processing and Conditioning	3
1.2.1 Acid Gas Removal	5
1.2.2 Amine Sweetening Process	6
1.3 Sources of Amine Wastewater	7
1.4 Amine Wastewater Characteristics	9
1.5 Problem Statement	10
1.6 Objectives of Study	11

1.7	Scope of Study	11
1.8	Thesis Organization	13
CHAPTER 2: LITERATURE REVIEW		15
2.1	Wastewater	15
2.1.1	Wastewater Constituents and Characterization	16
2.1.2	Wastewater Quality Indicators	18
2.1.3	Wastewater Treatment Objective and Regulation	19
2.1.4	Wastewater Treatment Methods	20
2.2	Treatment of Amine Wastewater	23
2.2.1	Adsorption	24
2.2.2	Advanced Oxidation Processes (AOPs)	25
2.2.3	Biological Treatment	26
2.3	Overview of Membranes Process	28
2.3.1	Definition	28
2.3.2	Membrane Morphology	29
2.3.3	Membrane Flow Geometries	30
2.3.4	Membrane Performance	30
2.3.5	Problems in Membrane Process	31
2.3.6	Advantages and disadvantages of membranes	33
2.4	Treatment of Industrial Wastewater Using Membrane Separation Process	34
2.4.1	Treatment of Palm Oil Mills Effluent Wastewater	34
2.4.2	Treatment of Petroleum Refining Wastewater	36
2.4.3	Treatment of Pulp and Paper Wastewater	37
2.4.4	Treatment of Textile Wastewater	38
2.4.5	Treatment of Tanning and Leather Wastewater	39
2.4.6	Electroplating wastewater treatment and Metal Recovery	40

CHAPTER 3: THEORY AND MODELING	42
3.1 Film Theory Model	43
3.2 Nonporous Model	45
3.2.1 Solution Diffusion Model	45
3.3 Porous Model	47
3.3.1 Irreversible Thermodynamics Models	47
3.4 Present Models	48
3.4.1 Combined film theory-solution diffusion model (CFSD)	49
3.4.2 Combined film theory-Spiegler Kedem model (CFSK)	49
3.4.3 Parameters Estimation	50
CHAPTER 4: MATERIALS AND METHODS	53
4.1 Materials	53
4.1.1 Membranes	53
4.1.2 Chemicals	54
4.1.3 Deionised Water	55
4.1.4 Artificial wastewater	55
4.2 Method 55	
4.2.1 Experimental Set-up	55
4.2.2 Experimental Procedure	57
4.3 Analysis	58
CHAPTER 5: RESULTS AND DISCUSSION	60
5.1 Experimental Result	60
5.1.1 Wastewater Characterization	60
5.1.2 Permeability Study	62
5.1.3 Rejection Study	76
5.2 Modeling of Membrane Processes	88
5.2.1 Estimation of Model Parameters	89
5.2.2 Results	90

5.2.3	Model Validation	99
CHAPTER 6: CONCLUSIONS AND RECOMMENDATIONS		104
6.1	Conclusions	104
6.2	Recommendations	106
REFERENCES		107
APPENDICES		117
Appendix A:	Effect of amine solution on permeate flux	117
Appendix B:	Effect of cross-flow velocity on permeate flux	118
Appendix C:	Physical properties of amines	121
Appendix D:	Experimental data for removal of amines from artificial wastewater across AFC99, AFC40 and CA202 membranes	122

LIST OF TABLES

Table 1.1: Fossil fuel emission levels, pounds per billion Btu of energy input.	2
Table 1.2: Major hydrocarbon components of natural gas.	3
Table 1.3: Typical composition of a contaminated DEA solution obtained from a gas treating plant in Western Canada.	9
Table 2.1: Heavy metals found in major industries.	17
Table 2.2: Malaysian effluent standard regulation for sewage and industrial effluents.	23
Table 2.3: Advantages and disadvantages of various methods of amine wastewater treatment.	27
Table 2.4: Dense and porous membranes for water treatment.	29
Table 4.1: Properties of AFC99, AFC40 and CA202 membranes.	54
Table 5.1: Characteristic of artificial amines wastewater in term of COD and pH.	61
Table 5.2: Percentage reduction of permeate fluxes of the amines.	72
Table 5.3: Estimated transport parameters for AFC99 membrane using CFSD model (pH 8).	93
Table 5.4: Estimated transport parameters for AFC99 membrane using CFSK model (pH 8).	94
Table 5.5: Estimated transport parameters for AFC40 membrane using CFSD model (pH8).	95
Table 5.6: Estimated transport parameters for AFC40 membrane using CFSK model (pH 8).	96
Table 5.7: Transport equations for CFSD and AFC99 membrane.	101
Table 5.8: Transport equations for CFSK and AFC99 membrane.	101
Table 5.9: Estimated transport parameters for AFC99 membrane using CFSD and CFSK models ($C_b=5000$ mg/l, $u= 5$ l/min, pH 8).	102

LIST OF FIGURES

Fig. 1.1: Primary sources of energy in the world in 2003. Total energy used was 405 quadrillion Btu.	1
Fig. 1.2: Schematic flow diagram of a typical natural gas processing plant.	4
Fig. 1.3: Typical amine sweetening system.	7
Fig. 2.1: Generalized flow diagram for wastewater treatment.	21
Fig. 2.2: Schematic diagram of membrane system.	28
Fig. 2.3: Membrane flow geometries: (a) Cross-flow filtration, (b) Dead-end filtration.	30
Fig. 2.4: Typical protocol used in fouling studies (Schafer <i>et al.</i> , 2003).	32
Fig. 3.1: Schematic diagram for film theory.	43
Fig. 3.2: Permeate flux as a function of transmembrane pressure: pressure-dependent and mass-transfer-limited permeate flux.	44
Fig. 3.3: Algorithm used for parameter estimation for CFSD and CFSK models.	52
Fig. 4.1: Schematic diagram of the Membrane test unit.	56
Fig. 4.2: Experimental flow diagram.	59
Fig. 5.1: Effect of operating pressure on pure water permeability across different type of membranes.	62
Fig. 5.2: Effect of operating pressure on MEA solutions and water flux across various membranes ($C_b=5000$ mg/l, $u=6$ l/min and pH=8).	64
Fig. 5.3: Effect of operating pressure on DEA solutions and water flux across various membranes ($C_b=5000$ mg/l, $u=6$ l/min and pH=8).	65
Fig. 5.4: Effect of operating pressure on MDEA solutions and water flux across various membranes ($C_b=5000$ mg/l, $u=6$ l/min and pH=8).	65

Fig. 5.5: Effect of amine molecular weight on permeate flux across AFC99 membrane ($C_b=5000$ mg/l, $u=6$ l/min and pH=8).	66
Fig. 5.6: Effect of cross-flow velocity on MEA permeate flux across AFC99 membrane ($C_b=5000$ mg/l and pH=8).	67
Fig. 5.7: Effect of cross-flow velocity on MEA permeate flux across AFC40 membrane ($C_b=5000$ mg/l and pH=8).	68
Fig. 5.8: Effect of cross-flow velocity on MEA permeate flux across CA202 membrane ($C_b=5000$ mg/l and pH=8).	68
Fig. 5.9: Effect of feed concentration on MEA permeate flux across various membranes ($u=6$ l/min and pH=8).	70
Fig. 5.10: Effect of feed concentration on DEA permeate flux across various membranes ($u=6$ l/min and pH=8).	70
Fig. 5.11: Effect of feed concentration on MDEA permeate flux across various membranes ($u=6$ l/min and pH=8).	71
Fig. 5.12: Effect of feed pH on MEA permeate flux across various membranes ($C_b=5000$ mg/l and $u=6$ l/min).	73
Fig. 5.13: Effect of feed pH on DEA permeate flux across various membranes	74
Fig. 5.14: Effect of feed pH on MDEA permeate flux across various membranes ($C_b=5000$ mg/l and $u=6$ l/min).	74
Fig. 5.15: Effect of operating pressure on observed rejection of MEA across various membranes ($C_b=5000$ mg/l, $u=6$ l/min and pH=8).	78
Fig. 5.16: Effect of operating pressure on observed rejection of DEA across various membranes ($C_b=5000$ mg/l, $u=6$ l/min and pH=8).	78
Fig. 5.17: Effect of operating pressure on observed rejection of MDEA across various membranes ($C_b=5000$ mg/l, $u=6$ l/min and pH=8).	79
Fig. 5.18: Effect of amine molecular weight on observed rejection across AFC99 membrane ($C_b=5000$ mg/l, $u=6$ l/min and pH=8).	80
Fig. 5.19: Effect of amine molecular weight on observed rejection across AFC40 membrane ($C_b=5000$ mg/l, $u=6$ l/min and pH=8).	80

Fig. 5.20: Effect of amine molecular weight on observed rejection across CA202 membrane ($C_b=5000$ mg/l, $u=6$ l/min and pH=8).	81
Fig. 5.21: Effect of cross-flow velocity on observed rejection of various amines across AFC99 membrane ($p=24$ bar, $C_b=5000$ mg/l and pH=8).	82
Fig. 5.22: Effect of cross-flow velocity on observed rejection of various amines across AFC40 membrane ($p=24$ bar, $C_b=5000$ mg/l and pH=8).	82
Fig. 5.23: Effect of cross-flow velocity on observed rejection of various amines across CA202 membrane ($p=24$ bar, $C_b=5000$ mg/l and pH=8).	83
Fig. 5.24: Effect of feed concentration on observed rejection across AFC99 membrane ($p=24$ bar, $u=6$ l/min and pH=8).	84
Fig. 5.25: Effect of feed concentration on observed rejection across AFC40 membrane ($p=24$ bar, $u=6$ l/min and pH=8).	85
Fig. 5.26: Effect of feed concentration on observed rejection across CA202 membrane ($p=24$ bar, $u=6$ l/min and pH=8).	85
Fig. 5.27: Effect of feed pH on observed rejection of various amines across AFC99 membrane ($p=24$ bar, $u=6$ l/min and $C_b=5000$ mg/l).	86
Fig. 5.28: Effect of feed pH on observed rejection of various amines across AFC40 membrane ($p=24$ bar, $u=6$ l/min and $C_b=5000$ mg/l).	87
Fig. 5.29: Effect of feed pH on observed rejection of various amines across CA202 membrane ($p=24$ bar, $u=6$ l/min and $C_b=5000$ mg/l).	87
Fig. 5.30: Estimation of parameters for AFC99 membrane using CFSD model for MEA-water system ($C_b=5000$ mg/l, $u=6.0$ l/min, pH 8).	89
Fig. 5.31: Estimation of parameters for AFC99 membrane using CFSK model for MEA-water system ($C_b=5000$ mg/l, $u=6.0$ l/min, pH 8).	90
Fig. 5.32: Comparison of experimental and calculated observed rejection for AFC99 membrane using CFSD model.	97
Fig. 5.33: Comparison of experimental and calculated observed rejection for AFC99 membrane using CFSK model.	97
Fig. 5.34: Comparison of experimental and calculated observed rejection for AFC40 membrane using CFSD model.	98

Fig. 5.35: Comparison of experimental and calculated observed rejection for AFC40 membrane using CFSK model.	98
Fig. 5.36: Estimation of k for AFC99 membrane using CFSD and CFSK models for MEA-water system ($C_b=5000$ mg/l, pH 8).	99
Fig. 5.37: Estimation of P_s and P_m for AFC99 membrane using CFSD and CFSK models for MEA-water system ($C_b=5000$ mg/l, pH 8).	100
Fig. 5.38: Estimation of reflection coefficient (σ) for AFC99 membrane using CFSK model for MEA-water system ($C_b=5000$ mg/l, pH 8).	100
Fig. 5.39: Comparison of experimental and calculated observed rejection for AFC99 membrane using CFSD model.	102
Fig. 5.40: Comparison of experimental and calculated observed rejection for AFC99 membrane using CFSK model.	103

NOMENCLATURES

SYMBOLS	NAME	UNIT
A_m	Membrane surface area	(m ²)
C	Solute concentration in the boundary layer	(mg/l)
C_b	Bulk phase solute concentration	(mg/l)
C_p	Permeate solute concentration	(mg/l)
C_{AM}	Solute concentration in the membrane pores	(mg/l)
C_m	Membrane surface solute concentration	(mg/l)
D	Diffusivity of solute in the boundary layer	(m ² /s)
D_{AM}	Diffusivity of solute in/ through membrane pores	(m ² /s)
$(D_{AM} K_m / \delta_m)$	Solute transport parameter	(m/s)
J	Permeate flux	(l/m ² ·h)
J_s	Solute flux	(mg/m ² ·s)
J_v	Solvent flux	(l/m ² ·h)
k	Mass transfer coefficient	(m/s)
K_m	Membrane-solute adsorption coefficient	(-)
L_p	hydraulic permeability	(l/m ² ·h·bar)
P_{so}	local solute permeability	(m ² /s)
P_w	local water permeability	(l/m.h. bar)
P_m	solute transport parameter	(m/s)
Q_p	permeate flow rate	(m ³ /s)
R	true rejection	(-)
R_o	observed rejection	(-)
SS	sum of squares of the residuals	(-)

δ	boundary layer thickness	(m)
δ_m	effective membrane thickness	(m)
σ	reflection coefficient	(-)
$\Delta\pi$	osmotic pressure difference across the membrane	(Pa)
ΔP	transmembrane pressure	(Pa)

ABBREVIATIONS

AFC40	Nanofiltration Membrane
AFC99	Reverse Osmosis Membrane
AOPs	Advanced Oxidation Processes
BHEP	Hydroxyethyl Piperazine
BOD	Biochemical oxygen demand
CA202	Ultrafiltration Membrane
CFSD	Combined film theory-solution diffusion
CFSK	Combined film theory-Spiegler Kedem
CMF	Continuous membrane filtration
COD	Chemical oxygen demand
CP	Concentration polarization
DEA	Diethanolamine
DO	Dissolved oxygen
ED	Electrodialysis
EG	Ethylene Glycol
EQA	Environmental quality act
HC	Hydrocarbons
HEI	Hydroxyethyl imidazolidone
HEOD	Oxazolidone
IE	Ion Exchange
IEP	Isoelectric Point
IT	Irreversible thermodynamics
MBR	Membrane bioreactor
MDEA	Methyldiethanolamine
MEA	Monoethanolamine

MF	Microfiltration
NF	Nanofiltration
NGLSs	Natural gas liquids
POME	Palm Oil Mills Effluent
RO	Reverse osmosis
SD	Solution Diffusion
SSL	Spent Sulfite Liquor
TEA	Triethanolamine
THEED	Triethylenediamine
TFC	Thin Film Composite
TSS	Total suspended solids
UF	Ultrafiltration
UV	Ultraviolet
WWTP	Wastewater treatment plant

CHAPTER 1

INTRODUCTION

This chapter provides the overview of natural gas and highlights the technologies used for purification. It also discusses the amine carries over from the gas sweetening process into the wastewater. Moreover, the objective and scope of the study are provided at the end of the chapter.

1.1 Overview of Natural Gas

The preservation of our environment is a very important and pressing topic, particularly when dealing with energy issues. There are a few types of fossils fuels that are widely used for energy production, including petroleum, coal and natural gas. The world commercial energy consumption by resource is summarized in Figure 1.1.

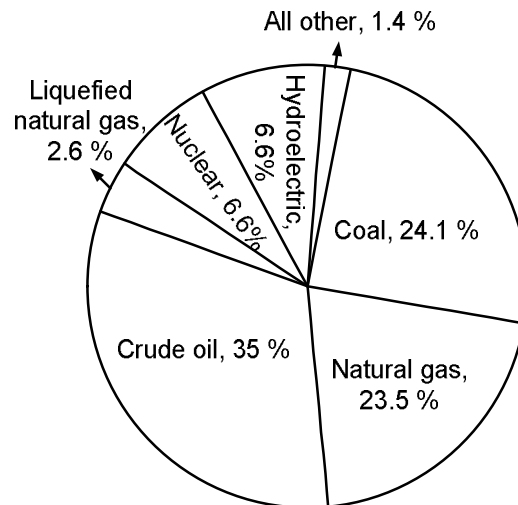


Fig. 1.1: Primary sources of energy in the world in 2003. Total energy used was 405 quadrillion Btu (Kidnay and Parrish, 2006).

Natural gas, the most flexible of all primary fossil fuels, is the fastest growing energy source in the world (Chandra, 2006). It is a mixture of hydrocarbon (HC) gases consisting predominantly methane (CH₄). Methane is highly flammable, burns easily and almost completely, while it emits very little air pollution. Although methane is always the main component, natural gas may also include ethane, ethylene, propane, butane, pentane and higher hydrocarbons (William and Gary, 2004). Other compounds found in natural gas include hydrogen sulfide (H₂S), carbon dioxide (CO₂), Nitrogen (N₂), water (H₂O), other sulfur and nitrogen compounds, and some helium (He). Natural gas is considered as an environmentally friendly clean fuel, offering important environmental benefits when compared to other fossil fuels. The superior environmental qualities over coal or oil are that commercialized natural gas is practically sulphur free and thus it produces virtually no sulphur dioxide (SO₂) or that the level of nitrous oxide (NO_x) and carbon dioxide (CO₂) emissions are lower (Chandra, 2006), as shown in Table 1.1.

Table 1.1: Fossil fuel emission levels, pounds per billion Btu of energy input (Kidnay and Parrish, 2006).

Pollutant	Natural Gas	Oil	Coal
Carbon dioxide	117,000	164,000	208,000
Carbon monoxide	40	33	208
Nitrogen oxides	92	448	457
Sulfur dioxide	0.6	1,122	2,591
Particulates	7	84	2,744
Mercury	0.000	0.007	0.016

Moreover, combustion of natural gas releases virtually no ash or particulate matter, an important environmental consideration because high levels of particulates may pose significant health problems. Thus increased use of natural gas helps to reduce or combat problems of acid rain, ozone layer or greenhouse gases.

1.2 Natural Gas Processing and Conditioning

Processing of natural gas is a very crucial step before it can be used for domestic and industrial purpose. Generally, the processing of natural gas involves the separation of methane (CH₄) from higher hydrocarbons, and removal of the impurities particularly carbon dioxide and hydrogen sulfide down to pipeline quality as shown in Table 1.2.

Table 1.2: Major hydrocarbon components of natural gas (Chandra, 2006).

Major Hydrocarbon Components of “Typical” Natural Gas			
	Wellhead composition mol %		Pipeline quality mol %
Methane	C ₁	65 to above 95	above 95.2
Ethane	C ₂	2 to 15	2.5
Propane	C ₃	0.25 to 5	0.2
Butanes	C ₄	≈ 0 to 5	0.06
Pentanes and heavier	C ₅₊	0.05 to 2	0.03
Non-hydrocarbon Components produced with Natural gas			
Nitrogen	N ₂	≈ 0 to 20	1.3
Carbon dioxide	CO ₂	≈ 0 to above 20	0.7
Hydrogen sulfide	H ₂ S	≈ 0 to 15	≈ 0

Natural gas processing and conditioning typically follows the following steps which can be simplified as shown in Figure 1.2.

- i. **Pretreatment:** Removal of free liquids, such as hydrocarbon condensate and water and entrained solids
- ii. **Dehydration:** A dehydration process is needed to eliminate water which may cause the formation of hydrates. Hydrates form when a gas or liquid containing water moisture experiences specific temperature and pressure conditions (Wilson and Yuvancic, 2004).

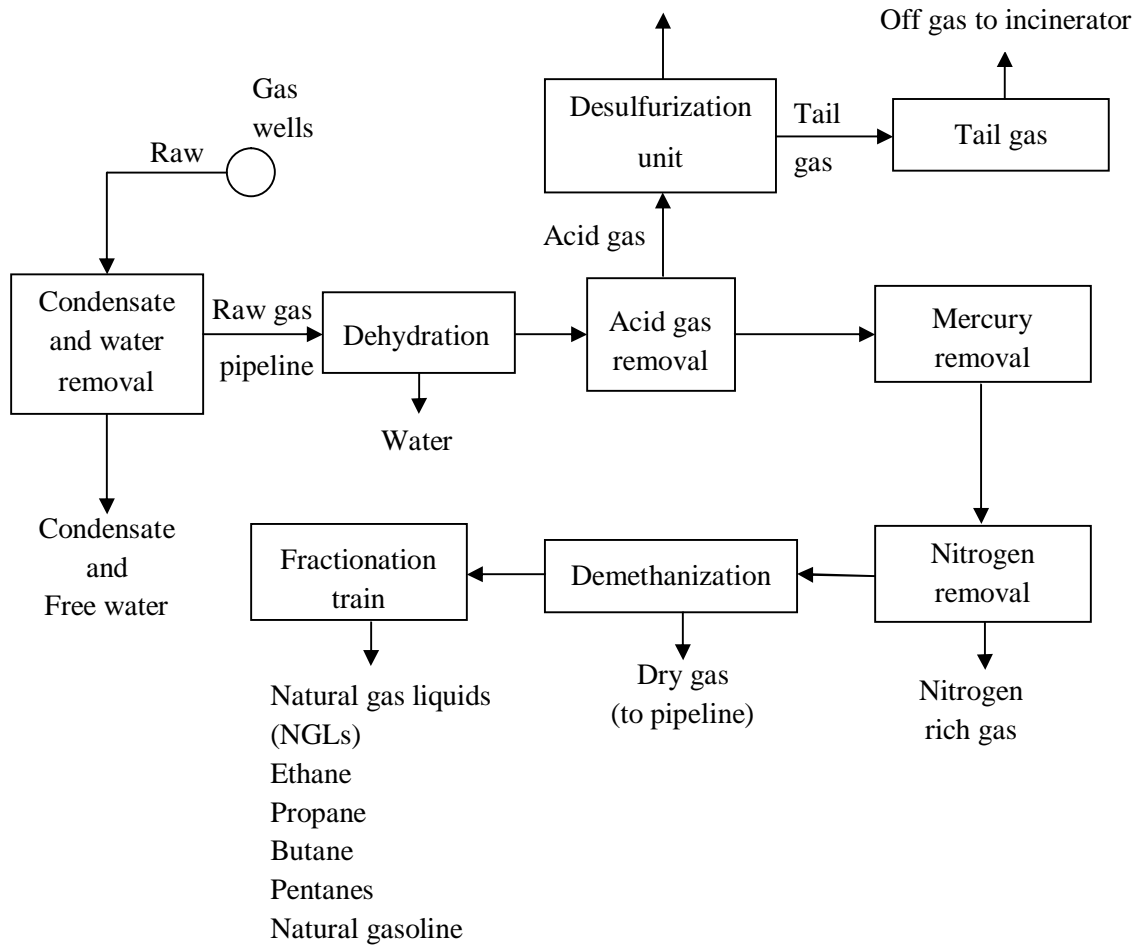


Fig. 1.2: Schematic flow diagram of a typical natural gas processing plant (Kohl and Nielsen, 1997).

- iii. **Contaminant Removal:** Removal of contaminants, including the elimination of hydrogen sulfide, carbon dioxide, mercury and nitrogen. The most commonly used technique is to first direct the flow through a tower containing an amine solution (Sohbi *et al.*, 2007). Amines absorb sulfur compounds and carbon dioxide from natural gas and can be reused repeatedly.
- iv. **Methane Separation:** The process of extractive distillation or absorption in which methane is separated from the heavier components of natural gas. The

process of demethanizing the natural gas stream can occur as a separate operation in the gas plant or as part of the nitrogen rejection unit operation (Kidnay and Parrish, 2006).

- v. **Fractionation:** Although the principal use of natural gas is the production of pipeline quality gas, a number of components in natural gas are often separated from the bulk gas and sold separately (Noronha, 2007). These include components that have greater value as petrochemical feed stocks, e.g., methane in the production of industrial chemicals, sulphur for production of sulphuric acid and vulcanization of rubber, industrial gases, e.g., ethane for the production of ethylene, or stand alone fuels, e.g., propane.

1.2.1 Acid Gas Removal

The removal of acid gas is important due a number of factors including:

- i. **Heating value:** One of the principal uses of natural gas is as a fuel, and consequently, pipeline gas is normally bought and sold on the basis of its heating value. On the other hand, CO₂ has no heating value and its removal may be required when it exists above 2 mol% to increase the energy content of the natural gas per unit volume (Kelkar, 2007).
- ii. **Pipeline requirements:** Acid gases particularly CO₂ and H₂S are corrosive to all metals normally associated with gas transporting, processing and handling systems (although it is less corrosive to stainless steel), and may lead to premature failure of most such systems (Kohl and Nielsen, 1997). Thus, the amount of H₂S must be reduced down to pipeline quality.
- iii. **Safety requirements:** On combustion, H₂S forms sulphur dioxide, which is highly toxic and corrosive (Veroba and Stewart, 2003). Thus, it cannot be

tolerated in pipeline gas that would be used as domestic fuel and has to be removed before distribution.

There are many acid gas treating processes available for removal of H₂S and CO₂ from natural gas. These processes include absorption processes using chemical or physical solvents including amines, potassium carbonate, and selexol (Granite and O'Brien, 2005), hybrid solution using mixed physical and chemical solvents such as sulfinol (Kidnay and Parrish, 2006), adsorption processes using activated carbon, and physical separation using membrane separation process (Kohl and Nielsen, 1997).

1.2.2 Amine Sweetening Process

Amine based sweetening processes are the most prominent and have been the process of choice for removal of H₂S and CO₂ from sour natural gas for decades (Jou *et al.*, 1997; Sohbi *et al.*, 2007). It provides flexibility, low cost and high reliability to industries seeking a proven acid gas removal technology. For low pressure acid gas removal applications, amine absorption is usually the technology of choice. Their selectivity can be optimized to remove the compounds desired, while minimizing process gas losses (Isa *et al.*, 2005).

Amine sweetening plant generally consists of an absorber, a stripper column, a flash separator and heat exchangers as well as accessory equipments as shown in Figure 1.3. Inlet sour gas should be extensively pretreated prior to entering amine sweetening system to eliminate pipeline solids and condensed gas liquids (Kidnay and Parrish 2006). The pretreated sour gas is then introduced into the absorber where it contacts with lean amine solution traveling down the column. The acid gas components, H₂S and CO₂, are absorbed by the amine solution and the sweet gas that leaves the absorber should be filtered to reclaim any entrained amine solvent.

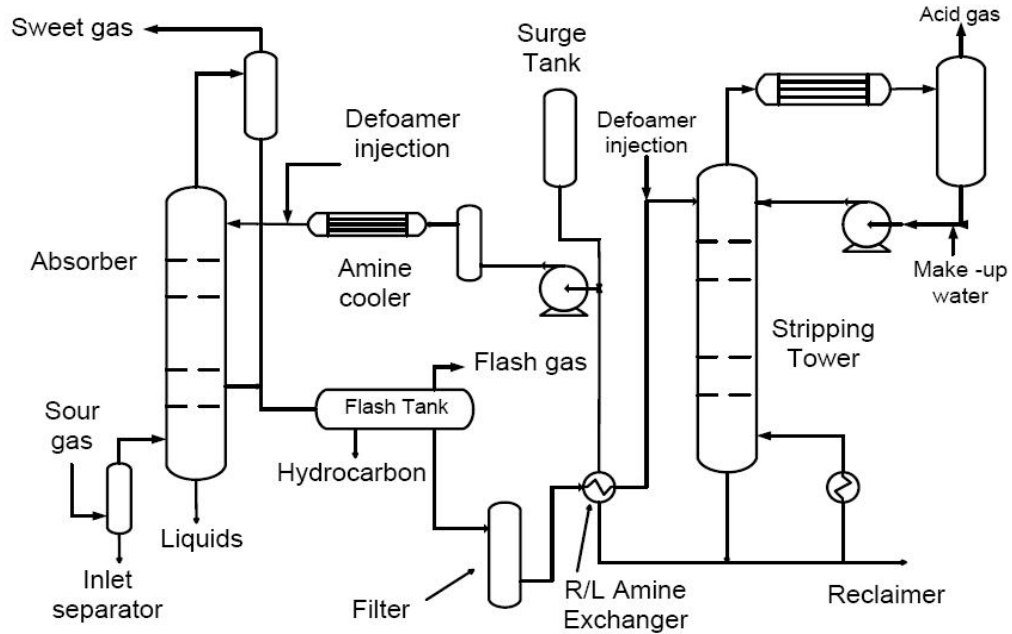


Fig. 1.3: Typical amine sweetening system (Kohl A. and Nielsen R., 1997).

The rich amine is sent to a flash tank and absorbed hydrocarbons exit as the flash-tank vapor. The rich amine flows through the lean/rich exchanger, which increases its temperature to about 377.7K (Kohl and Nielsen, 1997). The hot rich amine is stripped at low pressure removing the absorbed acid gases, dissolved hydrocarbons and some water. The stripped or lean amine is sent back through the lean/rich exchanger, which decreases its temperature. A pump boosts the pressure such that it is greater than the absorber column. Finally, a heat exchanger cools the lean solution before completing the loop back to the absorber (Sohbi *et al*, 2007).

1.3 Sources of Amine Wastewater

The losses of amine from the sweetening plant are mainly due to its operation, which eventually would be discharged to the effluent wastewater. The major sources of amine wastewater are originated from the following process units:

- i. **Absorption unit:** In the presence of contaminants such as condensed hydrocarbons, small suspended particulate matter, amine degradation products, or other surface active agents such as some pipeline corrosion inhibitors, amines develop a foaming problem in the absorber or the stripping tower (DuPart *et al.*, 1993). Foaming in amine plants increases operating costs and reduces treating efficiency. Thus, when foaming becomes severe, amine is often carried over into downstream treating equipment, and subsequently discharged to the effluent wastewater.
- ii. **Filter unit:** This unit is used to remove solid particles from the amine solution before being fed to the stripping unit. The solids must be removed in order to minimize the effect of amine foaming and system corrosion (Abry and DuPart, 1995). However, the cake that is formed on the filters has to be backwashed in order to maintain the operating pressure of the system. Consequently, any amine entrained in the cake enters to the wastewater stream.
- iii. **Reclaimer unit:** Normally the amine sweetening process involves absorption and desorption in order for continual use of the absorbent. However, the solution capacity to absorb acid gases decreases over an extended period of time due to accumulation of non-regenerable contaminants in the system (Meisen *et al.*, 1996). Reclaiming the amine from the contaminated solutions is a common and environmentally friendly technique, which ensures high solution purity necessary for optimal plant operation. The reclaimer is periodically stopped and flushed in order to remove the amine residual left, which finally end up in the effluent wastewater.

Generally, amine losses are largely through entrainment, caused by foaming or excessive gas velocities, leakage due to spills or corrosion, and during process turn around. Others are due to vaporization from the absorber and the overhead condenser (Abry and DuPart, 1995).

1.4 Amine Wastewater Characteristics

Amines wastewater is generally characterized by high chemical oxygen demand (COD) and high pH. Normally, the COD of the wastewater from the sweetening process reaches up to 17,000 mg/l (Omar *et al.*, 2010). Table 1.3 shows the analysis of a typical contaminated DEA solution obtained from a gas treating plant in Western Canada. The pH of the solution was about 10.

Table 1.3: Typical composition of a contaminated DEA solution obtained from a gas treating plant in Western Canada (Meisen *et al.*, 1996).

Compound	Wt. %
Water	68.6
Active Amines:	
Diethanolamine (DEA)	18.6
Triethanolamine (TEA)	0.5
Triethylenediamine (THEED)	4.2
Hydroxyethyl Piperazine (BHEP)	2.9
Residual Amine (Heat Stable Salts)	2.2
Hydroxyethyl imidazolidone (HEI)	0.2
Oxazolidone (HEOD)	0.2
Ethylene Glycol	0.1
Other contaminants (including suspended solids)	2.8

THEED, BHEP, HEI, HEOD and ethylene glycol are degradation products which are formed when the active amines react with carbon dioxide, carbonyl sulfide and oxygen present in the raw natural gas. On the other hand, the heat stable salts formed when strong acid anions such as formate, acetate, thiosulfate and chloride can tie up an amine molecule to form a salt that is not capable of being regenerated by the addition of heat (Meisen *et al.*, 1996).

Amine wastewater is generally not quite suitable to be treated using a conventional biological oxidation method due to its extremely high chemical oxygen demand (COD) and non-biodegradable character (Hawthorne *et al.*, 2005). Therefore, treatment of amine contaminated wastewater is a major concern in amine sweetening plants.

1.5 Problem Statement

Amine based sweetening processes are the most prominent and have been the process of choice for removal of H₂S and CO₂ from sour natural gas for meeting the pipeline quality (Sohbi *et al.*, 2007). However, during amine sweetening process, small amount of amine carry-over and discharged into the effluent stream. This carry-over usually comes from flushing of absorption column and discharged to the effluent water (Abry and DuPart, 1995). Moreover, amine wastewater comes from other sources including water used to wash vessels and other plant equipments, valve leakage and operational upset (Meisen *et al.*, 1996).

Amines wastewater is generally characterized by high chemical oxygen demand (COD) typically about 17,000 mg/l (Omar *et al.*, 2010). Treatment of amine wastewater using existing wastewater treatment plant (WWTP) without any dilution is very challenging since it can affect the performance of the activated sludge. However, dilution increases the volume of the wastewater and requires extension of the existing WWTP. In addition, the slow degradation rate and disposal requirement of excess sludge are the other drawbacks of existing WWTP. Therefore, the development of a technology which is suitable for effective removal of amines in the high COD amine wastewater is required. Thus, to fulfill this objective, membrane separation processes have been proposed as an alternative for the conventional WWTP under the present study.

Membranes have gained an important place in industries and are used in a broad range of applications including treatment of organic containing wastewater, wastewater from electroplating and metal recovery, palm oil industry, pulp and paper, petroleum

refinery, gas processing, and petrochemical (Duranceau, 2001; Singh, 2006; Driscoll T.P., 2008). Therefore, it is the objective of this study to investigate the efficiency of various membrane separation processes for the removal of amines from wastewater.

1.6 Objectives of Study

This study has the following objectives:

- i. To investigate the rejection of three different types of amines, including monoethanolamine (MEA), diethanolamine (DEA) and methyldiethanolamine (MDEA) using three different types of tubular membranes.
- ii. To evaluate the effect of various operating conditions including operating pressure, cross-flow velocity, feed concentration and feed pH on the rejection performance for those membranes against various types of amine solutions.
- iii. To determine the membranes transport parameters using combined film theory-solution diffusion (CFSD) and combined film theory-Spiegler Kedem (CFSK) models.
- iv. To validate the performance of the developed models using the experimental data.

1.7 Scope of Study

The scope of this study and the associated tasks can be briefly summarized as follows:

- i. **Flux Study:** Three different types of tubular membranes, namely AFC99, AFC40 and CA202 will be characterized in terms of permeability of pure water. AFC99 and AFC40 are reverse osmosis and nanofiltration membranes, respectively, and are made from thin film composite polyamide, whereas CA202 is made from

cellulose acetate and falls under ultrafiltration classification. The permeation test will be done at different operating pressures from 4 bar to 24 bar using deionised water. The pure water permeability study of the membranes will be extended to permeate flux study for three different types of amine solutions, namely MEA, DEA and MDEA solutions at various operating conditions including operating pressure, feed concentration, cross-flow velocity and pH. These amines were selected due to their principal commercial advantages for gas purification industries, including high acid gas absorption capacity, high reactivity, high stability and ability to meet pipeline specification (Kohl and Nielsen, 1997, Sohbi *et al.*, 2007). There are different types of membrane modules, including plate-and-frame, tubular, spiral-wound and hollow fiber modules that are widely available to perform the required separation on a useful scale. Thus, the choice of the most suitable membrane module type for a particular membrane separation must balance a number of factors. Cost is always important, but perhaps the most important issues are membrane fouling and concentration polarization (Baker, 2004). This is particularly true for liquid separations such as reverse osmosis and ultrafiltration systems. Thus, tubular modules were selected under present study due to their high resistant to fouling and concentration polarization, and subsequent use for treatment of highly contaminated wastewater.

- ii. **Rejection Study:** The three membranes will be tested for their rejection capability of the amines under the study. The solutions will be prepared with the concentration of 5000 mg/l to 15000 mg/l. The performance of the membranes will be tested under various operating conditions, including operating pressure, feed concentration, cross-flow velocity and feed pH.
- iii. **Modeling:** CFSD and CFSK models will be used to determine the membrane transport parameters, including solute transport parameters, mass transfer coefficients and reflection coefficients by curve-fitting the observed rejection and permeate flux data.

- iv. **Model Validation:** The estimated membrane transport parameters will be substituted into the modeling equations in order to validate the performance of the developed models. The calculated observed rejection will be validated with respect to a new set of experimental data.

1.8 Thesis Organization

This section briefly outlines the contents of this research and specifies the emphasis of each chapter. Chapter 1 provides a brief overview about the importance of natural gas and the problems associated with its processing and conditioning due to the presence of impurities, especially carbon dioxide and hydrogen sulfide. The existing acid gas removal technologies, especially amine based absorption process are discussed briefly. The chapter also discusses about sources of amine wastewater, the problem statement, objectives of the research and outlines the scope of the entire work presented in this study.

Chapter 2 discusses about general industrial wastewater characteristics and treatment methods. It also reviews various research works related to amine wastewater treatment including adsorption, advanced oxidation processes and biological treatment methods. The chapter also focuses on membrane separation processes and highlights the problems that undermine their performance. Additionally, it discusses the application of membrane process in selected industrial wastewater treatment.

Chapter 3 focuses on the theory and development of membrane transport models including combined film theory-solution-diffusion (CFSD) and combined Spiegler-Kedem-film theory (CFSK) models for performance prediction of reverse osmosis and nanofiltration membrane processes.

Chapter 4 presents details on the materials and methods employed to achieve the objectives of the study. The details of the experimental procedures and analytical

methods employed in order to study the membranes performance related to water and amine flux and observed rejection are discussed.

Chapter 5 discusses about the experimental results obtained under the study. The effects of operating parameters, including operating pressure, cross flow velocity, feed concentration and feed pH on the performance of the various membrane processes under the study are discussed briefly. The chapter also discusses estimation of transport parameters and the predictive capabilities of the two models used under the present study by comparing the model predictions with experimental results obtained from membrane filtration test.

Chapter 6 presents the conclusions of the entire research and discusses recommendations for future work.

CHAPTER 2

LITERATURE REVIEW

This chapter provides overview of the fundamental aspects of wastewater and membrane separation processes. The emphasis is to provide comprehensive summary of the most relevant information about amine wastewater treatment technologies and applications of membrane separation process for industrial wastewater treatment.

2.1 Wastewater

Wastewater is any water that has been adversely affected in quality by a wide range of potential contaminants and concentrations (Metcalf and Eddy, 2003). It is classified into two major categories by source: domestic wastewater and industrial wastewater.

Domestic sewage is wastewater discharged from sanitary conveniences in residential, commercial and various institutional properties. It is a complex mixture containing primarily water together with organic and inorganic constituents (Metcalf and Eddy, 2003). These constituents comprised suspended, colloidal and dissolved materials.

Industrial wastewaters are effluents, which are associated with raw-material processing and manufacturing. They have very varied compositions depending on the type of industry and materials processed. Some of these wastewaters can be organically very strong, largely inorganic or associated with high dissolved metal salts (Driscoll, 2008).

2.1.1 Wastewater Constituents and Characterization

Wastewater characterization study is essential in the design and operation of treatment and reuse facilities and in the engineering management of environmental quality (Asan and Levine, 1996). The characteristics of wastewater depend on the source and how the water is used. It is determined in accordance with several sets of laws and regulations that govern the quality of water bodies. Each of these laws defines several physical, chemical and biological characteristics and specifies a protocol to be used in determining each of the characteristics.

2.1.1.1 Physical Characteristics

Physically, wastewater is usually characterized by its color, odor, temperature, turbidity and solids content. The importances of these physical characteristics are summarized below (Baruth, 2005):

- i. **Color:** It is a qualitative characteristic that can be used to assess the general condition of wastewater. Wastewater that is dark grey or black is characteristics of wastewater typically septic, having undergone extensive bacterial decomposition under anaerobic conditions.
- ii. **Odor:** It has become increasingly important, as a variety of odorous compounds are released when wastewater is decomposed biologically under anaerobic conditions. The principal odorous compound is hydrogen sulphide, which cause offensive odor.
- iii. **Temperature:** Its measurement is important because most wastewater treatment schemes include biological processes that are temperature dependent.
- iv. **Suspended solids:** The solids in wastewater can be suspended, dissolved, and settleable. From a physical point of view, the suspended solids can

lead to the development of sludge deposits and anaerobic conditions when discharged into the receiving environment.

Generally, the importance of physical characterization is to determine the most suitable type of operations and processes for wastewater treatment and to assess the condition and quality of treated wastewater and its potential for reuse (Metcalf and Eddy, 2003).

2.1.1.2 Chemical Characteristics

Chemically, wastewater is composed of organic and inorganic compounds as well as heavy metals and various gases (Corbitt, 1999). Organic components may consist of carbohydrates, proteins, fats, hydrocarbons, phenols, etc. The principal inorganic chemicals of interest include free ammonia, organic nitrogen, nitrites, nitrates, organic phosphorus, inorganic phosphorus, chloride and sulphate. Several industries also discharge heavy metals, which are dangerous and toxic to living organisms including chromium, cadmium, lead, cyanide and mercury as shown in Table 2.1.

Table 2.1: Heavy metals found in major industries (Driscoll, 2008).

Industry	Al	As	Cd	Cr	Cu	Hg	Pb	Ni	Zn
Pulp & paper mills	-	-	-	√	√	√	√	√	√
Petroleum refinery	√	√	√	√	√	-	√	√	√
Electroplating	√	-	√	√	√	√	√	√	√
Textile mills	-	-	-	-	-	√	-	-	-
Tanning	-	-	-	-	√	-	-	-	-

The importance of chemical characterization is to assess the amount of nutrients present and their degree of decomposition in wastewater, to measure the buffering capacity of the wastewater and to assess the suitability of the wastewater for reuse.

2.1.1.3 Biological Characteristics

Biologically, wastewater contains various microorganisms including protista, plants and animals (Metcalf and Eddy, 2003). The primary importance of biological characteristics of wastewater is due to the extensive and fundamental role played by bacteria and other microorganisms in the decomposition and stabilization of organic matter, both in natural and in wastewater treatment plants.

2.1.2 Wastewater Quality Indicators

Wastewater quality indicators such as Dissolve Oxygen (DO), Biochemical Oxygen Demand (BOD) and Chemical Oxygen Demand (COD) are essentially laboratory tests to determine whether a specific wastewater will have a significant adverse effect upon aquatic life.

2.1.2.1 Dissolved Oxygen (DO)

Dissolved Oxygen (DO) is a relative measurement of the amount of oxygen (O_2) dissolved in the water (Metcalf and Eddy, 2003). Oxygen is sparingly soluble in water and its solubility decreases with increasing temperature. Moreover, the biological or chemical processes of microorganisms on organic compounds also lead to decline of DO levels.

2.1.2.2 Biochemical Oxygen Demand (BOD)

Biochemical Oxygen Demand (BOD) is a chemical procedure which is used most commonly to estimate the total quantity of biodegradable organic material in wastewater (Clair *et al.*, 2003). The use of BOD as a means of wastewater characterization offers a number of advantages, including determination of the approximate quantity of oxygen

that would be consumed by microorganisms in the process of oxidization of organic materials contained in a wastewater, determination of the size of waste treatment facilities and compliance with wastewater discharge permits.

2.1.2.3 Chemical Oxygen Demand (COD)

Chemical Oxygen Demand (COD) is a measure of the capacity of wastewater to consume oxygen during the decomposition of organic matter and the oxidation of inorganic chemicals such as ammonia and nitrite with a strong chemical oxidant (Clair *et al.*, 2003). COD is a vital test for assessing the quality of effluents and wastewaters prior to discharge. It is used for monitoring and control of discharges and for assessing treatment plant performance.

2.1.3 Wastewater Treatment Objective and Regulation

The focus on health concerns related to pollutants present in wastewaters has driven the development of various wastewater treatment technologies. Water quality standards have been established by most nations and have to be met as treatment goal in order to restore and maintain the physical, chemical and biological integrity of the water bodies (EQA, 2000). Generally, the principal objective of wastewater treatment is to allow industrial effluents to be disposed off without danger to human health, to reduce mass loadings and unacceptable damage to the natural environment, to draw on commercially proven technologies and to promote good industrial practices.

2.1.4 Wastewater Treatment Methods

Wastewater treatment consists of a combination of physical, chemical and biological processes and operations to remove solids, organic matter and sometimes, nutrients from wastewater (Asan and Levine, 1996).

2.1.4.1 Biological treatment method

It is the use of microorganisms, mostly bacteria, in the biochemical decomposition of wastewaters to stable end products. The method basically uses the same processes that would occur naturally in the receiving water, but it uses bacteria under controlled conditions, so that the cleansing reactions are completed before the water is discharged into the environment (Metcalf and Eddy, 2003).

2.1.4.2 Physical treatment method

A physical process usually treats suspended, rather than dissolved pollutants. It may be a passive process, such as simply allowing suspended pollutants to settle out or float to the top naturally depending on whether they are more or less dense than water (Asan and Levine, 1996). Or the process may be aided mechanically, such as by gently stirring the water to cause more small particles to pump into each other and stick together, forming larger particles which will settle or rise faster. Ultrafiltration, nanofiltration and reverse osmosis are also physical processes which force water through membranes and can remove colloidal materials and even dissolved matter.

2.1.4.3 Chemical treatment method

Chemical treatment processes involve converting a waste pollutant into an environmentally acceptable product, convenient to dispose, by changing the pollutant to a solid (precipitate), gaseous or another liquid form. Processes usually encountered in

waste treatment include neutralization, oxidation-reduction, precipitation, ion exchange and coagulation-flocculation (Metcalf and Eddy, 2003).

A typical treatment plant consists of a train of individual unit processes set up in a series, with the output (effluent) of one process becoming the input (influent) of the next process as shown in Figure 2.1. A common set of processes that might be found at a wastewater treatment plant would be:

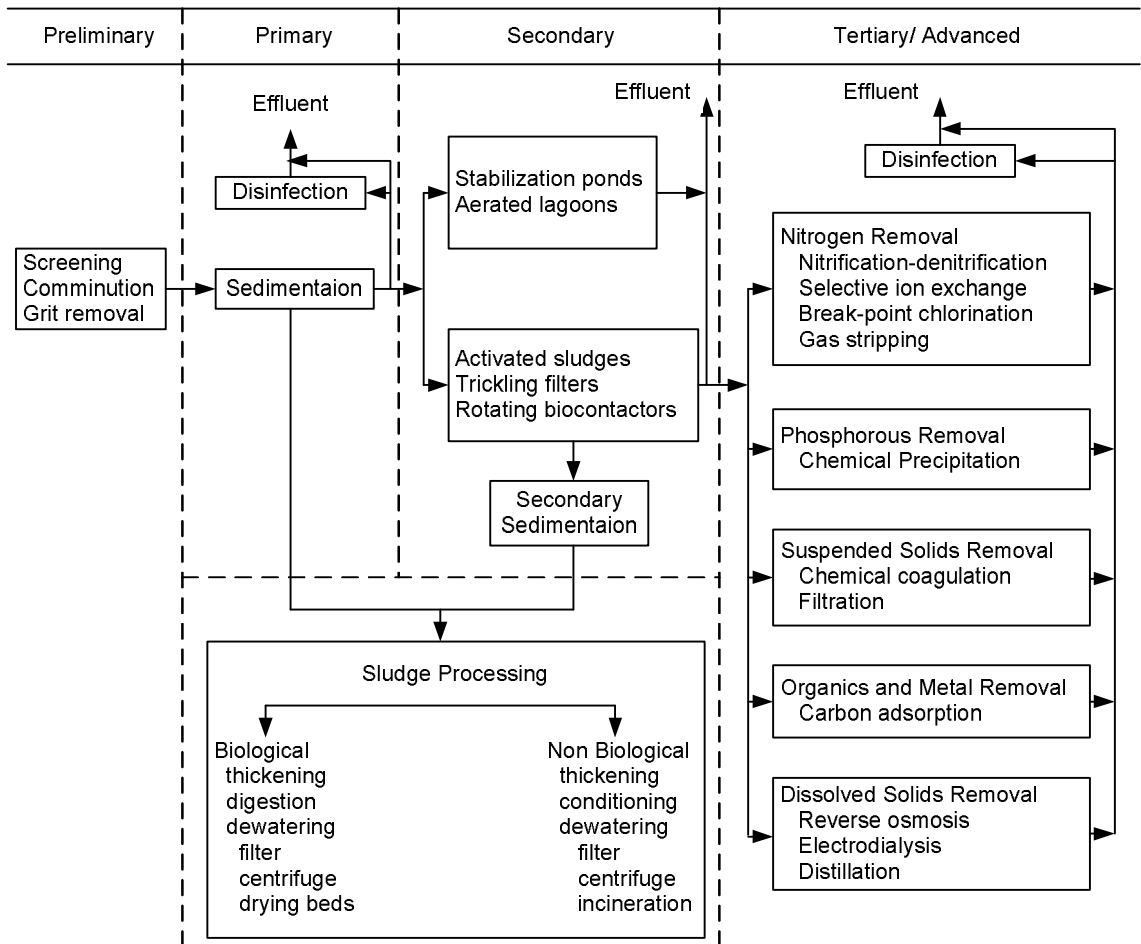


Fig. 2.1: Generalized flow diagram for wastewater treatment (Asan and Levine, 1996).

2.1.4.4 Preliminary Treatment

The objective of preliminary treatment is the removal of coarse solids and other large materials often found in raw wastewater (Baruth, 2005). Removal of these materials is necessary to enhance the operation and maintenance of subsequent treatment units. Preliminary treatment operations typically include coarse screening, grit removal and, in some cases, comminution of large objects.

2.1.4.5 Primary Treatment

The objective of primary treatment is the removal of settleable organic and inorganic solids by sedimentation and the removal of materials that will float (scum) by skimming (Asan and Levine, 1996). Some organic nitrogen, organic phosphorus and heavy metals associated with solids are also removed during primary sedimentation but colloidal and dissolved constituents are not affected.

2.1.4.6 Secondary Treatment

The objective of secondary treatment is the further treatment of the effluent from primary treatment to remove the residual organics and suspended solids. In most cases, secondary treatment involves the removal of biodegradable dissolved and colloidal organic matter using aerobic biological treatment processes (Metcalf and Eddy, 2003).

2.1.4.7 Tertiary and/or Advanced Treatment

Tertiary and/or advanced wastewater treatment is employed when specific wastewater constituents which cannot be removed by secondary treatment must be removed. Usually individual treatment processes, including selective ion exchange, break-point chlorination, air stripping, chemical precipitation, reverse osmosis and electro dialysis are

necessary to remove nitrogen, phosphorus, additional suspended solids, heavy metals and dissolved solids (Baruth, 2005).

2.2 Treatment of Amine Wastewater

The major problem associated with amines wastewater is its high chemical oxygen demand (COD). Normally COD of the wastewater from amine sweetening plant reaches up to 17,000 mg/l. Before the wastewater discharged to the environment, any treatment or series of treatments have to meet the stringent discharge quality, which is 100 mg/l in case of Malaysian law as shown in Table 2.2 (EQA, 1974). The table has listed some parameters that have certain standard limits, which must be obeyed by industries before discharging their wastewater to the environment.

Table 2.2: Malaysian effluent standard regulation for sewage and industrial effluents (Malaysian Environmental Quality, 1974 [Act 127]).

Parameters	Unit	Standard A	Standard B
Temperature	°C	40	40
pH value	mg.l ⁻¹	6.0-9.0	5.5-9.0
BOD ₅ at 20°C	mg.l ⁻¹	20	50
COD	mg.l ⁻¹	50	100
Suspended solids	mg.l ⁻¹	50	100
Mercury	mg.l ⁻¹	0.005	0.05
Cadmium	mg.l ⁻¹	0.01	0.02
Sulphide	mg.l ⁻¹	0.5	0.5
Oil and grease	mg.l ⁻¹	Not detectable	10.0

Standard A refers to the areas upstream of surface or above subsurface water supply intakes, for the purpose of human consumption including drinking, while standard B refers to areas of downstream.

There are few methods used for treating amine in wastewater and these are highlighted in the following section.

2.2.1 Adsorption

Adsorption is a treatment process which is used to remove dissolved waste contaminants, usually organics by employing adsorbent materials such as activated carbon. The adsorption is primarily due to van der Waals forces, although chemical or electrical attraction may also be important (Malik, 2004). The basic instrument for evaluating activated carbon use is the adsorption isotherm. The isotherm represents an empirical relationship between the amount of contaminant adsorbed per unit weight of carbon and its equilibrium water concentration. This relationship can be expressed by Freundlich isotherm as (Martin *et al.*, 2003),

$$X/m = KC^{1/n} \quad (2-1)$$

where, X/m (mg/g) is the amount of contaminant adsorbed per unit weight of carbon, C (mg/l) is concentration of contaminant in the water stream, K ((mg/g)(l/mg)^{1/n}) and n are experimentally described parameters .

Activated carbon has a highly porous internal structure providing large available surface area for adsorption (Fox, 1985). Thus, it had been proposed as an efficient adsorbent for removal of nitrogen containing compounds such as ammonia or amine. However, activated carbon showed poor adsorptivity for removal of amines from wastewater (Mitarai *et al.*, 1991). The adsorption decreases with increasing pH and resulted in very poor adsorption capacity at pH > 9.0 (Casey, 1997). Fritz *et al.* (1974) have proposed silica gel adsorbent to overcome the drawback of poor adsorptivity of activated carbon or active clay. However, when a highly concentrated amine containing wastewater at a level of 20000 ppm was treated with silica gel, the removal ratio was at a level of 57 percent. Fox (1985) also proposed silica-titania and silica-titania-magnesia gel

as a highly activated adsorbents. However, it was found that a removal of only 58 percent at best against a 100 ppm amine containing wastewater was achieved.

2.2.2 Advanced Oxidation Processes (AOPs)

Considerable research has been undertaken to enhance the oxidizing power of common reagents for improved treatment and removal of specific components resistant to oxidation. Fenton's reagent, for example, utilizes ferrous compounds as a catalyst to produce hydroxyl ion (OH·) and thereby enhance the oxidizing capacity of the peroxide (Gogate *et al.*, 2004):



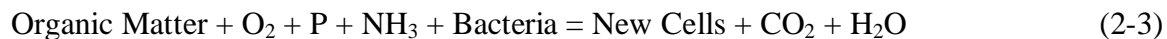
Advanced Oxidation Processes (AOPs), especially the photo-Fenton process has been widely used for degradation of amines. The photo-Fenton process is considered to be highly promising for the remediation of highly contaminated wastewater (Pignatello *et al.*, 2006). As compared to other conventional oxidant species, the hydroxyl radical is capable to completely oxidize (mineralize) even the less reactive pollutants. However, organic compounds oxidation by photo-Fenton process would be inhibited by inorganic species such as phosphate, sulphate, chloride and carbonate ions (DeLaat *et al.*, 2004). These anions can react with the hydroxyl radicals (HO·) and subsequently be scavenged from the aqueous solution leading to non-reactive species.

The main disadvantage of AOPs is the operational cost associated with their high electrical energy input (UV radiation generation) and expensive chemicals demand (H₂O₂, O₃, etc.). In fact, only wastewaters with relatively small concentration (COD ≤ 5,000 ppm) can be economically treated with these technologies (Pignatello *et al.*, 2006).

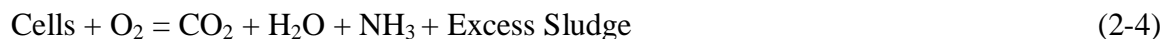
2.2.3 Biological Treatment

Biological treatment methods involve the use of microorganisms to break down hazardous organic compounds into non-hazardous materials. Stoichiometrically the process is commonly represented as two simple reactions as shown in Equations (2-3) and (2-4) (Metcalf and Eddy, 2003):

Oxidation and synthesis reaction



Endogenous respiration reaction



Biological systems are effective methods to economically remove large quantities of biodegradable wastewater organics, converting them to water and carbon dioxide. However, the use of biological processes to treat amine contaminated wastewater is limited to low concentration (Isa *et al.*, 2005). High COD amine wastewater can harm the bacteria populations and slowdown their activity, hence may take several weeks for complete degradation. Furacker (2003) studied aerobic degradation of methyldiethanolamine in a batch system. The findings showed that the degradation did not succeed within standardized batch experiments, whereas experiments with flow through reactors resulted in a removal of about 96% within 28 days. Moreover, all biological processes produce excess sludge that may have to be further reduced and stabilized before disposal (Hawthorne *et al.*, 2005). Generally, amine wastewater is not suitable for conventional biological oxidation methods due to high COD.

For the treatment of wastewaters discharged from plants, the methods and the optimum treating conditions vary depending upon: the natures and concentration of the wastewaters, the objective COD concentration level required for treatment, cost of operation and installation and reliability. Table 2.3 summarizes the advantages and disadvantages of various methods for treating wastewater containing amine.

Table 2.3: Advantages and disadvantages of various methods of amine wastewater treatment (Mitarai *et al.*, 1991; Hawthorne *et al.*, 2005).

Treatment methods	Advantages	Disadvantages
Adsorption using activated carbon	<ul style="list-style-type: none"> ▪ Very versatile technology ▪ Suitable for treating a wide variety of toxic organic compounds ▪ Suitable for removing low solubility organics 	<ul style="list-style-type: none"> ▪ Not suitable for treating high concentration wastewater containing amine ▪ High capital, operation and maintenance cost ▪ Intolerant of high suspended solids ▪ Pretreatment is required for oil and grease greater than 10 mg/l
Advanced oxidation processes (AOPs)	<ul style="list-style-type: none"> ▪ Complete degradation or mineralization 	<ul style="list-style-type: none"> ▪ Cost are very high ▪ Oxidizing chemicals are potentially hazardous ▪ Can be inhibited by inorganic ions
Activated sludge	<ul style="list-style-type: none"> ▪ Process reliable in absence of shock loading ▪ High degree of flexibility ▪ Can tolerate higher organic loads than most biological processes 	<ul style="list-style-type: none"> ▪ Generates high amount of sludge ▪ Sensitive to heavy metals and toxic organics ▪ Digestion rates are slow ▪ Requires large storage tanks, high capital cost ▪ Fairly energy intensive

Generally, the reliability of physicochemical processes for amine wastewater treatment is higher than conventional biological treatment methods. On the other hand, biological methods have the advantage of low cost operation.

Furacker (2003) studied that successful removal of poorly degradable amines can be achieved depending on the constitution and acclimatization of the applied activated sludge. The findings showed that the processing, the quality, the adaptation of bacteria and the reactor type are decisive parameters for the efficiency of biological treatment methods. Isa *et al.* (2005) also discussed that bacteria can easily adapt the environment and successfully degrade amines when the concentration is below 1000 mg/l. Hence, biological treatment method requires the support of an effective complementary

technique to improve the entire efficiency of the treatment in order to meet the stringent discharge quality when the COD of the wastewater is higher than 1000 mg/l.

Membranes, on the other hand, provide several advantages that make them attractive for wastewater treatment. They are capable of either fulfilling the stringent discharge quality or reducing the COD value of the amine wastewater to a level which is suitable for further biological treatment. Therefore, it is the objective of this study to investigate the efficiency of membranes for removal of amines from wastewater.

2.3 Overview of Membranes Process

2.3.1 Definition

A membrane is a thin layer of material which serves as a selective barrier between two phases and remains impermeable to specific particles, molecules, or substances when exposed to the action of a driving force. Some components are allowed passage by the membrane into a permeate stream, whereas others are retained by it and accumulate in the retentate stream (Zydney and Zeman, 1996) as shown in Figure 2.2.

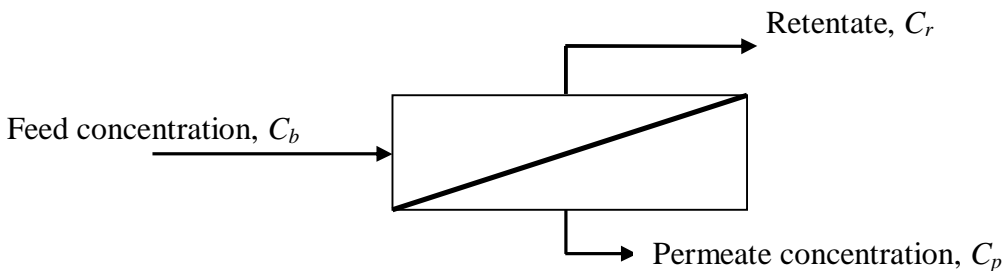


Fig. 2.2: Schematic diagram of membrane system (Jude and Jefferson, 2003).

2.3.2 Membrane Morphology

Membranes can be categorized based on their physical structure or morphology. Generally, membranes can be divided into: dense and porous membranes (Jude and Jefferson, 2003). The morphology can be classified further into a symmetric and an asymmetric structure. The thickness of symmetric membranes (porous or dense) ranges roughly from 10 to 200 μm , whereas asymmetric membranes consists of a dense top layer with thickness of 0.1 to 0.5 μm supported by a porous sub layer with a thickness of about 50 to 150 μm (Baker, 2004). Table 2.4 summarizes the types of pressure driven membrane processes, their physical structure and applications.

Table 2.4: Dense and porous membranes for water treatment (Jude and Jefferson, 2003).

Pressure Driven Membrane Processes Classification			
Membrane Process	Membrane Structure	Mechanism of Separation	Applications
Reverse osmosis (RO)	Dense	Separation achieved by virtue of differing solubility and diffusion rates of water (solvent) and solutes in water	Separation of salts, small organics, and microsolute
Nanofiltration (NF)	Micropores (< 1 nm)	Separation achieved through combination of charge rejection, solubility-diffusion and sieving	Separation of small organic compounds and selected salts
Ultrafiltration (UF)	Mesopores (2 – 50 nm)	sieving	Separation of colloids, emulsions, macromolecules, proteins
Microfiltration (MF)	Macropores (> to 50 nm)	sieving	Separation of small particles, microbial cells, large colloids

2.3.3 Membrane Flow Geometries

There are two main flow configurations of membrane processes: cross-flow and dead-end filtrations as shown in Figure 2.3. The dead-end membrane separation process is easy to implement and the process is usually cheaper than cross-flow membrane filtration. However, it is highly susceptible to extensive membrane fouling and concentration polarization. The tangential cross flow devices are more costly, but they are less susceptible to fouling due to the sweeping effects and high shear rates of the passing flow (Schafer *et al.*, 2005).

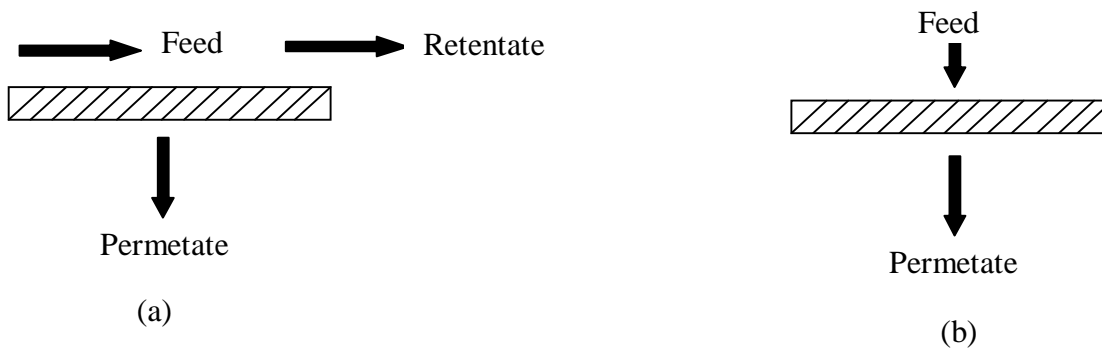


Fig. 2.3: Membrane flow geometries: (a) Cross-flow filtration, (b) Dead-end filtration (Baker, 2004).

2.3.4 Membrane Performance

Typically membrane performance is characterized in terms of flux and rejection. The permeate flux, J_v is the rate of material transported per unit membrane area and can be expressed as,

$$J_v = \frac{Q_p}{A_m} \quad (2-5)$$

where, J_v ($l/m^2 \cdot h$), Q_p (l/h) is solvent (water) flow rate through the membrane and A_m (m^2) is the surface area of the membrane.

The key elements of the membrane process that affect the overall permeate flux include the membrane resistance, the operational driving force per unit membrane area, the hydrodynamic conditions at the solution-membrane interface and the fouling and subsequent cleaning of the membrane surface (Baker, 2004). The permeate flux can also be expressed as,

$$J_v = \frac{\Delta P}{\mu(R_c + R_g + R_m)} \quad (2-6)$$

where, ΔP (Pa) is transmembrane pressure, μ (Pa.s) dynamic viscosity of the bulk solution, R_c (m^{-1}) resistance due to concentration polarization, R_g (m^{-1}) is resistance due to gel polarization, and R_m (m^{-1}) is membrane resistance.

The observed rejection is the relative change in concentration from the bulk stream to the permeate stream and can be expressed as,

$$R_o = 1 - \frac{C_p}{C_b} \quad (2-7)$$

where, C_p (mg/l) permeate concentration and C_b (mg/l) is the bulk concentration. The true rejection, R is obtained by replacing the bulk concentration, C_b in to membrane wall concentration, C_m (mg/l). It is expressed as,

$$R = 1 - \frac{C_p}{C_m} \quad (2-8)$$

2.3.5 Problems in Membrane Process

Membrane processes face two main challenges due to concentration polarization and membrane fouling.

2.3.5.1 Concentration Polarization

Concentration polarization (CP) is a fully reversible phenomenon inherent in all mass separation processes. It is caused by the accumulation of retained solutes on the

membrane surface during the separation process. CP creates a high solute concentration at the membrane surface compared to the bulk solution. This higher concentration at the film interface reduces permeate flux and quality due to a higher local osmotic pressure for a given driving force (Jude and Jefferson, 2003).

2.3.5.2 Membrane Fouling

The loss of performance of a membrane over a period of time is attributed to a variety of mechanisms known collectively as fouling (Van der Bruggen, *et al.*, 2002). There are many causes for fouling, including concentration polarization, gel formation, plugging of membrane pores by suspended matter and biological fouling. The effect of fouling can be minimized either by back washing or chemical cleaning as shown in Figure 2.4.

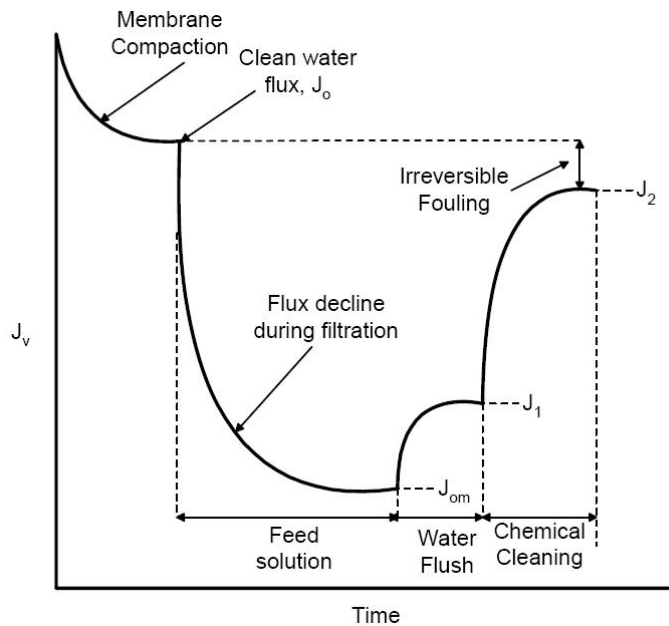


Fig. 2.4: Typical protocol used in fouling studies (Schafer *et al.*, 2003).

The membrane resistance is fixed, unless its overall permeability is reduced by components in the feed water permanently adsorbing onto or into the membrane (Damak *et al.*, 2004). Thus the feed water composition (specifically its foulant content) and the

process operating conditions largely determine process performance. Typically, fouling is addressed through pretreatment of feed or by changing the flow pattern from dead-end to cross-flow.

2.3.6 Advantages and disadvantages of membranes

Membranes provide several advantages that make them attractive for wastewater treatment. Some of the advantages and disadvantages of membrane separation processes are summarized below.

2.3.6.1 Advantages

- i. Simple to design and operate: Since membrane processes have few unit operations, membrane treatment plants are simple to design and operate. In addition, due to the few equipments involved, membrane treatment plants have much smaller foot print than the conventional plants of the same capacity.
- ii. Shortens treatment time: Since membrane separation process do not involve reaction or do not require retention pools like biological treatment methods, the removal process is fast.
- iii. Remove both inorganic and organic pollutants simultaneously: Since the mechanism of separation in membrane processes is based on size exclusion and electrostatic interaction, both inorganic and organic pollutants can be separated simultaneously based on their properties.
- iv. Allow recovery of waste process streams with no effect on the material being recovered: since membrane processes involve neither phase nor temperature changes, they are good for recovery of temperature sensitive materials.

- v. No formation of secondary chemical by-products: membrane separation is physical process and doesn't involve chemical reaction which could result secondary by-products.

2.3.6.2 Disadvantages

- i. Membrane feed usually requires pre-treatment: Membrane processes are highly susceptible to fouling which affects their performances. Hence, the feed requires pre-treatment which can incur additional cost for the process.
- ii. Low membrane life time: Membranes are also susceptible to free chlorine and bacteria which can damage their structure. Hence, usually they have short life time.

2.4 Treatment of Industrial Wastewater Using Membrane Separation Process

Nowadays, membrane processes are employed in various areas in wastewater treatment, including in textile, electroplating and metal recovery, pulp and paper, palm oil, petroleum refinery, metal working and metal finishing, tanning and leather, heavy metals and petrochemical industries (Koyuncu *et al.*, 1999; Cassano *et al.*, 2001; Duranceau, 2001; Jude and Jefferson, 2003; Hager, 2006; Jain *et al.*, 2006; Singh, 2006; Driscoll, 2008). Some of the applications of membranes for industrial wastewater treatment are discussed below.

2.4.1 Treatment of Palm Oil Mills Effluent Wastewater

Palm oil production industries are one of the few industries which produce highly polluted wastewater. Large quantities of water are used during the extraction of crude

palm oil from the fresh fruit bunch, and about 50% of the water results in palm oil mill effluent which contains high amounts of total solids (TDS = 40500 mg/L), oil and grease (4000 mg/L), COD (50000 mg/L) and BOD (25000 mg/L) (Ahmad *et al.*, 2005). The disposal of this highly polluting effluent may cause serious environmental pollution and damaging effects on the receiving water bodies.

Normally, treatment technologies of the palm oil mills effluent comprise screening and air flotation to remove fats and solids followed by biological treatment. For the biological treatment methods like aerobic or anaerobic digestion to be effective the ratio of BOD to COD should be > 0.6 . However, an effluent from the palm oil industry usually has its BOD/COD ratio around 0.2, which could cause destruction of microorganisms useful for the biodegradation (Koltuniewicz and Drioli, 2008). Other methods like multiple effect evaporation or incineration are highly energy intensive and hence very expensive. Thus, an efficient treatment technology is mandatory for treatment of palm oil mills effluent in order to comply with the stringent environmental regulation.

The uses of various membrane separation processes together with physicochemical processes for treatment of palm oil mills effluent have been conducted by many researchers (Ahmad *et al.*, 2005; Ahmad and Chan., 2009; Wu *et al.*, 2007 and 2010). Wong *et al.* (2002) studied the use of ultrafiltration together with filtration as pretreatment method for treatment of palm oil mills effluents. Their findings showed that removal efficiency of 99.2%, 98.2%, 85.0% and 78.8% was achieved for suspended solids, turbidity, COD and total nitrogen, respectively. Wu *et al.* (2007) also used ultrafiltration for treatment of palm oil mills effluent together with filter bed as a pretreatment mechanism. Their findings showed that a removal efficiency of 97.7%, 88.5% and 57% of total suspended solids, turbidity and COD, respectively was achieved at 0.8 MPa. The study by Ahmad *et al.* (2005) also showed that a rejection capacity of more than 96% of total suspended solids and BOD and COD removal of up to 56% was observed for treatment of palm oil mills effluent using ultrafiltration membrane. Ahmad and Chan (2009) also studied treatment of palm oil mills effluent using series of pretreatments, including coagulation-flocculation process and activated carbon and

membrane separation processes, including ultrafiltration and reverse osmosis. Their findings showed more than 99% removal of COD, total dissolved solids, nitrogen (organic) and almost 99% removal of ammonical nitrogen was observed.

2.4.2 Treatment of Petroleum Refining Wastewater

The hydrocarbon processing industry, including petroleum refining and natural gas production, generates large quantities of wastewaters that have high contents of oil, acid sludge, oil and grease, heavy metals, suspended solids, organic nitrogen, ammonia, organic carbon, hydrogen sulfide and dissolved solids (Ju *et al.*, 2008). The removal of a large portion of free oil is possible with conventional methods. However, refinery wastewater contains hydrocarbons that remain even after conventional wastewater treatment due to their limited biological degradation (Faksness *et al.*, 2004).

The removal of a large portion of free oil is possible with conventional methods; however, refinery wastewater contains hydrocarbons that remain even after conventional wastewater treatment due to their limited biological degradation (Vlasopoulos *et al.*, 2006). This makes further treatment necessary to meet discharge requirements, or for its reuse. Membrane purification can be a strong candidate for this application. Ultrafiltration membranes can remove essentially all free and dispersed oil from wastewater, hence the permeate can consistently be able to meet oil and gas standards for discharge (Teodosiu *et al.*, 1999). Reverse osmosis treatment can also be used to remove salts and small molecule contaminants from refinery wastewater (Cakmakci *et al.*, 2008).

The removal of oils by ultrafiltration pretreatment substantially reduces the fouling of RO membranes, making the process more feasible and economical for treatment of petroleum refining wastewater. Hydrophilic membranes generally are used for filtering these oily wastewaters since hydrophobic membranes can become wetted with oil and lose water flux during operation (Ahmadun *et al.* 2009). Hydrophilic membranes preferentially attract water rather than the oil, resulting in much higher flux. Tubular

membranes are particularly attractive since they are able to generate very concentrated retentates and require minimal pretreatment of the feed.

2.4.3 Treatment of Pulp and Paper Wastewater

The pulp and paper industry produce highly polluted water which contain cellulosic solids, resin acids, sludge, lignin, suspended solids and chlorinated phenolic compounds (Koyuncu *et al.*, 1999). In addition, the effluents are highly colored and non-biodegradable. The most significant environmental issues of textile wastewater are the discharge of chlorine-based organic compounds (from bleaching) and of other toxic organics (Wallberg *et al.*, 2003). In addition, the effluents are highly colored and non biodegradable for the most part.

Paper and pulp wastewater treatment typically includes (i) neutralization, screening, sedimentation and floatation to remove suspended solids and (ii) biological secondary treatment to reduce the organic content in wastewater and destroy toxic organics (Wallberg *et al.*, 2003). However, the conventional treatment cannot meet the requirements of water quality for the paper making process.

Membrane based processes are becoming very important alternative technologies for pulp and paper wastewater treatment. Zhang *et al.* (2007) used integrated membrane process in pilot scale which consists of membrane bioreactor (MBR), continuous membrane filtration (CMF) and reverse osmosis (RO) to treat wastewater from paper mill. Their findings showed that RO has achieved over 65% water recovery, less than 200 $\mu\text{S}/\text{cm}$ permeate conductivity, less than 15 mg/l permeate COD and less than 0.1 NTU turbidity. The results showed that the high quality RO permeate obtained could meet the whole standards of process water of paper mill.

Ultrafiltration (UF) can also be used to concentrate and recycle some of the effluents prior to discharge (Wallberg *et al.*, 2001). Some applications of UF include color removal from kraft mill bleaching effluents, concentration of dilute spent sulfite liquor (SSL) form

the sulfite process, recovery of lignin from kraft black liquor, and recovery of paper coatings (Guangli et al., 2004).

2.4.4 Treatment of Textile Wastewater

The textile wastewater is rated as one of the most polluting industrial sectors considering both volume and composition of the effluent (Vanndevivera *et al.*, 1998). The wastewater consist many pollutants including dissolved solids, suspended solids, organic chemicals, ionic salts, dye and sometimes heavy metals (Robinson *et al.*, 2001).

The common methods used for treating this kind of wastewater are usually biological, physical and chemical techniques as well as the various combinations of these (Banat *et al.*, 1996). However, it has been widely reported that many dye chemicals are either difficult to degrade using conventional biological treatment methods or results in highly biotoxic aromatic amines under anaerobic conditions.

The use of membranes in combination with physico-chemicals processes is very interesting in order to produce water to be reused from the textile effluent water (Wenzel *et al.*, 1996). Membrane processes can have many cost effective applications in textile industry. The cost competitiveness results from the ability to recover materials and recycle water, reducing fresh water consumption and waste water treatment costs, small disposal volumes which minimize waste disposal costs.

Bes-Pia *et al.* (2002) used a combination of coagulation, flocculation and nanofiltration (NF) for the purpose of reusing the wastewater after treatment. The permeate analysis of their finding showed that almost 100 % COD and 85 % conductivity removal for the DOW NF-70 membrane under their study. Chen *et al.* (2005) have also studied treatment of textile wastewater for reuse using electrochemical oxidation and NF membrane. Their finding showed that electrochemical oxidation achieved a high removal (89.8% efficiency) of the chemical oxygen demand (COD) of the wastewater while the

NF membrane has almost totally removed the total suspended solids (TSS) (nearly 100% reduction) and turbidity (98.3% elimination) in it.

Koyuncu et al. (2001) have also used pilot scale nanofiltration (NF) membranes in textile dyestuff effluents. They investigated the suitability of NF in separating COD, color and conductivity from textile industry dye house effluents. Their finding showed that overall removal efficiencies of COD, color and conductivity were found as greater than 97%. This significant reduction in color and COD can make possible the recycle of the permeate in the dye house.

2.4.5 Treatment of Tanning and Leather Wastewater

The wastewater of leather industry contains many toxic pollutants, including dyes, organic pollutants, amines, sulfide, chromium and suspended solids. The COD of this wastewater ranges between 20,000 and 40,000 mg/l of consumed oxygen (Cassano *et al.*, 2001).

Membrane processes can be used for the treatment of leather industry wastewaters in order to remove the salt content or to separate the biomass from the effluent after chemical–physical treatments (Ahmed *et al.*, 2006). The uses of membranes to treat the soaking, deliming/bating and pickling effluents were studied by many researchers (Cassano *et al.*, 2001; Cassano *et al.*, 2003; Jain, *et al.*, 2006). The findings of the studies showed that membranes especially microfiltration and ultrafiltration can be used for removal of organic components, protein components, fatty substances, COD, colloidal substances, etc. The findings of Cassano *et al.* (2001) showed that the use of non-cellulosic ultrafiltration tubular membranes achieved more than 85% protein and colloidal substances rejection. Their study also showed that reverse osmosis membrane exhibited about 95% removal of COD and fatty substances. Thus, membranes can be an alternative technology for efficient and economical treatment of industrial wastewaters.

The recovery of chromium from spent tanning and retanning baths provides a significant economic advantage in terms of both its reuse and the simplification of processing of the wastewaters (Winston Ho et al., 2001; Scholz et al, 2003). Membrane technology can also be used to concentrate the chromium and salts from the tannery operation for reuse. This not only cost-effectively solves disposal problems, but also it reduces manufacturing costs for a more profitable waste operation (Scholz et al, 2003). Extensive studies involving microfiltration (MF), ultrafiltration (UF), nanofiltration (NF) and reverse osmosis (RO) have been studied widely (Cassano et al., 2001; Cassano et al., 2003; Ahmed et al., 2006; Jain et al., 2006).

Das et al. (2006) proposed an integrated NF/RO system to treat the chrome tanning effluent in a cross-flow cell. The NF permeate was passed through a RO unit to obtain clean water and concentrated salt solution for reuse. In this industry, the spent tanning liquors can be subjected to a preliminary MF and UF step to remove most suspended solids and fat substances, to recover sulfides and recycle or at least remove dissolved chromium from spent chrome tannin (Cassano et al., 2001). The permeate coming from the UF treatment is then subjected to a NF process in which chromium salts are concentrated to a final value.

2.4.6 Electroplating wastewater treatment and Metal Recovery

The electroplating industry is one of the major industries which generate a large portion of wastewater containing heavy metals. Heavy metals are important sources of environmental pollution and present one of the most critical industrial waste problems (Gijzen, 2000). Contaminants in the effluent from electroplating industries mainly come from rinse water and used or spent process solutions. Accidental spills, leaks, and drips of process solutions also can contribute to effluent contamination (Waalkes, 2000).

The conventional alkaline–chlorination-oxidation-reduction process with further chemical precipitation of the metals presents some deficiencies and can result in

additional environmental problems due the production of highly toxic chlorine by products and metallic hydroxide (Gijzen, 2000). The appropriate disposition of this sludge constitutes a serious environmental and economical problem for the involved industries (Monser et al., 2002). Therefore, there is a growing interest in developing an effective method for recovery of metals from electroplating waste stream and the recovery of water using membrane technology.

RO process has become increasingly attractive for the treatment and recycling of wastewater in metal plating industries as it is highly efficient, easy to operate and low on cost (Chaci et al., 1997). Simultaneous water recycling and recovery of valuable materials are of utmost importance because precious metals are used. The RO process has been used in the treatment and recovery of wastewater containing nickel, acid copper, zinc, copper cyanide, cadmium, silver, tin, iron, lead, palladium, platinum, rhodium, fluoride, chromium, aluminum, and gold (Benito et al., 2002).

There are many studies in the industrial or pilot scale regarding the use of membranes for recovery of metals and water in electroplating industries. Imasu (1985) reported the use of cellulose acetate and polyamide (FT30) membranes with nickel, chromium, and gold plating lines. Up to 80 percent water recoveries with high metal and TDS (> 95 %) rejections were possible. Slater et al. (1987) reported on the use of RO membranes to remove cadmium from metal processing wastewaters. The FT30 membranes used had cadmium rejection of > 99.5 percent in the most cases and produced high quality product water suitable for reuse. Jian-Jun (2003) proposed the treatment of spent rinse water from metal plating using RO to meet the requirements for reuse as alkaline rinse water. He used ESPA1 polyamide composite, RO Film Tec TW30 and UF membranes. For a combination of alkaline, acid and nickel-plating rinses, he found a rejection of conductivity 97 %, nickel 99.8 %, nitrate 95 % and total organic carbon 87 %. The finding showed that the permeate quality met the requirements for reuse as an alkaline rinse water.

CHAPTER 3

THEORY AND MODELING

The purpose of this chapter is to provide a detailed summary of membrane transport models and their ability to predict membrane performance (usually expressed in terms of solute rejection) at different operating conditions. The success of the models can be measured in terms of their ability to describe mathematically the data with coefficients that are reasonably constant over a range of operating conditions.

There are several models available for modeling of reverse osmosis and nanofiltration membranes processes, including nonporous and porous membrane models. The nonporous membrane models include the solution-diffusion, solution-diffusion-imperfection, and extended solution-diffusion models (Lonsdale *et al.*, 1965; Paul, 2004). The porous models include preferential sorption-capillary flow, surface force-pore flow models, and irreversible thermodynamics models such as Kedem-Katchalsky and Spiegler-Kedem models (Spiegler and Kedem, 1966). Donnan exclusion and extended Nernst-Planck models can also be used to describe nanofiltration process which includes electrostatic effects for charged membranes (Bowen and Mukhtar, 1996). Most of these models were developed with fundamental equations that consider a mass balance around the membrane element, pressure driven solvent and concentration gradient driven solute transport. In addition, since the separation process causes accumulation of solutes on the membrane surface, the concentration polarization phenomenon also needs to be included in the mass transport equations.

3.1 Film Theory Model

In order to model the transport mechanism of solvent and solute across the membrane, the intersection between the bulk solution and the membrane interface is crucial to be studied. This relation is described by using film theory. As membranes are permselective, they allow solvent (water) to pass through while rejecting the solutes. The accumulation of the retained solutes at the solution-membrane interface develops a concentration gradient within this interface. This phenomenon is known as concentration polarization and well described by film theory as shown in Figure 3.1.

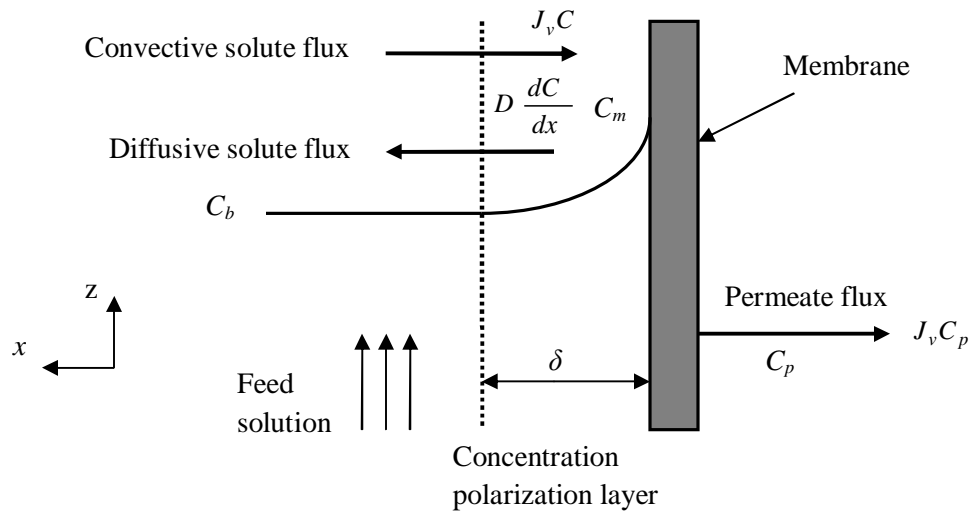


Fig. 3.1: Schematic diagram for film theory (Baker, 2004).

This theory assumes a fully developed boundary layer with thickness of δ and the flow is in one dimension, x . At steady state, a material balance of solute on a differential fluid element within the concentration polarization boundary layer can be expressed as (Baker, 2004; Paul, 2004),

$$\text{Convection solute flux} - \text{diffusive solute flux} - \text{permeate flux} = 0 \quad (3-1)$$

$$J_v C - J_v C_p - D \frac{dC}{dy} = 0 \quad (3-2)$$

where, C (mg/l) is the solute concentration in the boundary layer and D is the diffusivity of the solute in the boundary layer (m^2/s). Integrating Equation (3-2) with the following boundary conditions,

(i) $C=C_m$ at $x=0$ and (ii) $C=C_b$ at $x= \delta$

Will result,

$$\frac{C_m - C_p}{C_b - C_p} = \exp\left(\frac{J_v}{k}\right) \quad (3-3)$$

where, k is mass transfer coefficient (m/s)($=D/\delta$), and δ is boundary layer thickness (m).

Equation (3-3) is known as the concentration polarization equation for partially rejected solutes. It predicts that under mass-transfer-limited conditions, permeate flux is independent of transmembrane pressure. In practice, permeate flux is often limited by the mass transfer coefficient at higher transmembrane pressures as shown from Figure 3.2. At lower transmembrane pressures, permeate flux may be proportional to the transmembrane pressure.

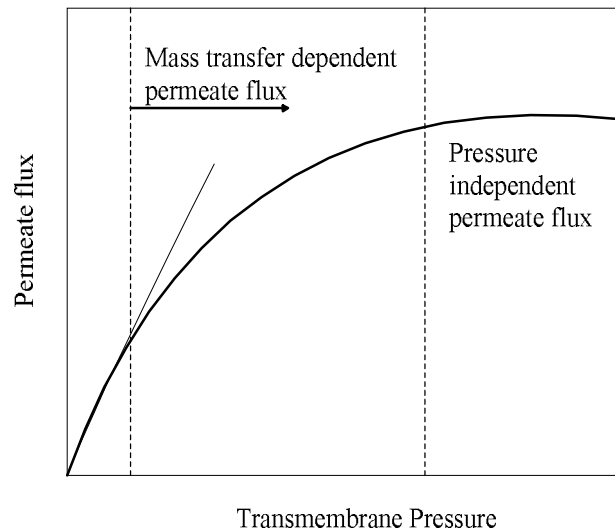


Fig. 3.2: Permeate flux as a function of transmembrane pressure: pressure-dependent and mass-transfer-limited permeate flux (Jude and Jefferson, 2003).

Inserting observed and true rejections given in Equation (2-7) and (2-8), respectively in Equation (3-3) gives,

$$\frac{1-R_o}{R_o} = \frac{1-R}{R} \cdot \exp\left(\frac{J_v}{k}\right) \quad (3-4)$$

Equation (3-4) can be rearranged and expressed as,

$$\ln \frac{1-R_o}{R_o} = \ln \frac{1-R}{R} + \left(\frac{J_v}{k}\right) \quad (3-5)$$

Hence, by plotting $\ln \frac{1-R_o}{R_o}$ versus J_v , a linear correlation will be drawn, the slope of the plot will be $(1/k)$ with intercept of $\ln \frac{1-R}{R}$. Solving the slope and intercept will give the value of mass transfer coefficient, k and true rejection, R , respectively.

3.2 Nonporous Model

The basic principle of the nonporous models concept is that permeating species dissolve in the membrane material and molecularly diffuse through it as a consequence of a concentration gradient in contrast to the pore flow mechanism where the membrane material is not an active participant at a molecular level (Paul, 2004). Also, the models assume equilibrium or steady state condition is achieved in the membrane.

3.2.1 Solution Diffusion Model

The solution diffusion model (SD) proposed by Lonsdale *et al.* (1965) assumes:

- i. Solute and solvent transport across membranes depend on the relative affinities of these components for the membrane and their diffusive transport within the membrane phase.
- ii. The water flux is proportional to the solvent chemical potential difference (usually expressed as the effective pressure difference across the membrane), and

the solute flux is proportional to the solute chemical potential difference (usually given as the solute concentration difference across the membrane).

iii. The solute and solvent diffusion across the membrane is uncoupled.

The derivation of the SD model is given by Lonsdale *et al.* (1965), and subsequently the solvent (J_v) and solute fluxes (J_s), respectively, can be expressed as,

$$J_v = L_p(\Delta P - \Delta\pi) \quad (3-6)$$

$$J_s = (D_{AM} K_m / \delta_m)(C_m - C_p) \quad (3-7)$$

$$J_s = J_v C_p \quad (3-8)$$

where, L_p (l/m².h.bar) is the hydraulic permeability coefficient; ΔP (bar) is the transmembrane pressure; $\Delta\pi$ (bar) is osmotic pressure across the membrane, D_{AM} (m²/s) is the diffusivity of the solute through the membrane, K_m is partition coefficient, δ_m (m) is the effective membrane thickness and $D_{AM} K_m / \delta_m$ (m/s) is a single parameter defined as solute transport parameter.

Based on SD model, differences in the solubilities (partition coefficients) and diffusivities of the solute and solvent in the membrane phase are extremely important since these parameters strongly influence fluxes through the membrane. The real rejection based on the boundary layer concentration is expressed as in Equation (2-8). Combining Equation (2-8) and Equations (3-6) to (3-8), the real rejection for the SD model can be expressed as,

$$\frac{1}{R} = 1 + \left(\frac{L_p}{P_s} \right) \left(\frac{1}{\Delta P - \Delta\pi} \right) \quad (3-9)$$

where P_s (m/s) is equivalent to $D_{AM} K_m / \delta_m$, the solute transport parameter.

The principal advantage of the SD model is that only two parameters (L_p and P_s) are needed to characterize the membrane system. As a result, it has been widely applied to model both inorganic salt and organic solute systems. On the other hand, the restriction of the SD model is that the separation obtained at infinite flux is always equal to 1.0.

However, this limit is not reached for many solutes. For this reason, the SD model is appropriate for solute-solvent-membrane systems where the separation is close to 1.0.

3.3 Porous Model

The models based on irreversible thermodynamics treat the phase-separating membrane as a black box in which relatively slow processes proceed near equilibrium. They give general guidelines for membrane separation and insight into the underlying mechanisms of separation (Spiegler and Kedem, 1966; Soltanieh and Gill, 1981). Spiegler Kedem model is the most popular model that widely used to model porous nanofiltration.

3.3.1 Irreversible Thermodynamics Models

Based on the irreversible thermodynamics (IT) equations given by Kedem Katchalsky, Speigler and Kedem (1966) defined the solvent, J_v and solute, J_s fluxes in differential form as given below (Soltanieh and Gill, 1981):

$$J_v = P_w \left(\frac{dP}{dx} - \sigma \frac{d\pi}{dx} \right) \quad (3-10)$$

$$J_s = P_{so} \frac{dC_M}{dx} + (1 - \sigma) C_M J_v \quad (3-11)$$

where, P_w (l/m.h.bar) is the local water permeability, σ is the reflection coefficient, P_{so} (m^2/s) is the local solute permeability, x is the coordinate direction perpendicular to the membrane and C_M (mg/l) is the solute concentration in the membrane. Equation (3-10) can be integrated over the thickness of the membrane, δ_m to give:

$$J_v = L_p (\Delta P - \sigma \Delta \pi) \quad (3-12)$$

where, $L_p = \frac{P_w}{\delta_m}$.

Equations (3-8) and (3-11) can be combined to give:

$$\frac{dC_M}{dx} = \frac{J_v}{P_{so}} (C_p - (1-\sigma)C_M) \quad (3-13)$$

Equation (3-13) can be integrated over the thickness of the membrane, δ_m and combined with Equation (2-8) to give (Murthy and Gupta, 1999; Ballet *et al.*, 2004):

$$\frac{1}{R} = \frac{1 - \sigma \exp\left(- (1-\sigma) \left(\frac{\delta_m}{P_{so}}\right) J_v\right)}{\sigma \left[1 - \exp\left(- (1-\sigma) \left(\frac{\delta_m}{P_{so}}\right) J_v\right) \right]} \quad (3-14)$$

Equation (3-14) can be further simplified by defining an overall solute permeability, P_m (m/s) as $P_m = P_{so} / \delta_m$. Thus, Equation (3-14) can be expressed as,

$$R = \frac{\sigma \left[1 - \exp\left(- J_v \frac{(1-\sigma)}{P_m}\right) \right]}{1 - \sigma \exp\left(- J_v \frac{(1-\sigma)}{P_m}\right)} \quad (3-15)$$

Equation (3-15) approximates the true rejection of a solute for Spiegler Kedem theory. The equation shows that the true rejection increases with increasing solvent flux and at the limiting case, when $J_v \rightarrow \infty$, the rejection becomes equal to the reflection coefficient, σ which is the limiting retention.

3.4 Present Models

In order to model the separation mechanism for this work, membrane transport models are combined with film theory in order to incorporate the effect of concentration polarization during the separation process. The two models developed for this work, namely combined film theory-solution diffusion (CFSD) and combined film theory-Spiegler Kedem (CFSK) models are discussed below.

3.4.1 Combined film theory-solution diffusion model (CFSD)

In order to incorporate the effect of concentration polarization with the transport equation, the combined film theory-solution diffusion model was selected. The approach is selected to model the AFC99 and to some extent AFC40 membrane processes. Equations (3-8) and (2-8) are inserted into Equation (3-7) in order to correlate the solute transport parameter with the real rejection. The correlation is rearranged to give,

$$\frac{1-R}{R} = \left(\frac{P_s}{J_v} \right) \quad (3-16)$$

The solute transport parameter can be determined by plotting $\frac{1-R}{R}$ versus $\frac{1}{J_v}$. However, the $\frac{1-R}{R}$ cannot be obtained since the real rejection depends on membrane wall concentration, which is not measurable. Alternatively, Equation (3-16) is substituted into Equation (3-4) to give,

$$\frac{1-R_o}{R_o} = \left(\frac{P_s}{J_v} \right) \exp\left(\frac{J_v}{k} \right) \quad (3-17)$$

Equation (3-17) is the working equation of the combined film theory-solution diffusion (CFSD) model (Murthy and Chaudhari, 2009). $\frac{1-R_o}{R_o}$ and J_v can be obtained from the experiment. Hence, the model parameters, namely solute transport parameter, P_s and the boundary layer mass transfer coefficient, k can be estimated by curve fitting method using R_o and J_v .

3.4.2 Combined film theory-Spiegler Kedem model (CFSK)

Similar to CFSD model, CFSK model was also selected in order to incorporate the effect of concentration polarization with the transport equation. The solute transport parameter,

P_m and reflection coefficient, σ can be estimated from Equation (3-15) using curve fitting methods. However, the real rejection, R cannot be obtained experimentally. Thus, the true rejection must be substituted with other experimentally measurable variables in order to estimate the model parameters. Consequently, Equation (3-4) can be inserted into Equation (3-15), and rearranged to give,

$$\frac{1-R_o}{R_o} = \frac{1-\sigma}{\sigma} \left[1 - \exp\left(-J_v \frac{1-\sigma}{P_m}\right) \right]^{-1} \left[\exp\left(\frac{J_v}{k}\right) \right] \quad (3-18)$$

Equation (3-18) is the combined film theory-Spiegler Kedem model (CFSK). CFSK model is capable of modeling highly complex and nonlinear systems for reverse osmosis and nanofiltration membranes, especially for solute-solvent-membrane systems where the convection transport is significant (Spiegler and Kedem, 1966). $\frac{1-R_o}{R_o}$ and J_v can be obtained from the experiment. Hence, the model parameters, namely solute transport parameter, P_m , reflection coefficient, σ and the boundary layer mass transfer coefficient, k can be estimated by curve fitting method using R_o and J_v .

3.4.3 Parameters Estimation

A nonlinear parameter estimation software, namely SigmaPlot (version 6) was used to estimate the membrane transport parameters and mass transfer coefficients from equations (3-17) and (3-18). The data supplied to the nonlinear parameter estimation software were R_o and J_v taken at different operating pressures keeping cross-flow velocity and feed concentration constant for each set of data. The software is based on the Levenberg–Marquardt method, which is widely accepted and used by many researchers (Murthy and Chaudhari, 2009). The Levenberg–Marquardt algorithm estimates the coefficients (parameters) of the independent variable(s) that give the best fit between the modeling equation and the experimental data. The algorithm seeks the values of the

parameters that minimize the sum of the squared differences between the values of the observed and predicted values of the dependent variable as given in the equation below.

$$\sum_{i=1}^n (y_i - \bar{y}_i)^2 \quad (3-19)$$

where, y_i is the observed (experimental rejection) and \bar{y}_i is the value of the predicted dependent variable (calculated rejection).

The algorithm is iterative and it begins with a guess at the parameters, checks to see how well the modeling equation fits, and then continues to make better guesses until the differences between the residual sums of squares no longer decreases significantly. This condition is known as convergence test. The algorithm used to estimate the membrane transport parameters and mass transfer coefficients is shown in Figure 3.3.

CFSD and CFSK models have been used by many researchers in order to estimate the transport parameters and predict the experimental values mathematically (Murthy and Gupta, 1999; Ballet *et al.*, 2004; Murthy and Chaudhari, 2009). Their findings showed the variation of the solute transport parameters from the two models is almost the same whereas, the mass transfer coefficient value can vary significantly. This is due to the presence of the reflection coefficient in the CFSK model. In fact, it may be noted that the CFSK model (Equation (3-18)) can be reduced to the CFSD model (Equation (3-17)) when the reflection coefficient, σ value approaching 1.

Murthy and Gupta (1997) used the published data of Sourirajan (1977) in order to verify the variation in mass transfer coefficient from different models. Their findings showed that the values of k and P_s obtained from CFSD model were nearly the same as those obtained by Sourirajan using Kimura-Sourirajan Analysis (KSA), which is mathematically similar to the solution-diffusion model (Lonsdale *et al.*, 1965). On the other hand, the k values obtained from CFSK model are different from the k values of Sourirajan. The above finding clearly showed that the values of estimated mass transfer coefficients depend on the membrane transport model used in the analysis.

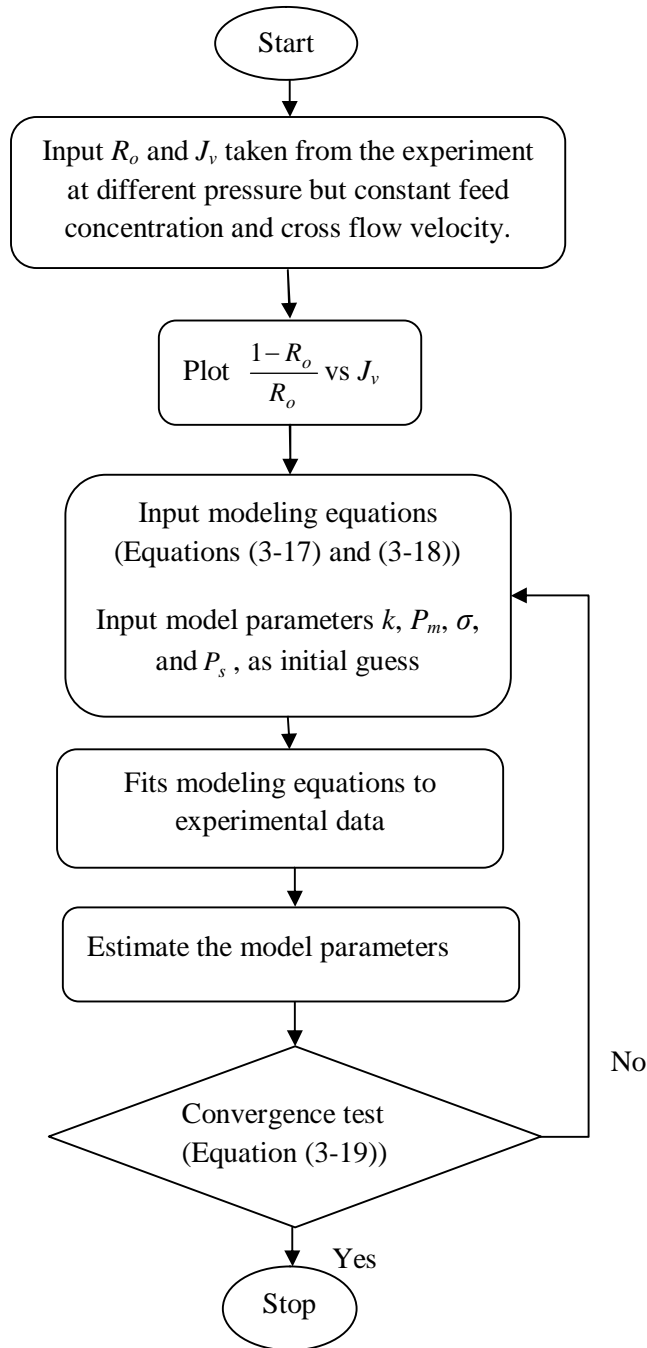


Fig. 3.3: Algorithm used for parameter estimation for CFSD and CFSK models.

Generally, previous studies show that the models predictions are in excellent agreement with the experimental results. Therefore, CFSD and CFSK models are used for the predictions of the experimental rejection values under present study as provided in Chapter 5.

CHAPTER 4

MATERIALS AND METHODS

This chapter describes the materials used and research methodology employed in the study. The experimental study was conducted to determine the pure water permeability, permeate flux and observed rejection of the membranes under the study. The performance of the membranes were investigated with respect to operating pressure, cross-flow velocity, feed concentration and feed pH.

4.1 Materials

4.1.1 Membranes

The membranes used in the experimental study covered three classification of membrane processes including reverse osmosis (RO), nanofiltration (NF) and ultrafiltration (UF). They are tubular membranes and commercially known as AFC99, AFC40 and CA202, respectively. These membranes were purchased from PCI Limited, United Kingdom. They have internal diameter of 12.5 mm, length of 1.2 m and effective membrane surface are of 0.05 m². AFC99 and AFC40 membranes are thin film composite membranes made from polyamide, whereas CA202 is made from cellulose acetate. Table 4.1 summarizes the important characteristics of the membranes.

Table 4.1: Properties of AFC99, AFC40 and CA202 membranes
(PCI membrane user manual).

Membrane type	Reverse osmosis AFC99	Nanofiltration AFC40	Ultrafiltration CA202
Material	Thin film Polyamide	Thin film Polyamide	Cellulose acetate
Recommended maximum pressure (bar)	64	60	25
Maximum Temperature, (°C)	80	60	30
Apparent retention character	99% NaCl	60% CaCl ₂	2,000 MWCO

4.1.2 Chemicals

4.1.2.1 Amines

Three different amines were used for preparation of the artificial wastewater under the study. These amines are monoethanolamine (MEA), diethanolamine (DEA), and methyldiethanolamine (MDEA). MEA and DEA were obtained from R&M chemicals, whereas MDEA was obtained from MERCK. All amines under the study had purity of >98%. The physical properties of the amines under the study are given in Appendix C.

4.1.2.2 COD Reagent

Potassium dichromate is used as an oxidizing agent in order to oxidize the amines in the feed and treated wastewater. The dichromate oxidant is preferred compared to other oxidants (e.g. potassium permanganate) because of its superior oxidizing ability, applicability to a wide variety of samples and ease of manipulation.

4.1.2.3 Hydrochloric acid

The pH of the prepared artificial amines wastewater was alkali in nature and it varied in the range from 10 to 12. Thus, hydrochloric acid (36%) was used in order to adjust the pH of the artificial wastewater in order to investigate its effect on the membranes performance. The pH was measured using Mettler Toledo 320 pH meter.

4.1.3 Deionised Water

Deionised water was used for all experimental work, including for cleaning of the membranes, preparing the amine solution as well as for dilution of the treated water and preparation of the blank reagent for COD analysis.

4.1.4 Artificial wastewater

Artificial amine wastewater was used to study flux and rejection characteristics of amines for the three membranes under the study. The artificial wastewater was prepared by diluting different amounts of MEA, DEA and MDEA in deionised water. The range of concentrations of the feed synthetic wastewater under the study was from 5000 to 15000 mg/l.

4.2 Method

4.2.1 Experimental Set-up

A Membrane Test Unit, TR 08 from Solution Engineering, was used for conducting the permeation and filtration experiments under the study. Figure 4.1 shows the schematic diagram of the Test Unit.

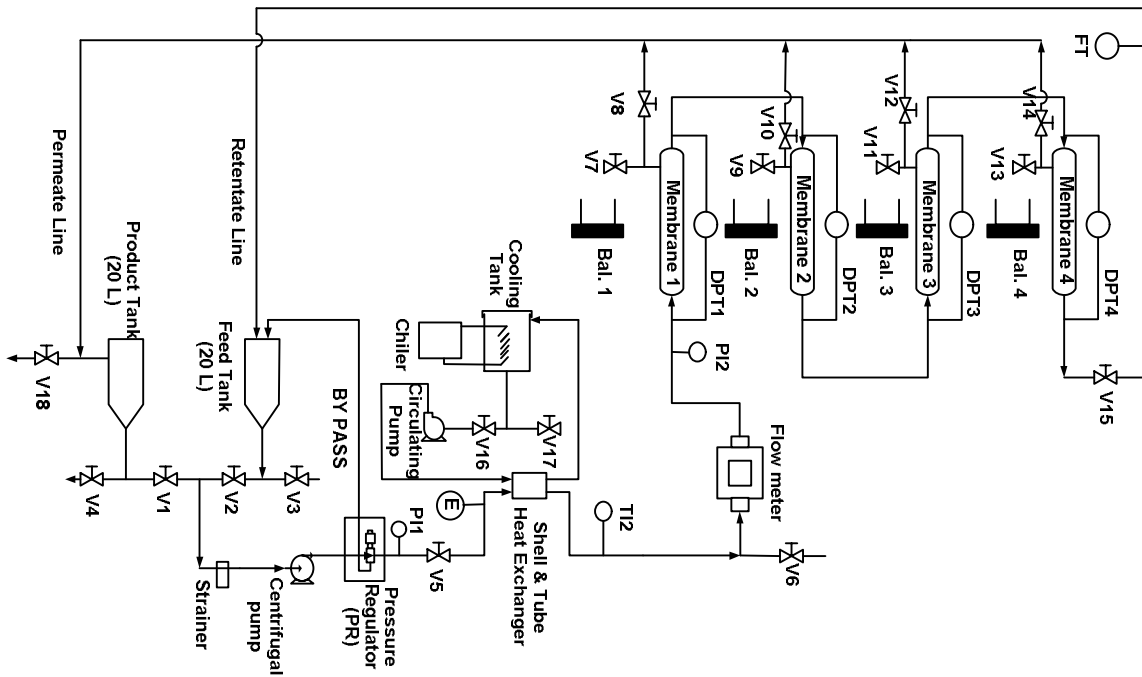


Fig. 4.1: Schematic diagram of the Membrane test unit (PCI membrane user manual).

The system is in a cross-flow configuration where the feed solution is pumped to four parallel tubular membranes simultaneously. The unit is supplied with a feed tank and a product tank, each having a maximum capacity of 20 liters. The feed line is equipped with a unit of shell and tube heat exchanger in order to control the temperature of the fluid entering to the membranes. The cooling system uses ammonia as a chiller. The test unit has also two pumps, centrifugal and triple plunger pumps. The centrifugal pump is used to circulate cooling water from the heat exchanger to the cooling water tank, whereas the triple plunger pump is used to pump the feed stream from the feed tank into the tubular membrane module. This plunger pump is capable of delivering pressure up to 60 bar. Pressure regulator, flow meters and temperature sensors are also installed in order to regulate the operating pressure, cross-flow velocity and temperature of the feed and retentate streams. The system is also supplied with four units of electronic balances to weigh the permeate automatically using a computer with respect to time.

4.2.2 Experimental Procedure

4.2.2.1 Membrane Pretreatment

Before the water flux study was carried out, the membranes were stabilized at 25 bar for 10 hrs in order to offset membrane compaction, which leads to reduction in permeability during the experiment.

4.2.2.2 Flux Study

a. Water Flux Study

The pure water permeation was studied using deionised water under different operating pressures. The range of operating pressure was varied between 4 and 24 bars for each membrane under the study. The volume of permeate collected versus time was recorded online for the four membrane modules, simultaneously. The pure water permeability (PWP ($l/m^2 \cdot h \cdot bar$)) of each membrane type was determined by taking the slope of pure water flux versus pressure graph.

b. Permeate Flux Study

The experiments to study the permeate fluxes were carried out at different operating conditions: (i) feed concentrations (5000, 10000 and 15000 mg/l); (ii) cross-flow velocity (1.5, 3, 4.5, and 6 l/min); (iii) feed pH (3 and 8); and (iv) operating pressures (4, 8, 12, 16, 20 and 24 bar). The feed temperature was maintained constant at 25 ± 1 °C for all experiments by means of a temperature controller. The system was operated in batch circulation mode. Consequently, both permeate and retentate (concentrated) streams were returned back to the feed vessel (except during sample collection for analyses) in order to maintain constant bulk concentration. Sufficient time was given (usually an hour) for the process to reach steady state before collecting the permeate sample for every change in the operating conditions. The permeate from the membrane modules was collected into bottles mounted on the four electronic balances. The volume of permeate collected versus

time was recorded online for the four membrane modules, simultaneously. These data were used for calculation of the permeate flux. Both the water and permeate flux were calculated using equation (2-5).

4.2.2.3 Rejection Study

This study was conducted to evaluate observed rejection characteristics of the three membranes using artificial amine wastewater. The same procedure was followed as Section 4.2.2.1 part (b) in order to collect the permeate sample for rejection study. The concentration of the bulk artificial wastewater and the permeate were determined using HACH Spectrophotometer, at 620nm. Then, the observed rejection of the membranes was calculated using Equation (2-7).

4.3 Analysis

Two milliliter of the permeate samples from each membrane modules that were collected during the permeate flux study were taken and mixed with the COD reagent for observed rejection study. The mixed samples were heated in a thermoreactor at 150°C for two hours. The bulk and permeate concentration of the samples were measured using HACH DR5000 Spectrophotometer based on dichromate standard procedure at a wave length of 620 nm. A blank sample prepared by mixing 2 milliliter of deionised water with the COD reagent was used to calibrate the spectrophotometer. The overall procedure of the experimental study is given in the figure shown below.

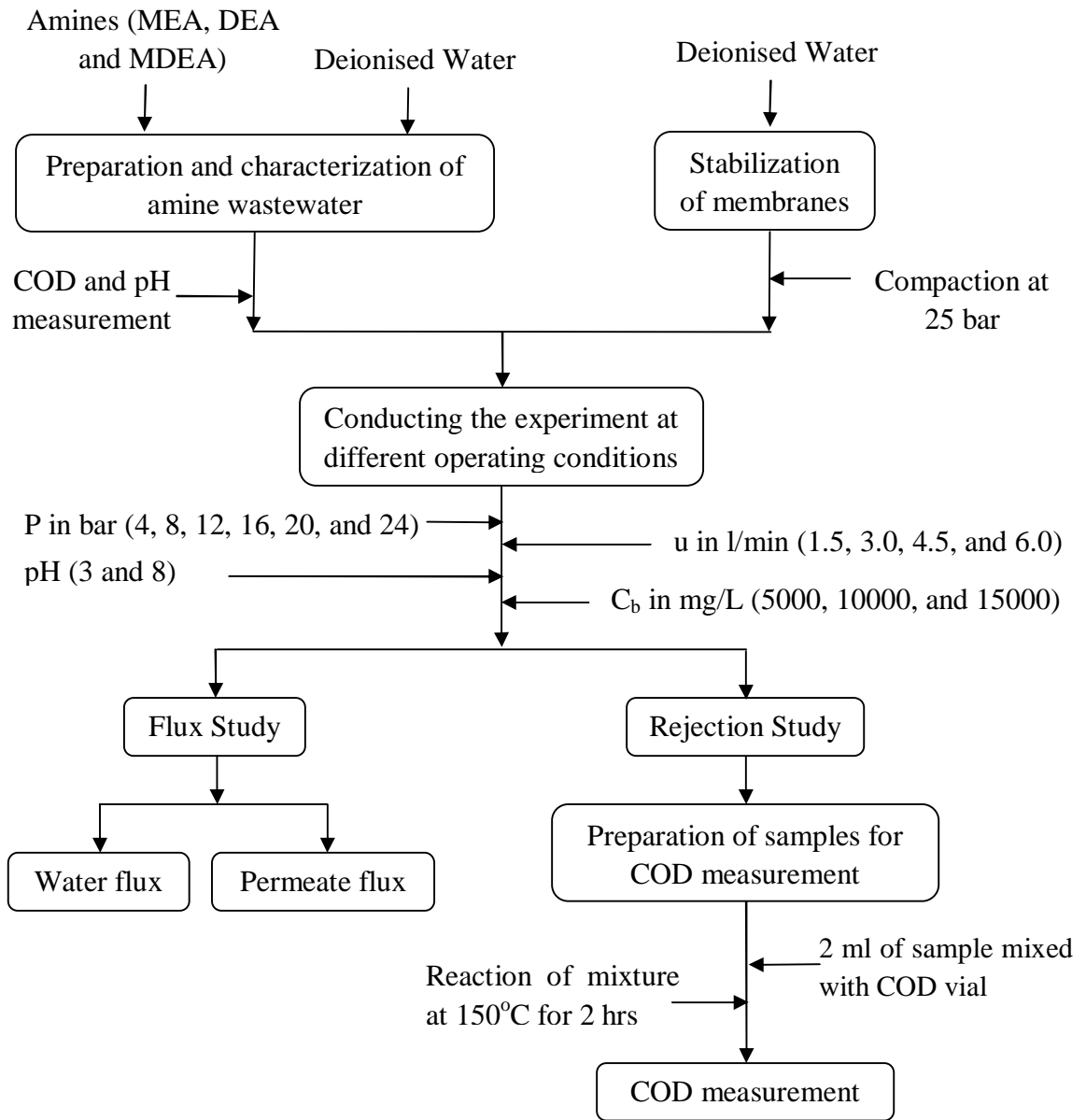


Fig. 4.2: Experimental flow diagram.

CHAPTER 5

RESULTS AND DISCUSSION

This chapter is divided into two main sections, which provide the experimental and modeling results. The experimental section discusses about the membranes' performance in separating the artificial amines wastewater with respect to membrane and solute types, operating pressure, cross-flow velocity, feed concentration and feed pH. The modeling section discusses about membrane transport parameters, i.e. solute transport parameter and reflection coefficient and mass transfer coefficient. Two transport models, namely combined film theory-solution diffusion (CFSD) model and combined film theory-Speigler Kedem (CFSK) model were used to estimate the membrane transport parameters and predict their performances.

5.1 Experimental Result

5.1.1 Wastewater Characterization

Table 5.1 shows the characteristic of artificial amine wastewater in terms of chemical oxygen demand (COD) and pH. Both properties form the critical characteristic of the artificial amine wastewater. Results showed that as the concentration of amines increased, the COD has also increased as shown in Table 5.1. This is understood due to the presence of more pollutants in the artificial wastewater (Fürhacker *et al.*, 2003; Isa *et al.*, 2005). The higher amount of pollutants in the wastewater results in consumption of more dissolved oxygen during the oxidation reaction. Hence, the oxygen demand required to oxidize the wastewater increases with increase in concentration. It was also

found that the concentration of COD was dependent on the type of amine present. For example, for the same concentration of amines, the COD for MDEA was found to be the highest followed by DEA and MEA, respectively. This is due to the increase in the oxygen equivalent of the organic matter of the amines, which is associated with weight of the alkyl substituent attached to the nitrogen atom (Rooney *et al.*, 1998). These alkyl substituent of the amines are $\text{OHCH}_2\text{CH}_2-$, $(\text{OHCH}_2\text{CH}_2)_2-$ and $\text{CH}_3(\text{CH}_2\text{CH}_2\text{OH})_2-$ for MEA, DEA and MDEA, respectively. Hence, the COD of the samples increases with the molecular weight of the amines under the study.

Table 5.1: Characteristic of artificial amines wastewater in term of COD and pH.

Concentration (mg/l)	Monoethanolamine (MEA)		Diethanolamine (DEA)		Methyldiethanolamine (MDEA)	
	COD (mg/l)	pH	COD (mg/l)	pH	COD (mg/l)	pH
1500	1982	11.00	2355	10.62	2580	10.46
3500	4625	11.17	5425	10.80	6020	10.63
6000	7930	11.29	9215	10.91	10325	10.75
9000	11890	11.38	13825	10.99	15480	10.83
12000	15855	11.44	18430	11.05	20650	10.89
15000	19820	11.49	23440	11.09	25810	10.94

Table 5.1 also shows that the pH of the artificial wastewaters increased with increasing in concentration of amines. The pH was found to be in the range between 10 and 12 for all types of amine solutions under the study. For any given concentration of the amines, the highest pH value was observed for MEA followed by DEA and MDEA, respectively. This is due to the effect of steric hindrance offered by the alkyl substituents on the nitrogen atom and the degree of solvation of the protonated amines (Zemaitis *et al.*, 1986). The solvation energy increases with the number of hydrogen bonding of the

protonated amines, which are 1, 2 and 3 for MDEA (R_3NH^+), DEA ($R_2NH_2^+$) and MEA (RNH_3^+), respectively. In addition, there is also a decrease in solvation energy from MEA to MDEA due to the steric hindrance offered by the increased number of the alkyl substituents to the approaching proton. Thus, MEA exhibited the highest pH value followed by DEA and MDEA, respectively.

5.1.2 Permeability Study

5.1.2.1 Water Flux

Figure 5.1 shows the water flux against operating pressure for the three membranes under the study. Results show that the water flux increased linearly with respect to the operating pressure. It is understood that the increment of the operating pressure has increased the driving force, hence increasing the permeate flux. These results also show that there are no sign of membranes compaction occurred within the range of operating pressure.

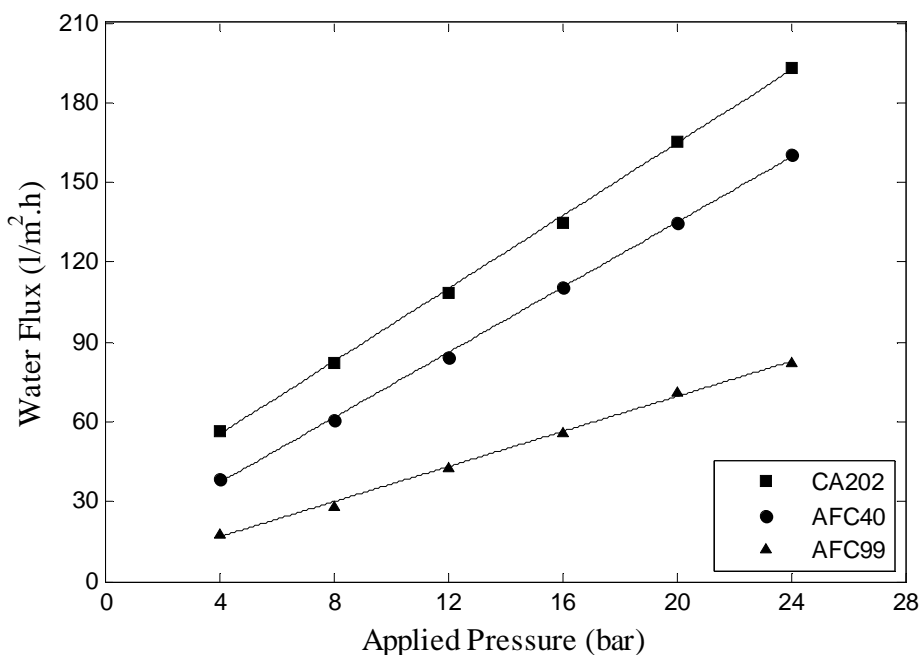


Fig. 5.1 : Effect of operating pressure on pure water permeability across different type of membranes.

It was found that the water flux of CA202 membrane was the highest followed by AFC40 and AFC99 membranes, respectively. This is attributed to the difference in the pore sizes of the membranes as CA202 is the UF membrane, while AFC40 is the NF membrane and AFC99 is the RO membrane. Studies show that membranes with lowest pore size like AFC 99 would give the highest resistance for the solvent (water) transportation across the membrane (Baker, 2004). Under present study, CA202 has the largest pore size as compared with very tight pore size for AFC40 or non-pore for AFC99 membranes. Hence, CA202 exhibited the highest amount of water flux. On the other hand, AFC99 exhibited the lowest water flux since the mechanism of transport depends on diffusion which is a slow process as compared to convection transport through membrane pores (Paul, 2004; Greenleea *et al.*, 2009).

5.1.2.2 Permeate Flux

Membrane filtration experiments were performed to determine the permeate flux and observed rejection characteristics under different operating conditions, including operating pressure, cross-flow velocity, feed concentration and feed pH for different types of amines such as monoethanolamine (MEA), diethanolamine (DEA) and methyldiethanolamine (MDEA).

a. Effect of Membranes Type on Permeate Flux

Figures 5.2 to 5.4 show the permeate flux for AFC99, AFC40 and CA202 membranes under different operating pressure conditions for MEA, DEA and MDEA solutions. As expected, the figures show that the permeate flux increases linearly with increases in operating pressure for all the membranes. As explained earlier, increasing the operating pressure would increase the net pressure as well, hence increases the permeate flux.

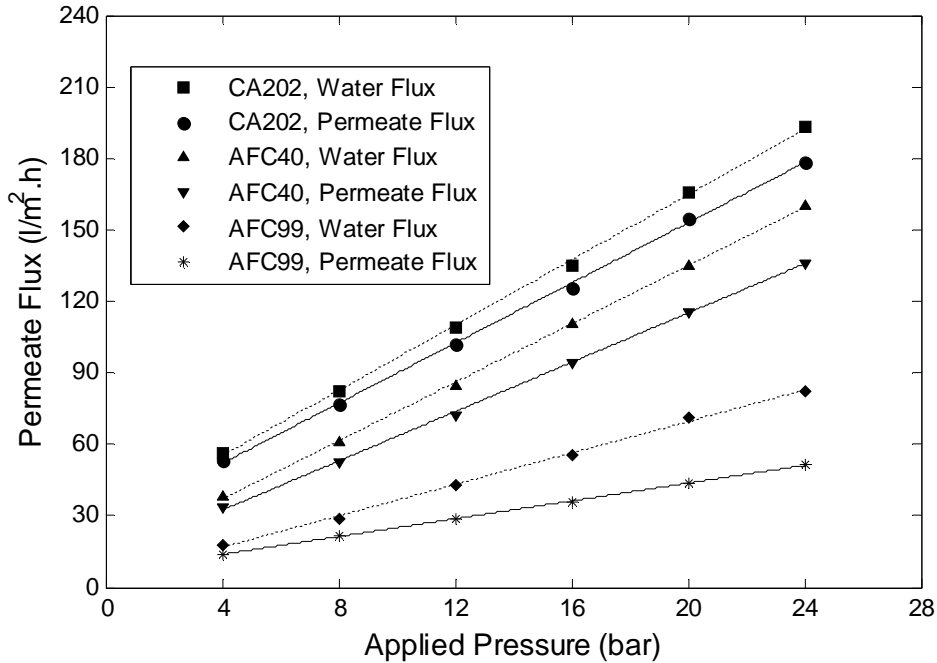


Fig. 5.2 : Effect of operating pressure on MEA solutions and water flux across various membranes ($C_b=5000$ mg/l, $u=6$ l/min and pH=8).

As discussed earlier in Section 5.1.2.1, the same sequential trend was also found for the permeate flux of the three membranes. It was also found that the permeate flux of the amine solutions for all membranes was lower as compared with permeate flux for pure water. This is due to the presence of osmotic pressure in the amine solutions which reduce the net driving pressure, hence reduces the permeate flux. In addition, the presence of solutes on the membrane surface increases the overall membrane resistance due to concentration polarization, hence reduces the permeate flux (Baker, 2004; Greenleea *et al.*, 2009). Thus, Figures 5.3 to 5.5 strongly indicate that both phenomena are present on the three membranes under the study.

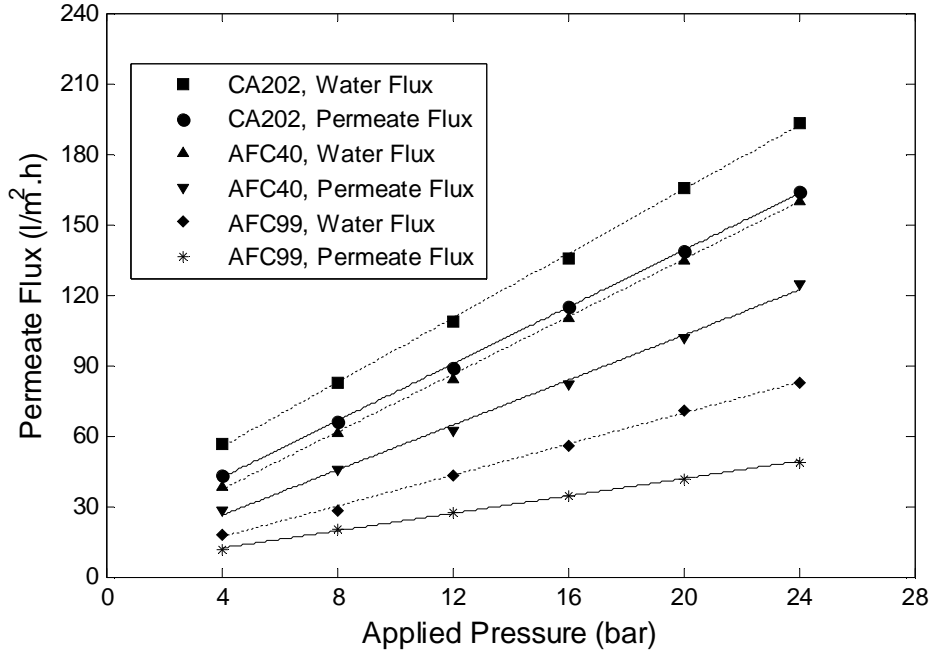


Fig. 5.3: Effect of operating pressure on DEA solutions and water flux across various membranes ($C_b=5000$ mg/l, $u=6$ l/min and pH=8).

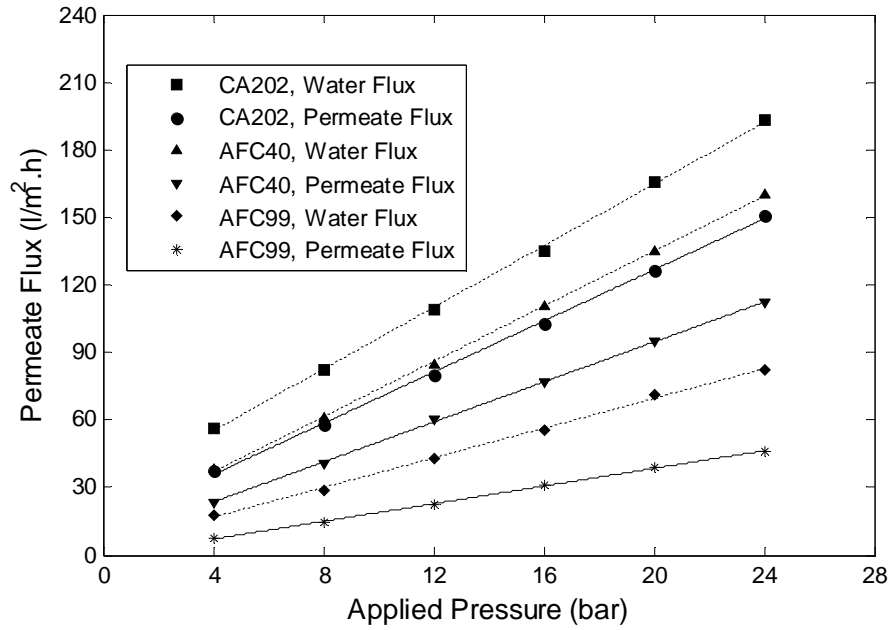


Fig. 5.4: Effect of operating pressure on MDEA solutions and water flux across various membranes ($C_b=5000$ mg/l, $u=6$ l/min and pH=8).

b. Effect of Amine Molecular Weight on Permeate Flux

Figure 5.5 shows the effect of amine molecular weight on permeate flux of the amines under the study across AFC99 membrane. The results show that the permeate flux of MEA solution gives the highest permeate flux followed by DEA and MDEA solutions, respectively. This is due to the difference in molecular weight of the amines. The smallest molecular weight of MEA with 61.0 g/mol could allow it to move faster with high flux as compared to DEA with molecular weight of 105.14 g/mol and MDEA with molecular weight of 119.16 g/mol. Higher molecular weight substances may diffuse through the membrane at a slower rate due to an increase in the pore resistance resulting in lower permeate flux (Ozaki and Li, 2002).

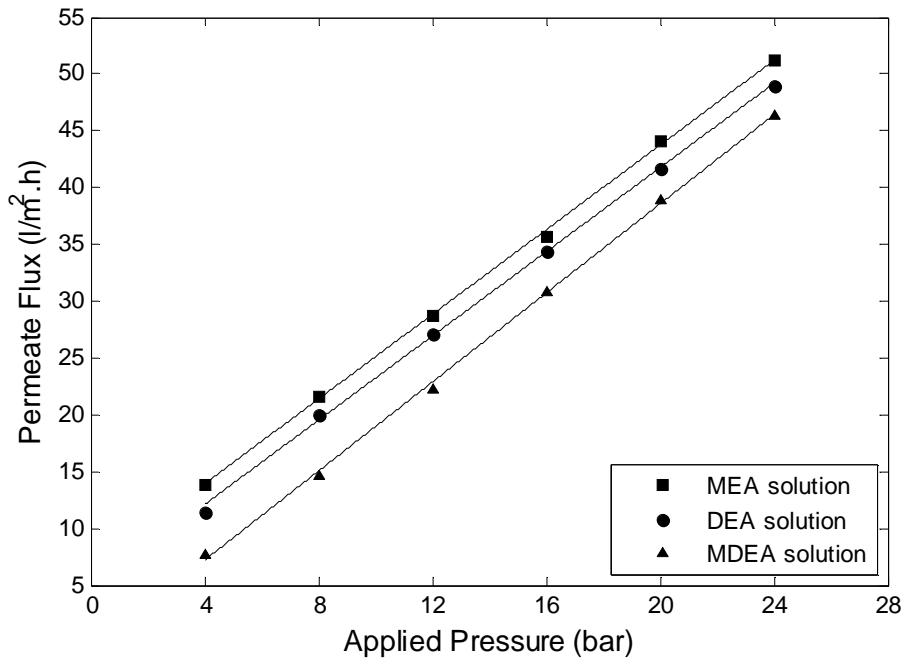


Fig. 5.5: Effect of amine molecular weight on permeate flux across AFC99 membrane ($C_b=5000$ mg/l, $u=6$ l/min and pH=8).

Similar trend was also observed for the permeate flux of AFC40 and CA202 membranes and the results are given in the Appendix A, Figures A.1 and A.2.

c. Effect of Cross-flow Velocity on Permeate Flux

Figures 5.6 to 5.8 show the effect of cross-flow velocity on permeate flux of MEA solution across AFC99, AFC40 and CA202 membranes, respectively. Results show that the permeate flux increases with increasing in cross-flow velocity for the range of operating conditions. This is because the increase in the cross-flow velocity can increase the mass transfer coefficient at the boundary layer, and subsequently increases the permeate flux (Murthy and Gupta, 1997; Damak *et al.*, 2004). Similar trend was also observed for the permeate flux of DEA and MDEA solutions as given in the Appendix B, from Figures B.1 to B.6.

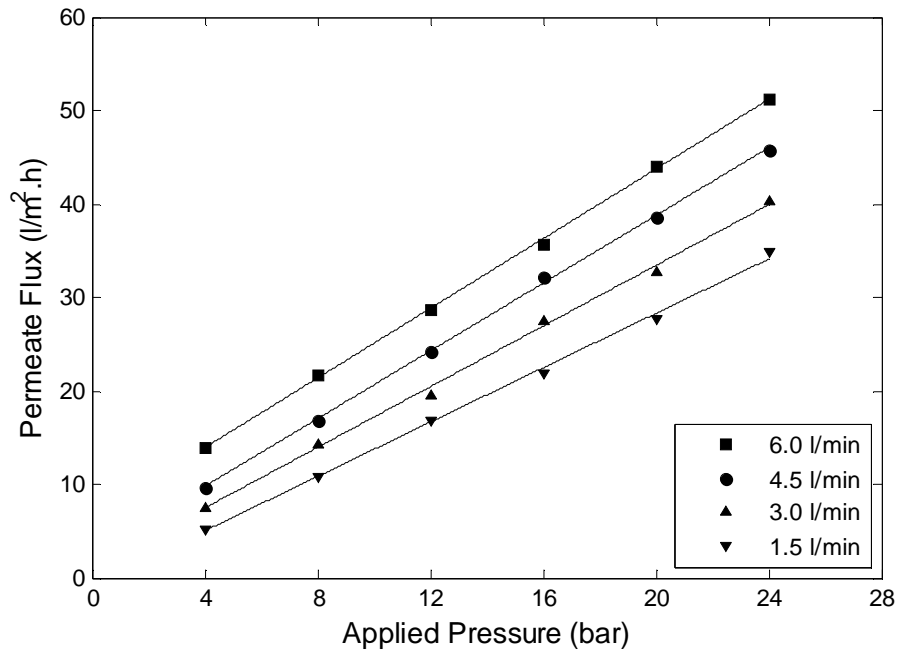


Fig. 5.6: Effect of cross-flow velocity on MEA permeate flux across AFC99 membrane ($C_b=5000$ mg/l and pH=8).

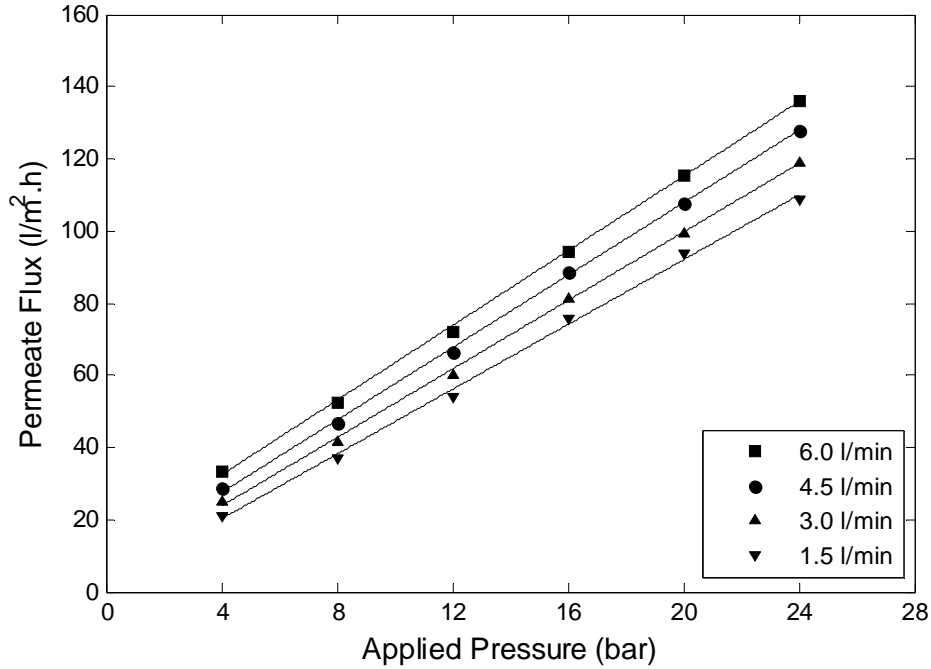


Fig. 5.7: Effect of cross-flow velocity on MEA permeate flux across AFC40 membrane ($C_b=5000$ mg/l and pH=8).

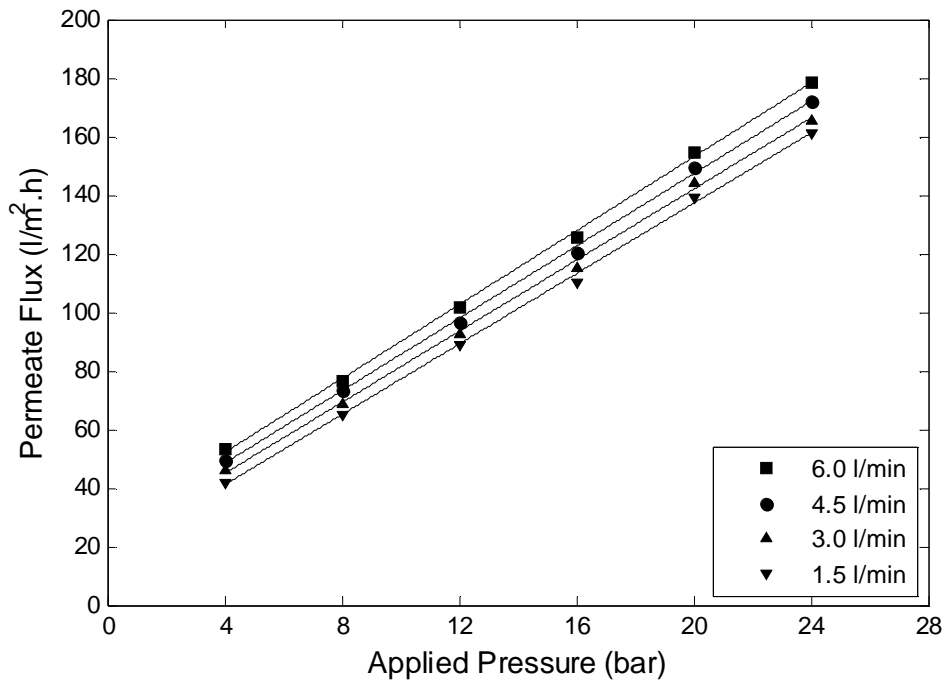


Fig. 5.8: Effect of cross-flow velocity on MEA permeate flux across CA202 membrane ($C_b=5000$ mg/l and pH=8).

Under present study, the AFC99 and AFC40 membranes reject more solutes, as a result they can develop significant concentration polarization layer as compared to CA202 membrane (Damak *et al.*, 2004). Hence, the increase in the cross-flow velocity can give considerable flux improvement for AFC99 followed by AFC40 and CA202 membranes, respectively as shown on Figures 5.7 to 5.9. Under higher cross-flow velocity, the investigation shows that the permeate fluxes of MEA solutions across the AFC99, AFC40 and CA202 membranes increase by 32.0%, 20.26% and 9.52%, respectively, whereas the permeate fluxes of DEA solutions increase by 29.65%, 20.61% and 9.66% across the AFC99, AFC40 and CA202 membranes, respectively. The findings also show that the permeate fluxes of MDEA solutions across the AFC99, AFC40 and CA202 membranes increase by 28.46%, 18.89% and 8.09%, respectively.

d. Effect of Feed Concentration on Permeate Flux

Figures 5.9 to 5.11 show the effect of feed concentration on MEA, DEA and MDEA permeate fluxes at different operating pressure across different membranes. Results show that the permeate flux decreases as the concentration of the feed increases. Increasing the feed concentration effectively increases the osmotic pressure in the solution and also increases the overall membrane resistance. As the result, it reduces the net driving force which causes reduction in the permeate flux of the amines (Baker, 2004).

The investigation shows that the permeate fluxes of the MEA solution across AFC99, AFC40 and CA202 membranes decreases by 29.18%, 19.19% and 6.96%, respectively when the feed concentration increases from 5000 to 15000 mg/l. For DEA solutions, the permeate flux has decreased by 34.72%, 22.61% and 8.32% across AFC99, AFC40 and CA202, respectively. In addition, 35.42%, 19.74% and 7.70% of reductions in permeate fluxes of MDEA solutions were observed across AFC99, AFC40 and CA202 membranes, respectively.

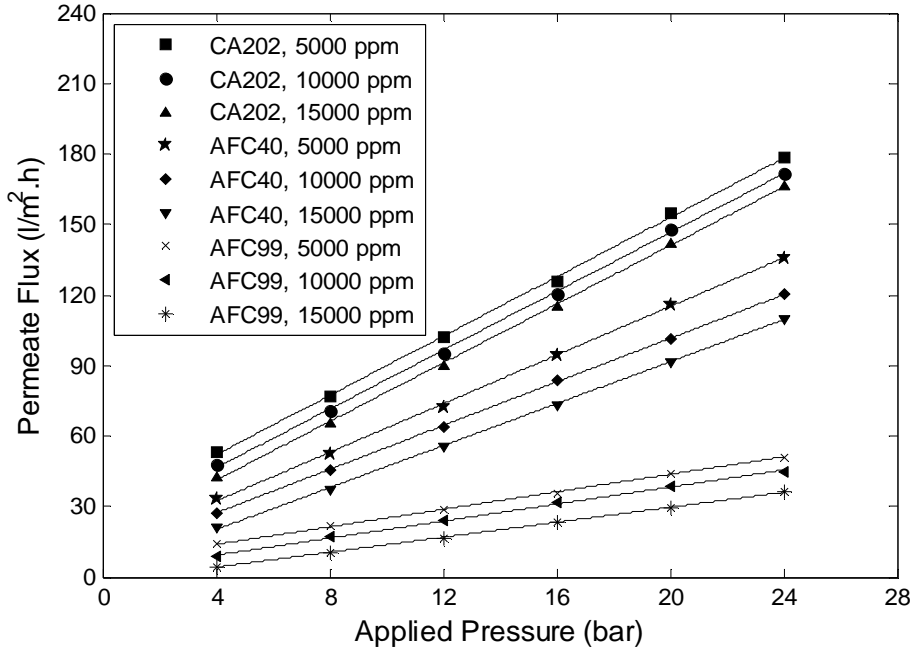


Fig. 5.9: Effect of feed concentration on MEA permeate flux across various membranes ($u=6$ l/min and $pH=8$).

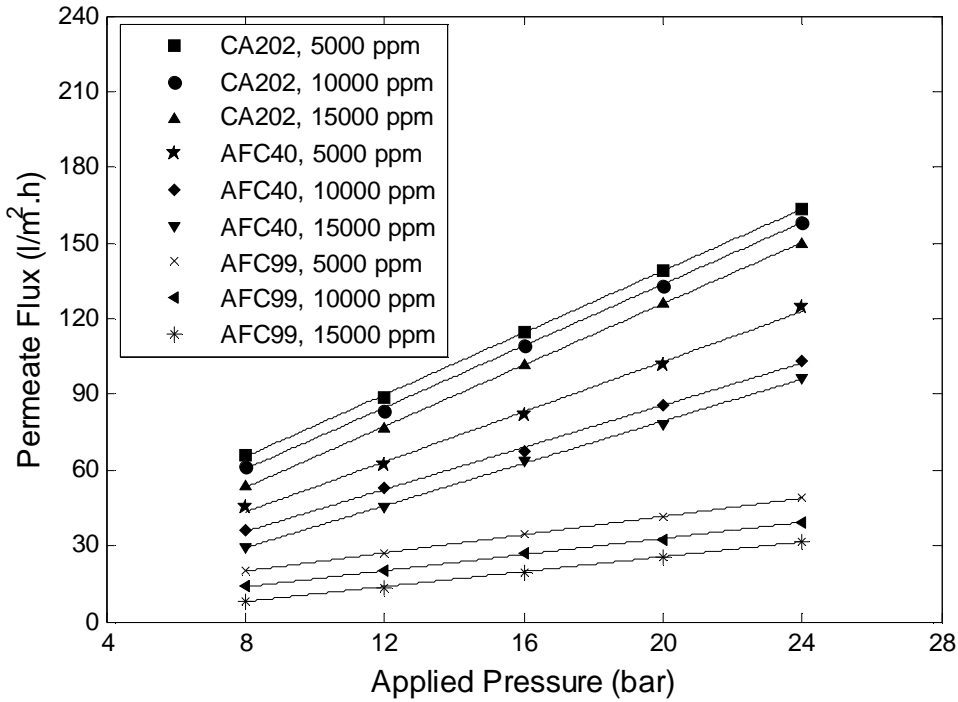


Fig. 5.10: Effect of feed concentration on DEA permeate flux across various membranes ($u=6$ l/min and $pH=8$).

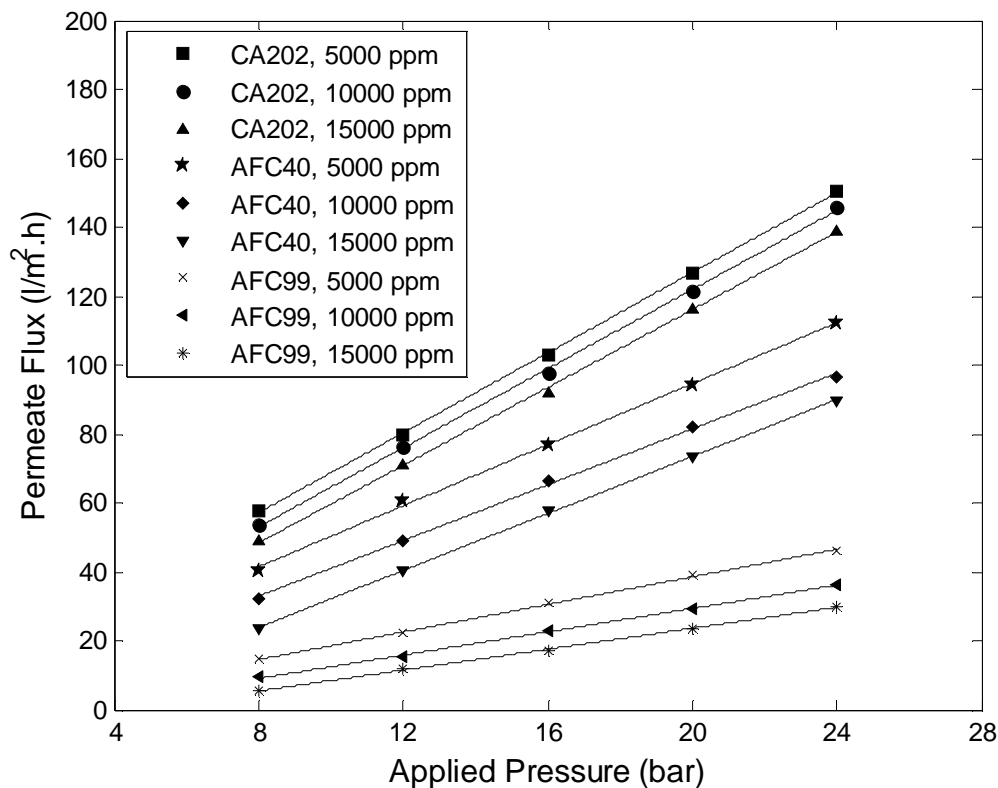


Fig. 5.11: Effect of feed concentration on MDEA permeate flux across various membranes ($u=6$ l/min and $\text{pH}=8$).

Table 5.2 summarizes the percentage reduction of permeate fluxes of MEA, DEA and MDEA solutions against concentration and type of membrane, in comparison with the permeate of water flux. The table shows that the permeate flux reduction is highest for AFC99 followed by AFC40 and CA202, respectively. In addition, the reduction of the permeate fluxes increased with increase in the molecular weight of the amines.

Table 5.2: Percentage reduction of permeate fluxes of the amines.

Change in concentration	% reduction of MEA permeate flux			% reduction of DEA permeate flux			% reduction of MDEA permeate flux		
	Across AFC99	Across AFC40	Across CA202	Across AFC99	Across AFC40	Across CA202	Across AFC99	Across AFC40	Across CA202
Water as compared to 5000 mg/l feed solution	37.78	15.06	7.12	40.53	22.28	15.29	43.67	30.12	22.00
Water as compared to 15000 mg/l feed solution	55.93	31.36	13.92	61.18	39.86	22.34	63.62	43.91	28.00
5000 mg/l as compared to 15000 mg/l feed solution	29.18	19.19	6.96	34.72	22.61	8.32	35.42	19.74	7.70

e. Effect of pH on Permeate Flux

Figures 5.12 to 5.14 show the effect of feed pH on permeate flux against operating pressure for MEA, DEA and MDEA solutions across AFC99, AFC40 and CA202 membranes. The results show that the membranes exhibited different behavior as the pH reduces from 8 to 3 as shown in the figures. It is observed that the permeate flux increased for AFC99 membrane, whereas decreased for AFC40 and CA202 membranes as the pH decreases from 8 to 3.

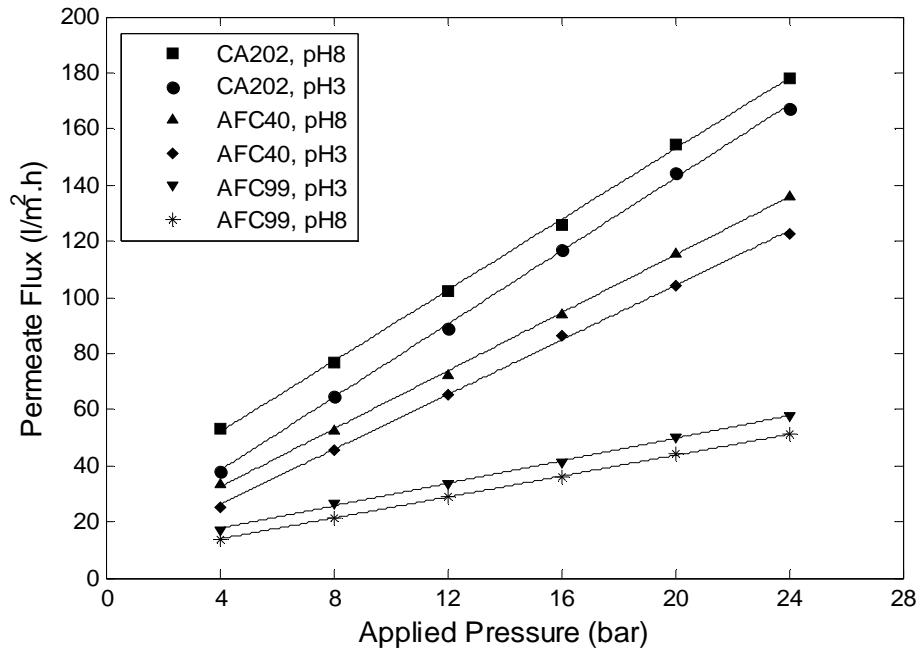


Fig. 5.12: Effect of feed pH on MEA permeate flux across various membranes ($C_b=5000$ mg/l and $u=6$ l/min).

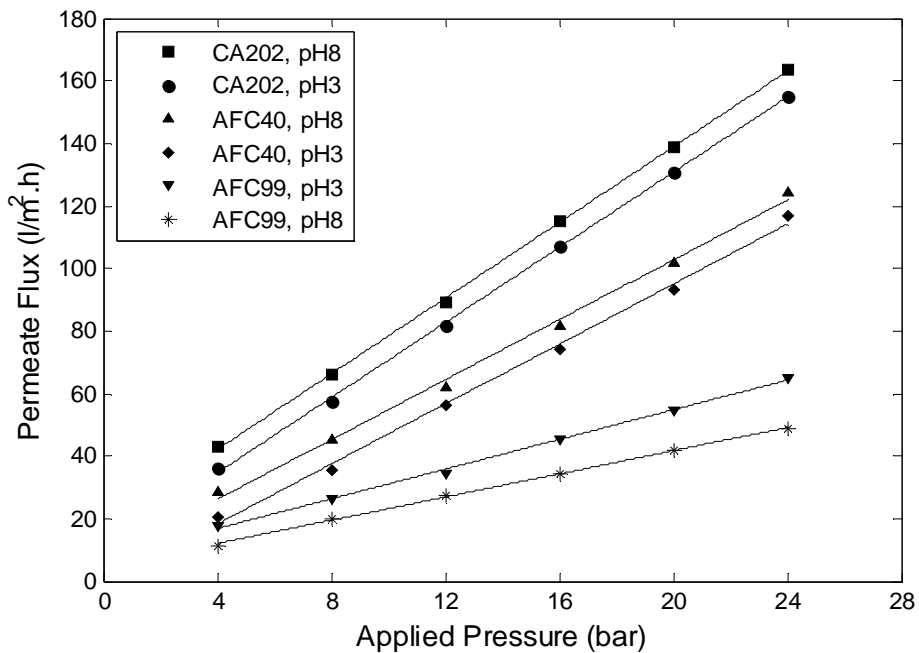


Fig. 5.13: Effect of feed pH on DEA permeate flux across various membranes ($C_b=5000$ mg/l and $u=6$ l/min).

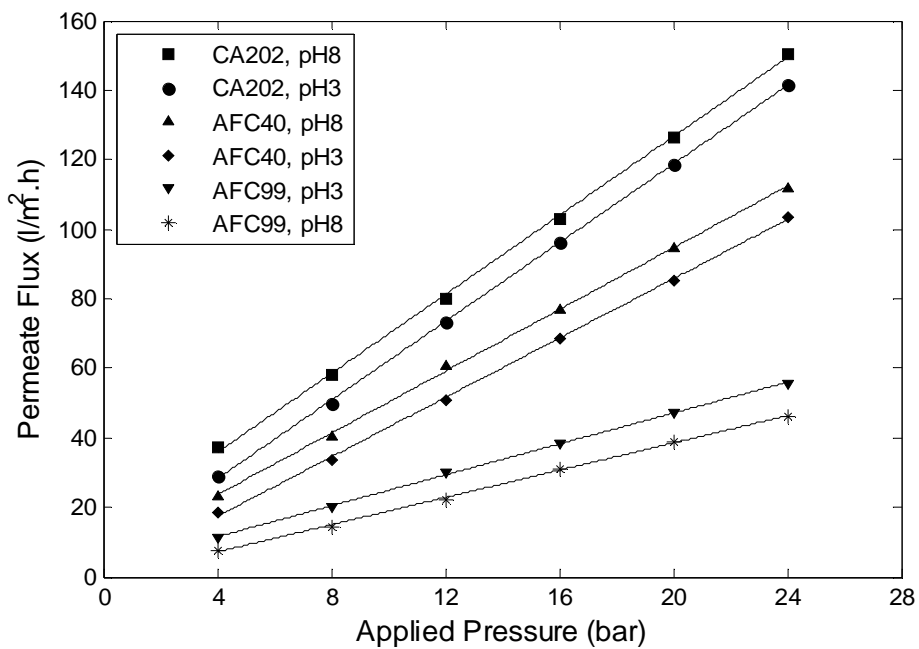


Fig. 5.14: Effect of feed pH on MDEA permeate flux across various membranes ($C_b=5000$ mg/l and $u=6$ l/min).

The effect of pH on membrane performance can be explained by the surface chemistry of the membranes such as the presence of dissociable functional groups, the degree of their dissociability and the orientation of the functional groups (Zydney and Zeman, 1996). Several researchers discussed the presence of excess carboxylic and amine functional groups at the surface of thin film composite polyamide membranes, which give them either positive or negative surface charge depending on the pH of the surrounding medium (Freger *et al.*, 2002; Freger and Srebnik, 2003; Manttari *et al.*, 2006; Hurwitz *et al.*, 2010; Lee *et al.*, 2010). The positive surface charge is due to the protonation of the amine functional groups in strongly acidic medium, and the negative charge is due to deprotonation of the carboxylic groups in alkaline medium (Chung *et al.*, 2005; Liu *et al.*, 2008). In both cases, the electrostatic repulsion between the charged groups would cause an increase in pore size or free volumes between the polymer chains of the membranes, resulting in permeate flux increase (Manttari *et al.*, 2006). However, the orientation of the functional groups affect the response of the membranes as the pH varies.

The results show that higher permeate flux was obtained for AFC40 membrane at high pH value. This could be attributed to the high density of carboxylic functional groups at the surface of AFC40 membrane (Van der Bruggen *et al.*, 1999). Thus, the membrane would be negatively charged in the neutral pH region and the effective charge density increases at higher pH (Freger *et al.*, 2002). Therefore, charge repulsion among the carboxylic functional groups make the membrane more loose, resulting in an increase in the permeate flux. The permeate flux of AFC99 membrane, on the other hand, increases when the pH decreases from 8 to 3. This could be attributed to the presence of high amine functional group at the outer most active layer of the membrane. Thus, as the pH of the surrounding medium becomes strongly acidic, the amine functional groups easily protonated and the effective charge density increase when the pH further decreases. Hence, the repulsion between the amine functional groups would be strong at lower pH and results in a more loose surface structure. Hence, the permeate flux increases. This difference in permeate flux characteristics of polyamide RO and NF membranes could be attributed to the different types of monomers and solvents used during

fabrication of the membranes, as it is discussed by Freger *et al.*, 2002. The ATR-FTIR study of the researchers on polyamide RO and NF exhibited different spectra characteristics due to the different types of amine monomers used for the reaction. Ghosh *et al.* (2008) also discussed that selecting the organic solvent is also critical for morphology of the thin film since it governs the solubility and diffusivity of the amine monomer in the reaction zone during the interfacial polymerization. In addition, AFC99 and AFC40 membranes also have different hydrophilicities, which could result in different permeability behavior of the membranes (PCI membrane user manual).

The study also shows that the permeate of CA202 membrane increases as the surrounding pH increases. The streaming potential study by Arkhangelsky *et al.*, (2008) showed that the effective surface charge density of cellulose acetate membrane was about 5 mV at pH 3 and -16 mV at pH 8. Thus, due to the higher surface charge density at pH 8 there would be greater repulsion between the functional groups resulting in wider pores. Hence, the permeate flux increases with increases in pH.

5.1.3 Rejection Study

a. Effect of Operating Pressure on Observed Rejection

Figures 5.15 to 5.17 show the effect of operating pressure on observed rejection of MEA, DEA and MDEA across AFC99, AFC40 and CA202 membranes. The observed rejections of the amines across the membranes were found to increase as the operating pressure increases.

Generally, in pressure driven membrane processes, the water flux is proportional to the operating pressure, but the solute flux is independent of operating pressure (Baker, 2004). Thus, as the operating pressure increases the solute passage is increasingly overcome as solvent (water) is pushed through the membrane at a faster rate than solute

can be transported. This means that the membrane becomes more selective as the pressure increases, hence the observed rejection increases.

The findings show that AFC99 membrane is the most effective membrane followed by AFC40 and CA202 membranes, respectively. Generally, AFC99 membrane has achieved the highest rejection efficiency (above 96%) for all the amines under the study. The observed rejection of the amines across AFC40 and CA202 membranes was also found to increase with operating pressure and reaches a plateau region at higher operating pressure. The AFC40 and CA202 membranes exhibited the highest rejection efficiency up to 59% and 26%, respectively at pH8 for the range of operating pressure in MEA solution. The highest rejection of DEA and MDEA by AFC40 was found to be 65.9 % and 72.8 %, respectively. However, the rejection of DEA and MDEA by CA202 was found to be much lower, i.e. 33.3% and 35.3%, respectively. This is due to the difference in the membranes pore size. AFC99 membrane has a tight or pore less structure and hence, the mechanism of solute transport is only due to diffusion. AFC40 and CA202, on the other hand, have relatively loose and porous structure, hence there would also be convection transport of solutes through the membranes pores which results in higher permeate concentration and lower rejection efficiency (Jude and Jefferson, 2003; Baker, 2004).

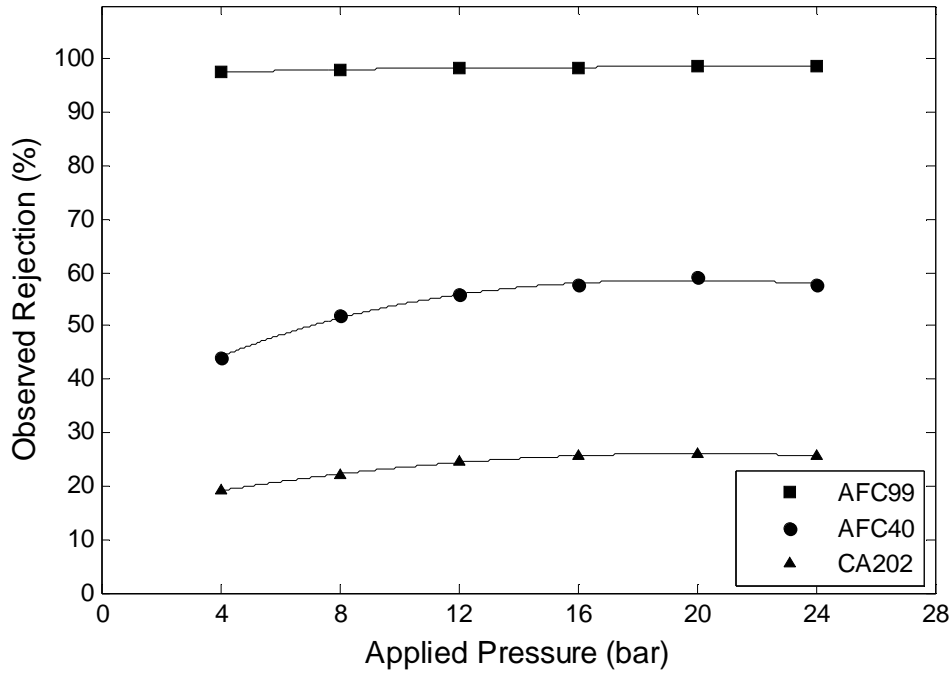


Fig. 5.15: Effect of operating pressure on observed rejection of MEA across various membranes ($C_b=5000$ mg/l, $u=6$ l/ min and pH=8).

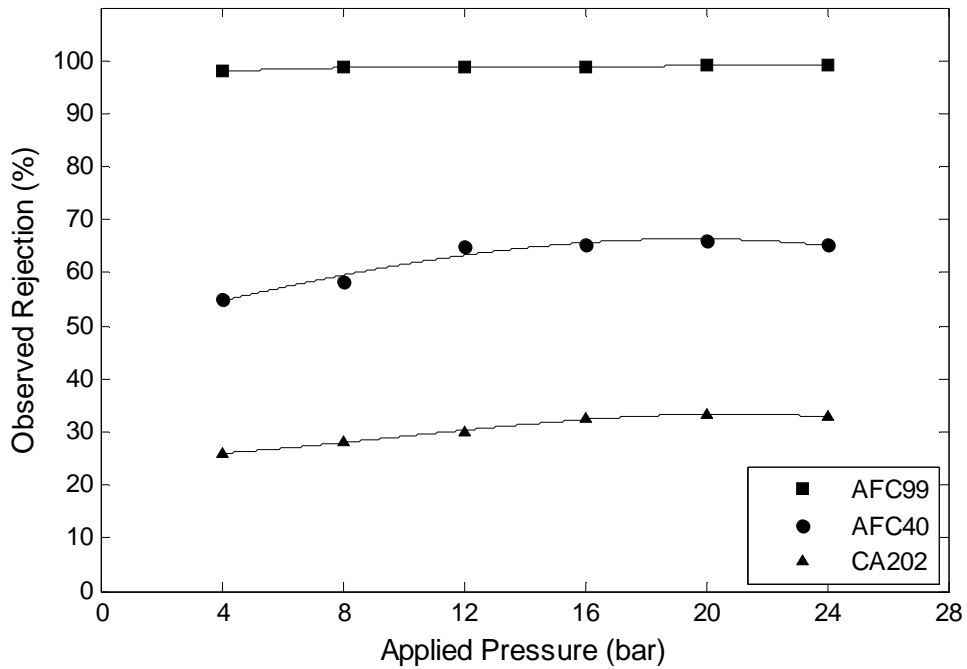


Fig. 5.16: Effect of operating pressure on observed rejection of DEA across various membranes ($C_b=5000$ mg/l, $u=6$ l/ min and pH=8).

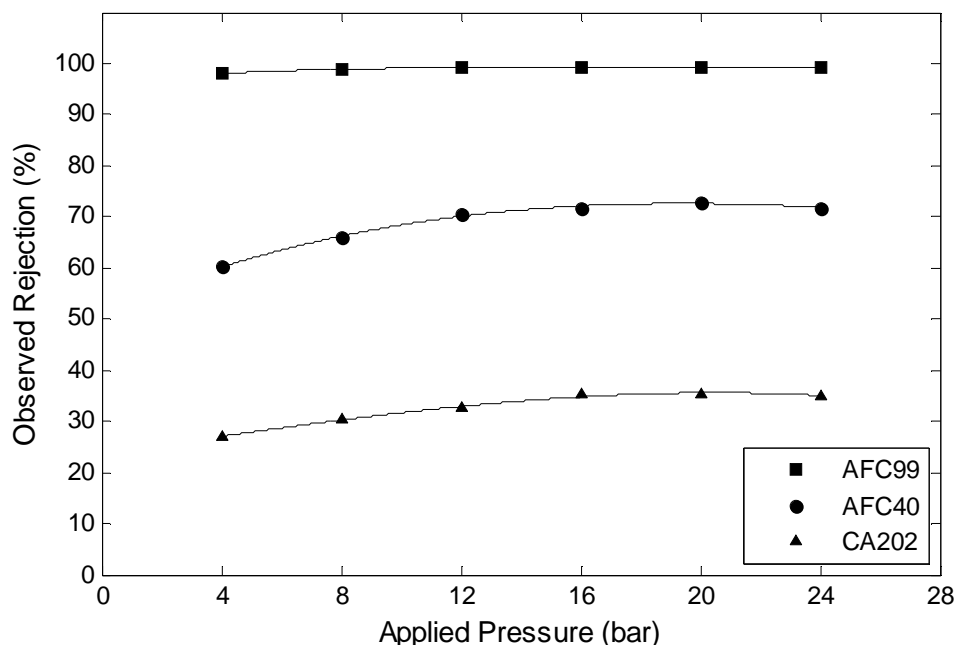


Fig. 5.17: Effect of operating pressure on observed rejection of MDEA across various membranes ($C_b=5000$ mg/l, $u=6$ l/min and pH=8).

b. Effect of Amine Molecular Weight on Observed Rejection

Figures 5.18 to 5.20 show the variation of the observed rejection with amine types across AFC99, AFC40 and CA202 membranes. The findings show that MDEA was found to be the highest rejected amine followed by DEA and MEA, respectively for all the membranes under the study. As mentioned in Section 5.1.2 (a), the findings show that the rejection behavior of the membranes increases with the increase in the molecular weight of the amines studied, where the molecular weight for MDEA (119 g/mol) > DEA (105 g/mol) > MEA (61 g/mol). The increase in rejection is due to the molecular sieving effect of the membranes (Van der Bruggen *et al.*, 1999; Ozaki and Li, 2004; Schafer *et al.*, 2005). Higher molecular weight increases the molecular sieve effect of the membranes causing an increase in the surface resistance to the amines flux through the membranes, hence increases the observed rejection.

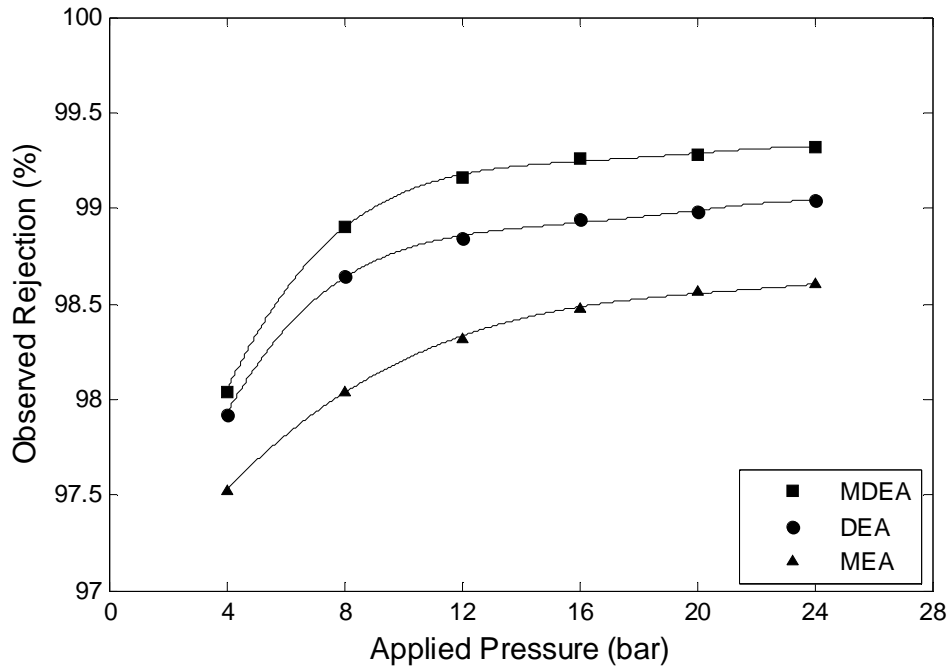


Fig. 5.18: Effect of amine molecular weight on observed rejection across AFC99 membrane ($C_b=5000$ mg/l, $u=6$ l/ min and pH=8).

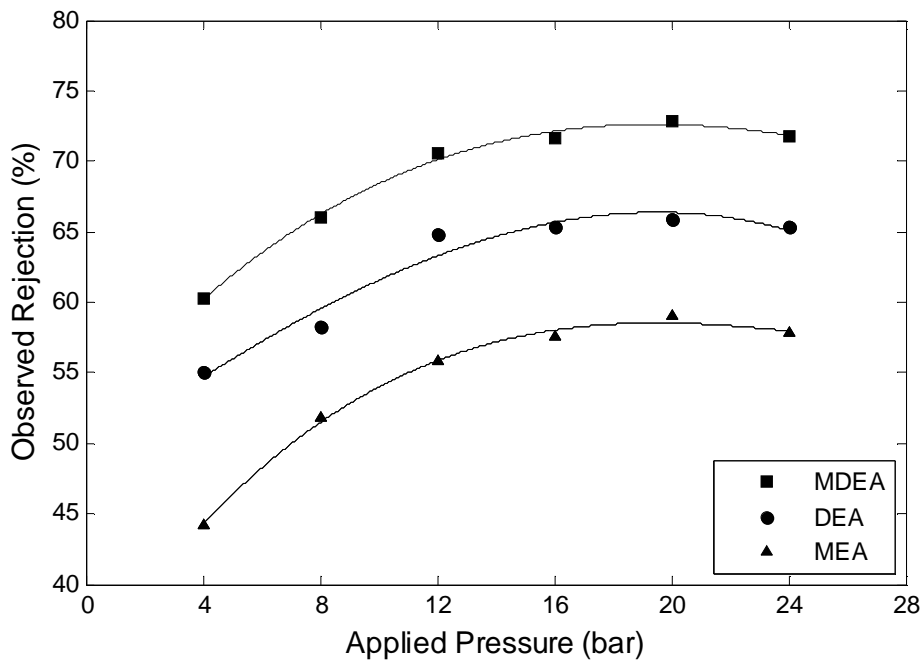


Fig. 5.19: Effect of amine molecular weight on observed rejection across AFC40 membrane ($C_b=5000$ mg/l, $u=6$ l/ min and pH=8).

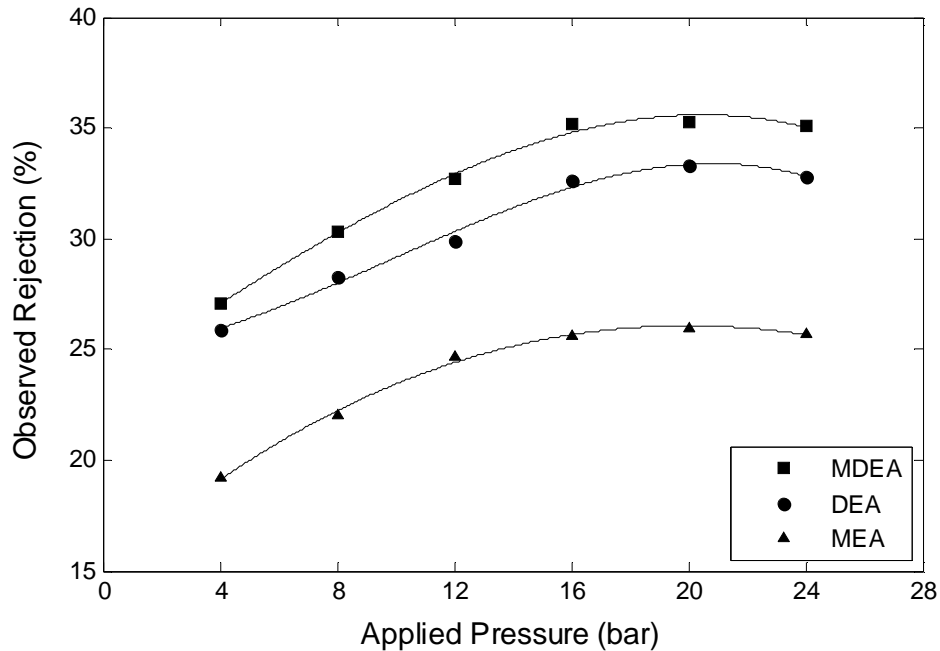


Fig. 5.20: Effect of amine molecular weight on observed rejection across CA202 membrane ($C_b=5000$ mg/l, $u=6$ l/ min and pH=8).

The investigation also shows that the ratio of the observed rejections of the amines increases with increase in the ratio of their molecular weight. For example, a ratio of observed rejections of 1.100, 1.130 and 1.242 were found for molecular weight ratios of 1.133 (MDEA/DEA), 1.721 (DEA/MEA) and 1.951 (MDEA/MEA), respectively. However, the findings show that the increase in observed rejection of the amines has no direct relationship with the increment of the molecular weight.

c. Effect of Cross Flow Velocity on Observed Rejection

Figures 5.21 to 5.23 show the effect of cross-flow velocity on observed rejection for MEA, DEA and MDEA solutions across AFC99, AFC40 and CA202 membranes. The results show that the observed rejection increases with an increase in cross-flow velocity for all the membranes under the study. The investigation shows that the observed rejection of MEA solution across the membranes increases from 97.92% to 98.60% for

AFC99, from 40.0% to 57.80% for AFC40 and from 24.3% to 25.7% for CA202 when the cross-flow velocity increases from 1.5 to 6.0 l/min.

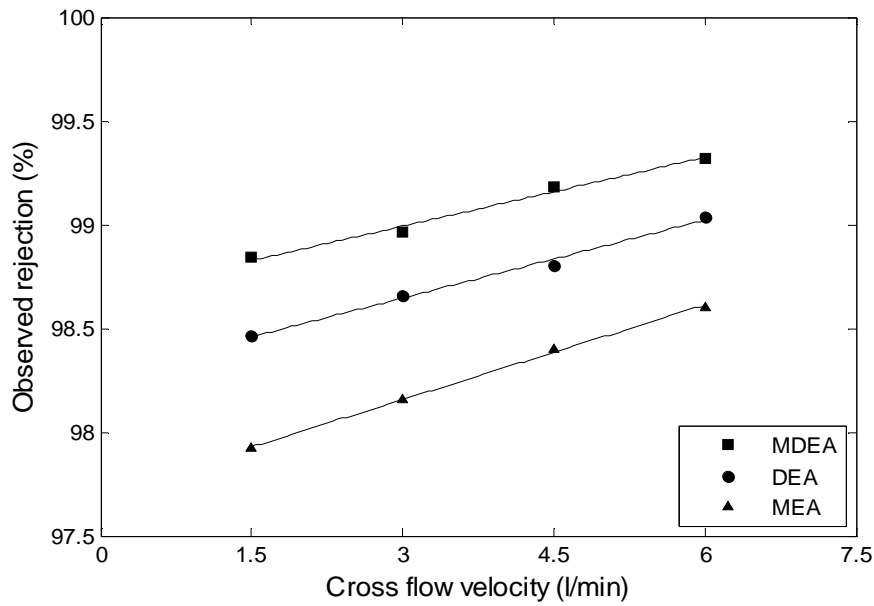


Fig. 5.21: Effect of cross-flow velocity on observed rejection of various amines across AFC99 membrane ($p=24$ bar, $C_b=5000$ mg/l and $pH=8$).

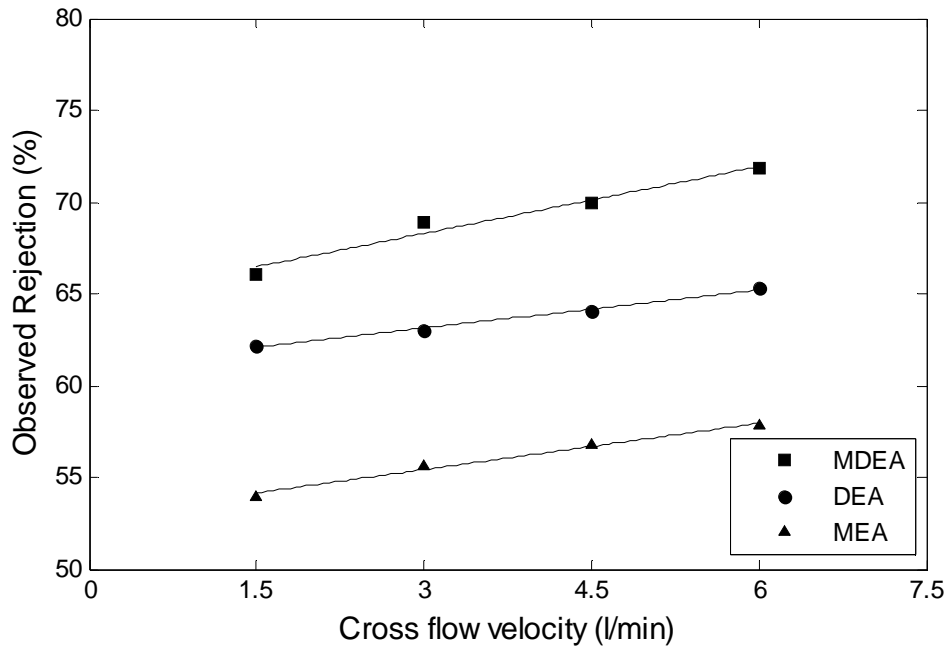


Fig. 5.22: Effect of cross-flow velocity on observed rejection of various amines across AFC40 membrane ($p=24$ bar, $C_b=5000$ mg/l and $pH=8$).

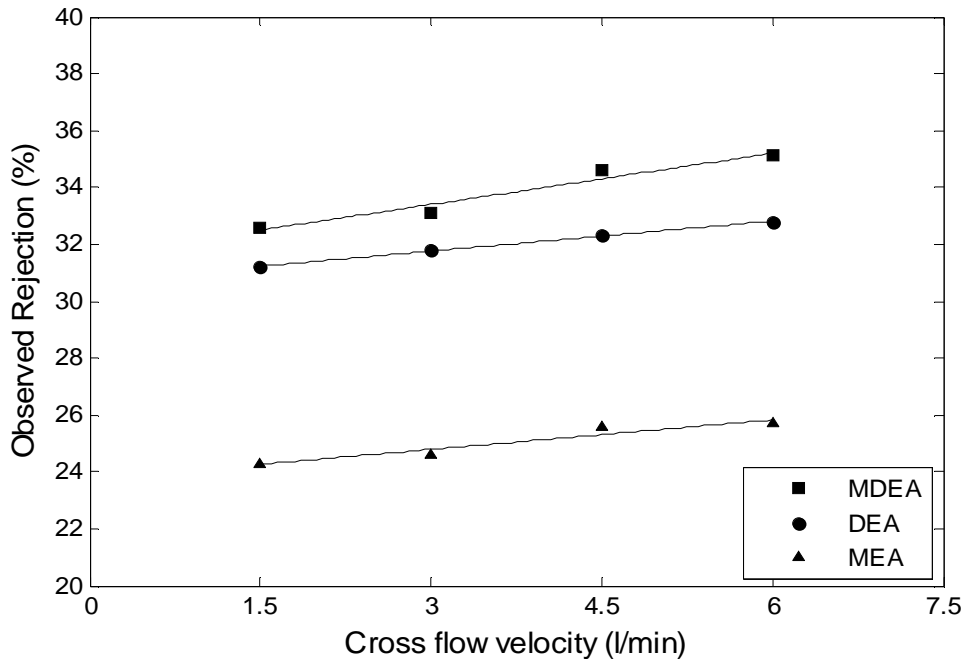


Fig. 5.23: Effect of cross-flow velocity on observed rejection of various amines across CA202 membrane ($p=24$ bar, $C_b=5000$ mg/l and $pH=8$).

Cross-flow velocity is one of the hydrodynamic factors that affect the accumulation of membrane fouling. Usually, a higher cross-flow velocity increases the mass transfer coefficient, and subsequently minimizes the effect of concentration polarization, resulting in higher observed rejection of the solutes by the membranes (Hilal *et al.*, 2005).

d. Effect of Feed Concentration on Observed Rejection

Figures 5.24 to 5.26 show the effect of feed concentration on the observed rejection for MEA, DEA and MDEA solutions across AFC99, AFC40 and CA202 membranes. The findings show that the observed rejection of the amines decreases as the feed concentration increases. This is because solute flux across the membranes increases with increases in feed concentration due to the increment of concentration gradient of the solutes across the membranes. As a result, the flux of the amines through the membranes increases resulting in higher solute concentration in the permeate stream. Hence, the net

effect would be a decrease in solute rejection when the feed concentration increases (Baker, 2004). The investigation shows that the observed rejection of MEA across AFC99, AFC40 and CA202 membranes decreases by 0.41%, 15.69% and 21.01%, respectively when the feed concentration increases from 5000 to 15000 mg/l. For DEA solutions, the observed rejection has decreased by 0.61%, 12.86% and 5.27% across AFC99, AFC40 and CA202, respectively. In addition, 0.60%, 9.33% and 6.90% reductions in observed rejection of MDEA solutions were observed across AFC99, AFC40 and CA202 membranes, respectively.

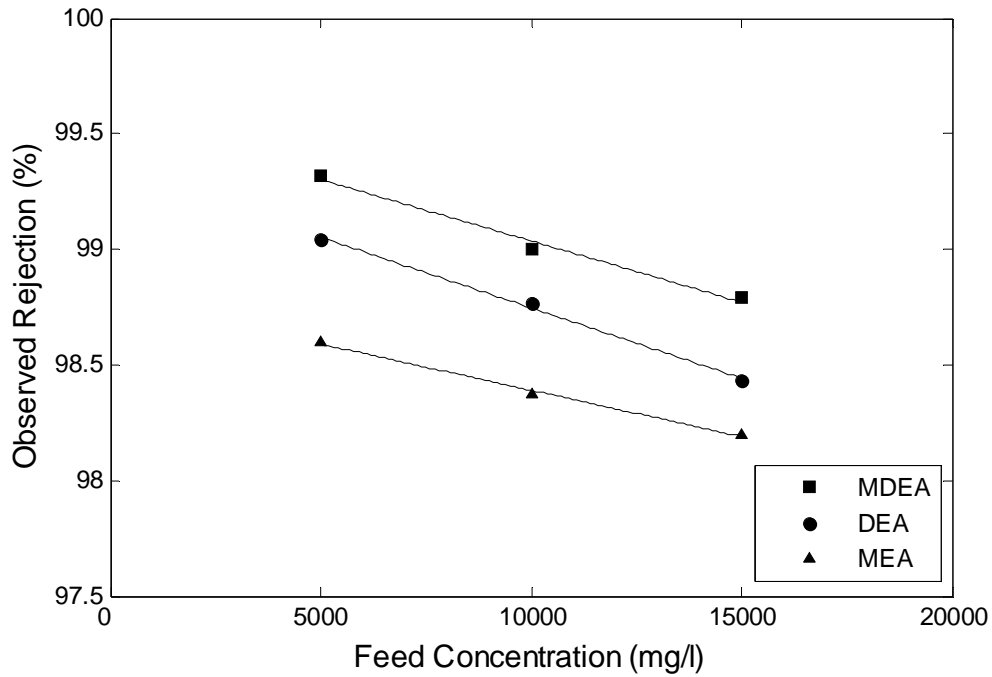


Fig. 5.24: Effect of feed concentration on observed rejection across AFC99 membrane ($p=24$ bar, $u=6$ l/min and $pH=8$).

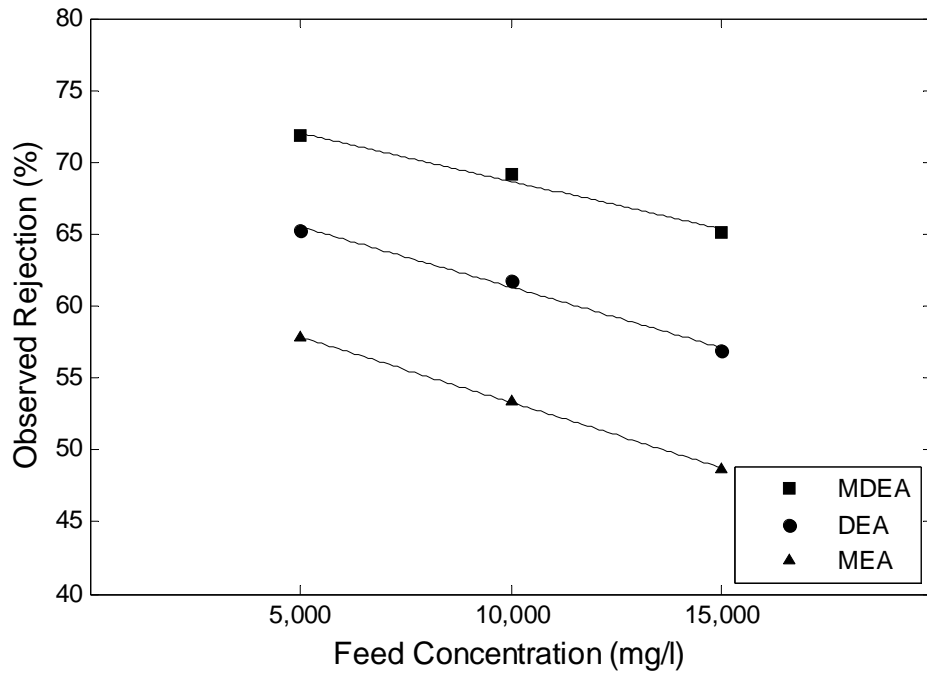


Fig. 5.25: Effect of feed concentration on observed rejection across AFC40 membrane ($p=24$ bar, $u=6$ l/min and $pH=8$).

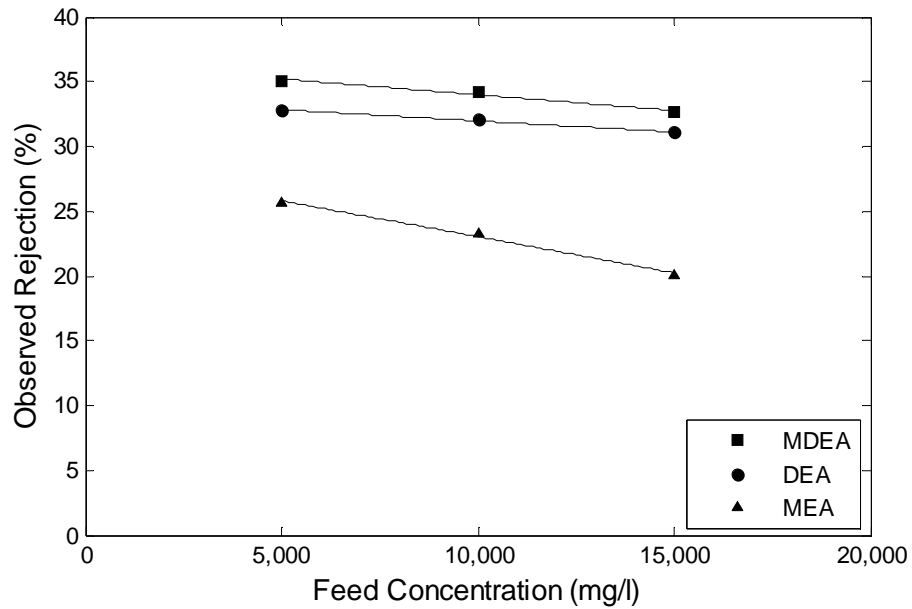


Fig. 5.26: Effect of feed concentration on observed rejection across CA202 membrane ($p=24$ bar, $u=6$ l/min and $pH=8$).

e. Effect of pH on Observed Rejection

Figures 5.27 to 5.29 show the effect of feed pH on observed rejection of MEA, DEA and MDEA solutions across AFC99, AFC40 and CA202 membranes. The results show that the observed rejection increases as the pH of the feed decreases. As discussed earlier in Section 5.1.2.2 (e), the membranes exhibited positive charge at pH 3 and negative charge at pH 8. On the other hand, amine solutions are alkaline and form R_3NH^+ , $R_2NH_2^+$ and RNH_3^+ due to protonation of the amines (where R is an alkyl substitute of $CH_3(CH_2CH_2OH)_2$, $(CH_2CH_2OH)_2$ and CH_2CH_2OH for MDEA, DEA and MEA, respectively). As the pressure increases, more solutes would be brought closer to the membrane surface. Thus, the electrostatic repulsion between the positively charged membranes and the protonated amines increases and gives higher rejection (Bowen and Mukhtar, 1996; Van der Bruggen *et al.*, 1999; Manttari *et al.*, 2006). However, at high pH, the observed rejection decreases due to the electrostatic attraction between the positively charged amine and the negatively charged surface of the membranes (Seidel *et al.*, 2001).

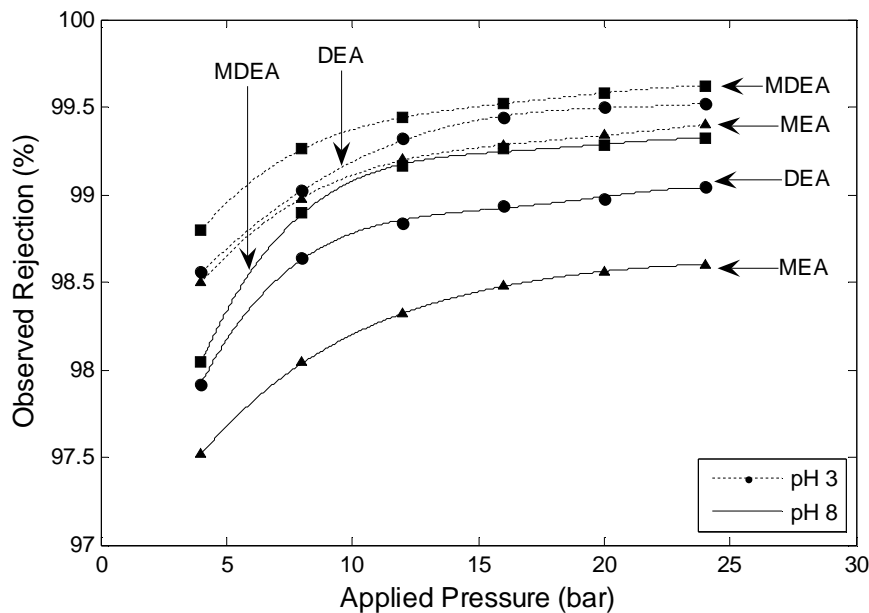


Fig. 5.27: Effect of feed pH on observed rejection of various amines across AFC99 membrane ($p=24$ bar, $u=6$ l/min and $C_b=5000$ mg/l).

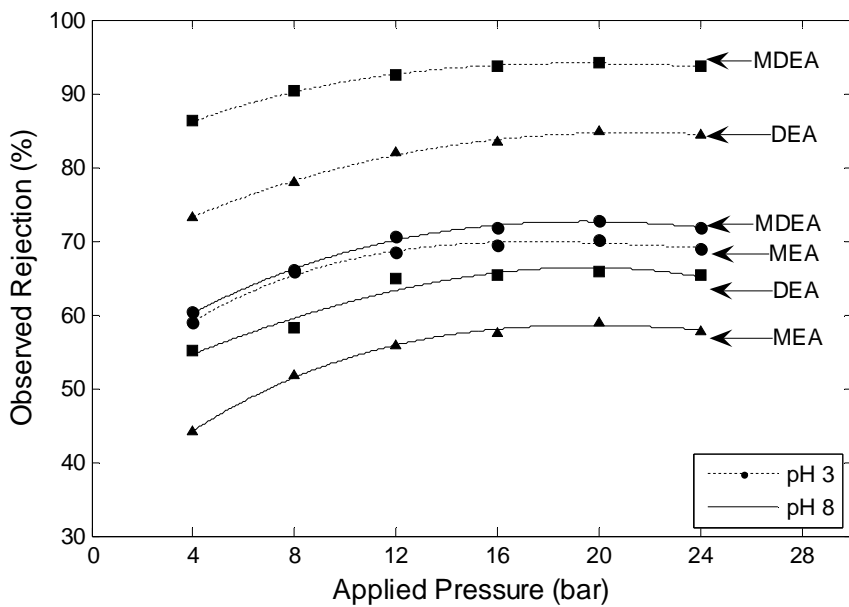


Fig. 5.28: Effect of feed pH on observed rejection of various amines across AFC40 membrane ($p=24$ bar, $u=6$ l/min and $C_b=5000$ mg/l).

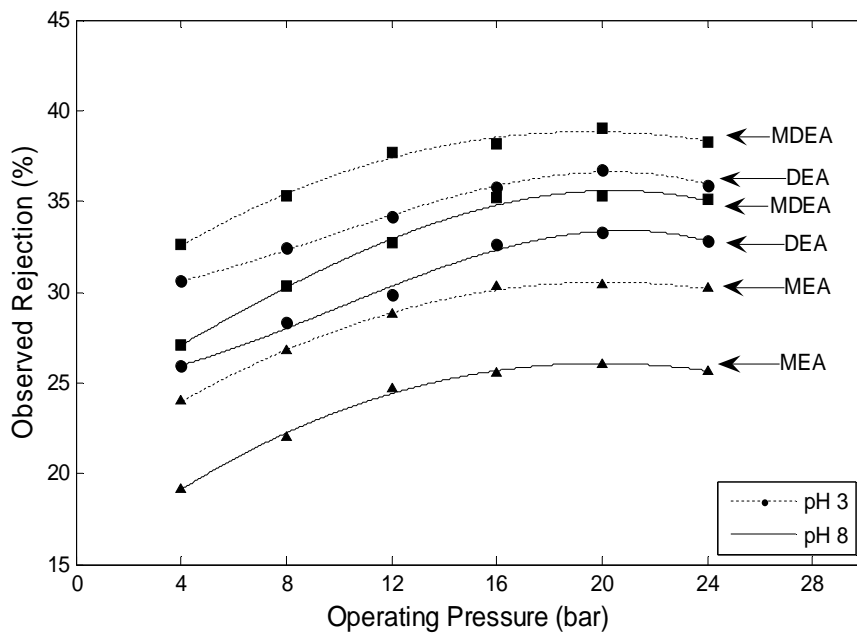


Fig. 5.29: Effect of feed pH on observed rejection of various amines across CA202 membrane ($p=24$ bar, $u=6$ l/min and $C_b=5000$ mg/l).

The finding shows that the rejection effect of the pH is more significant for AFC40 membrane compared to AFC99 and CA202 membranes. The investigation shows that the observed rejection of the membranes increases on average by 0.50%, 21%, and 11% for AFC99, AFC40 and CA202 membranes, respectively when the pH decreases from 8 to 3. This shows that for AFC40 and CA202 membranes, the rejection mechanism depends not only on sieving but also on the charge interaction between the feed solution and the membranes, whereas for AFC99 membrane, the rejection was almost due to sieving.

5.2 Modeling of Membrane Processes

In this section, two membrane models were used to estimate the membrane transport parameters in order to predict the membranes performance. These membrane transport models are known as combined film-theory solution-diffusion model (CFSD) and combined film-theory Spiegler-Kedem model (CFSK). These two models best describe either AFC99 or AFC40 membrane processes but are not suitable for CA202 membrane process. This is due to the difference in the relative pore size of the membranes. Studies show that a transition in mechanisms of transport between solution-diffusion and pore-flow models exists in the range 5–10 °A of pore diameter (Baker, 2004). AFC99 membrane has a dense polymer layer with no visible pores, through which the separation occurs. Hence, its transport mechanism is best described by the CFSD model (Murthy and Gupta, 1999). CA202 membrane, on the other hand, has relatively large and fixed pores. Hence, its transport mechanism is best described by a pore-flow model. AFC40 membrane contains tight pores with diameters between 5 °A and 10 °A and is intermediate between CA202 and AFC99 membranes. Hence, its transport mechanism is best described by CFSK model (Spiegler and Kedem, 1966; Murthy and Chaudhari, 2009).

5.2.1 Estimation of Model Parameters

Based on the present study, the experimental results for the flux and rejection were used to estimate the transport parameters, including solute transport parameter, P_s or P_m , reflection coefficient, α and mass transfer coefficient, k . These parameters were determined by curve fitting of the permeate flux and the observed rejection data into combined film theory-solution-diffusion model, (CFSD) as given by Equation (3-17), and combined film theory-Spiegler-Kedem model, (CFSK) as given by the Equation (3-18) as discussed in Section 3.4.3. Sets of experimental data at various operating conditions, including operating pressure, cross-flow velocity and feed concentration for all amine types were used in the curve fitting. Figures 5.30 and 5.31 show a typical plot of $\frac{1-R_o}{R_o}$ versus J_v . The fittings were excellent with about 2% error. From these fittings the best transport equation were obtained.

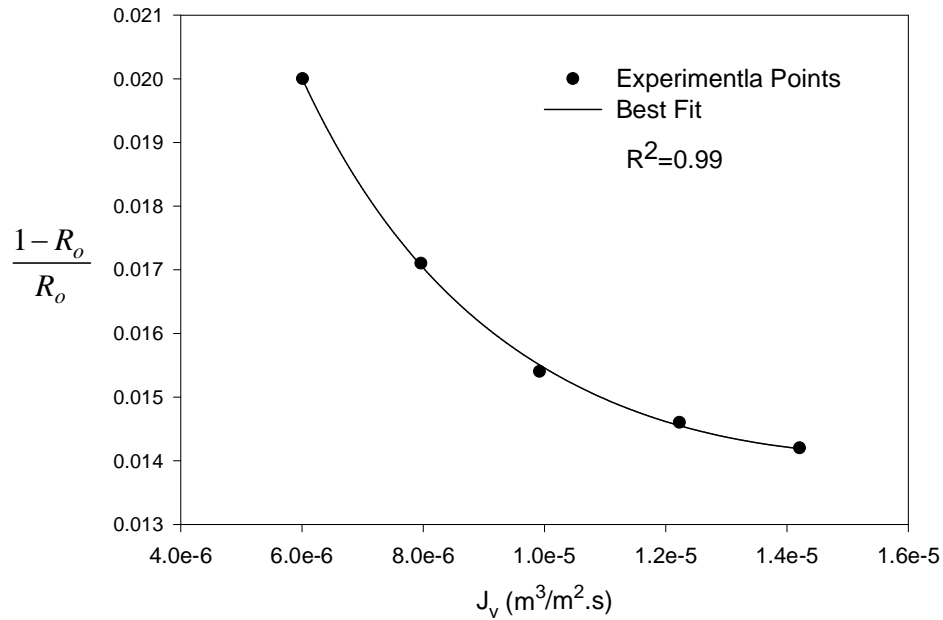


Fig. 5.30: Estimation of parameters for AFC99 membrane using CFSD model for MEA-water system ($C_b=5000$ mg/l, $u=6.0$ l/min, pH 8).

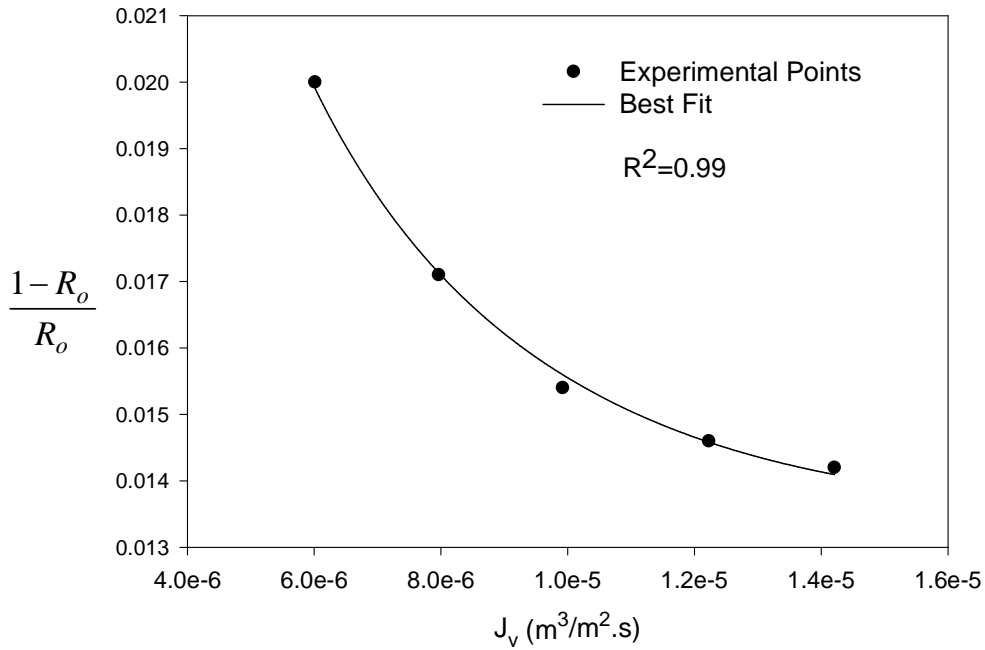


Fig. 5.31: Estimation of parameters for AFC99 membrane using CFSK model for MEA-water system ($C_b=5000$ mg/l, $u=6.0$ l/min, pH 8).

5.2.2 Results

The membrane transport parameters estimated from the curve fitting using Equations (3-17) and (3-18) are given in Tables 5-3 to 5-6. The results show that the values of the solute transport parameter, reflection coefficient and mass transfer coefficients are dependent on the feed concentration and cross-flow velocity. The solute transport parameter increased with increase in cross-flow velocity and feed concentration for both models. It can also be seen from the tables that the solute transport parameter from the CFSK model is lower than the value obtained from CFSD model under the same operating conditions. This is because the CFSK model assumes that the solute transport through the membrane is a result of both convection and diffusion, whereas the CFSD assumes the transport of the solute is only due to diffusion. Because of this fact, the amount of accumulated solute at the membrane-solution interface under CFSK model

assumption would be less as compared to CFSD model assumption resulting in lower solute transport parameter values in CFSK model. The finding is in agreement with cited literatures (Murthy and Gupta, 1997; Murthy and Gupta, 1999)

The mass transfer coefficient also increases with increasing in cross-flow velocity and decreases as the feed concentration increases. This is because, when the cross-flow velocity increases, the shear force on the membrane surface increases and sweeps away the retained solutes from the membrane surface. Consequently, the back diffusivity of the solutes increases while the concentration polarization boundary layer decreases resulting in higher mass transfer coefficient. On the other hand, the CFSK model exhibited higher mass transfer coefficients as compared to CFSD model. This is because the concentration polarization boundary layer is lower in CFSK model as compared to CFSD model due to the additional convection transport of the solutes (Murthy and Gupta, 1999). In addition, the back diffusivity of the solutes slightly increases as the solute concentration at the solution-membrane interface decreases. Therefore, these phenomena increase the mass transfer coefficient. The same trend of the parameters was observed by other authors (Murthy and Gupta, 1997; Murthy and Gupta, 1999).

The tables also show that the reflection coefficient increased with increase in cross-flow velocity and decreased with increase in concentration. This is due to the increase in concentration gradient of the amines across the membrane as the feed concentration increases. However, when the cross-flow velocity increases the retained solutes at the interface of the membrane will be carried away by the tangential flow of the feed, resulting in an increase of the reflection coefficient.

Figures 5.32 to 5.35 compare the experimental and calculated observed rejection of AFC99 and AFC40 membranes using CFSD and CFSK models for the optimum transport parameters. The figures show that the calculated rejection values are in good agreement with the experimental results and the errors are about 3 % for AFC99 and 7% for AFC40. Figures 5.32 and 5.33 show that both transport models are excellent in prediction of the membranes performance for AFC99 membrane. On the other hand, for AFC40

membrane, CFSK model exhibited better prediction as compared to CFSD model as can be seen from Figures 5.34 and 5.35. This is due to the inclusion of convection flow of solutes through the membrane pores by CFSK model. As can be seen from the reflection coefficient values given in Tables 5.4 and 5.6, the convection flow of solutes through AFC40 membrane is higher than AFC99 membrane due to its wider pore size. Thus, CFSK model can predict the AFC40 membrane performance better than CFSD model, which assumes the solute transport across the membrane is only due to diffusion.

Table 5.3: Estimated transport parameters for AFC99 membrane using CFSD model (pH 8).

Operating conditions		MEA solution			DEA solution			MDEA solution		
Feed concentration (mg/l)	Cross-flow velocity (l/min)	$k*10^6$ (m/s)	P_s*10^8 (m/s)	R^2	$k*10^6$ (m/s)	P_s*10^8 (m/s)	R^2	$k*10^6$ (m/s)	P_s*10^8 (m/s)	R^2
5000	1.5	7.889	6.242	0.92	6.449	3.816	0.91	5.87	2.482	0.90
	3.0	10.240	7.114	0.98	7.906	4.101	0.99	7.13	2.766	0.89
	4.5	12.000	7.381	0.97	11.155	5.017	0.99	9.90	3.110	0.98
	6.0	15.830	8.220	0.99	14.450	5.243	0.99	12.75	3.269	0.99
10000	1.5	5.638	4.443	0.94	5.731	3.236	0.98	3.715	1.552	0.87
	3.0	8.360	6.158	0.91	7.416	3.836	0.89	4.523	1.817	0.87
	4.5	10.932	7.403	0.98	9.472	4.564	0.99	6.553	2.627	0.95
	6.0	12.640	7.790	0.99	10.702	4.923	0.99	8.040	3.012	0.98
15000	1.5	2.984	2.090	0.88	2.561	1.640	0.87	-	-	-
	3.0	4.325	3.261	0.88	3.865	2.580	0.90	-	-	-
	4.5	6.006	4.482	0.90	4.967	3.120	0.88	3.919	1.868	0.86
	6.0	8.910	6.109	0.98	6.937	4.105	0.94	5.828	2.687	0.88

Note: For AFC99 membrane and MDEA solution at 15000 mg/l and cross flow velocities of 1.5 and 3.0 l/min the membrane parameters were not estimated since no permeate flux was observed at 4 and 8 bar.

Table 5.4: Estimated transport parameters for AFC99 membrane using CFSK model (pH 8).

Operating conditions		MEA solution				DEA solution				MDEA solution			
Feed concentration (ppm)	Cross-flow velocity (l/min)	σ	$k*10^6$ (m/s)	P_m*10^8 (m/s)	R^2	σ	$k*10^6$ (m/s)	P_m*10^8 (m/s)	R^2	σ	$k*10^6$ (m/s)	P_m*10^8 (m/s)	R^2
5000	1.5	0.9861	29.04	5.699	0.95	0.9891	24.96	3.542	0.88	0.9921	22.09	2.248	0.94
	3.0	0.9867	49.96	6.490	0.97	0.9892	46.47	3.766	0.99	0.9922	34.04	2.467	0.97
	4.5	0.9876	71.73	6.692	0.99	0.9908	67.21	4.503	0.99	0.9935	59.08	2.866	0.98
	6.0	0.9898	94.41	7.644	0.99	0.9928	85.69	4.859	0.99	0.9949	75.64	3.062	0.99
10000	1.5	0.9846	24.54	3.929	0.89	0.9896	23.40	2.984	0.99	0.9904	21.70	1.347	0.94
	3.0	0.9855	45.01	5.628	0.98	0.9897	40.97	3.525	0.99	0.9904	31.94	1.536	0.90
	4.5	0.9865	66.73	6.813	0.98	0.9902	62.88	4.227	0.99	0.9909	56.97	2.330	0.99
	6.0	0.9874	86.13	7.135	0.99	0.9904	78.90	4.514	0.99	0.9916	71.45	2.683	0.99
15000	1.5	0.9809	21.40	1.590	0.88	0.9828	16.04	1.255	0.87	-	-	-	-
	3.0	0.9811	41.26	2.672	0.92	0.9834	33.01	2.090	0.94	-	-	-	-
	4.5	0.9822	62.69	3.741	0.93	0.9845	54.40	2.542	0.96	0.9868	50.87	1.508	0.88
	6.0	0.9850	80.28	5.472	0.99	0.9864	70.67	3.565	0.99	0.9890	65.03	2.356	0.92

Table 5.5: Estimated transport parameters for AFC40 membrane using CFSD model (pH8).

Operating conditions		MEA solution			DEA solution			MDEA solution		
Feed concentration (ppm)	Cross-flow velocity (L/ min)	$k*10^6$ (m/s)	P_s*10^6 (m/s)	R^2	$k*10^6$ (m/s)	P_s*10^6 (m/s)	R^2	$k*10^6$ (m/s)	P_s*10^6 (m/s)	R^2
5000	1.5	22.730	6.9970	0.9614	17.300	3.7100	0.8909	15.3400	2.7170	0.9151
	3.0	27.660	7.8500	0.9791	20.050	4.1650	0.9022	18.6900	3.0660	0.8820
	4.5	30.720	8.4260	0.9977	22.460	4.5120	0.8916	20.7900	3.2170	0.9219
	6.0	33.960	8.8750	0.9971	26.080	4.9770	0.9286	23.8200	3.3690	0.9662
10000	1.5	16.780	6.7890	0.9448	12.250	2.9430	0.9046	11.5600	1.9800	0.8737
	3.0	19.650	7.4560	0.9098	14.280	3.3230	0.8909	13.2300	2.2250	0.9190
	4.5	23.320	7.6710	0.9874	16.600	3.7520	0.8998	14.8800	2.4120	0.9296
	6.0	27.090	8.2810	0.9949	18.810	4.0750	0.9019	16.9200	2.6760	0.8887
15000	1.5	13.900	5.7310	0.8852	9.5450	2.4790	0.8967	8.0820	1.2450	0.9013
	3.0	15.980	6.3730	0.9132	10.920	2.7900	0.9037	10.1200	1.7380	0.9137
	4.5	18.540	7.2090	0.9401	12.580	3.2120	0.9109	11.4600	1.9870	0.9410
	6.0	21.180	7.9580	0.9660	14.670	3.6740	0.8995	13.2400	2.2700	0.9732

Table 5.6: Estimated transport parameters for AFC40 membrane using CFSK model (pH 8).

Operating conditions		MEA solution				DEA solution				MDEA solution			
Feed concentration (ppm)	Cross-flow velocity (l/min)	σ	$k*10^6$ (m/s)	P_m*10^6 (m/s)	R^2	σ	$k*10^6$ (m/s)	P_m*10^6 (m/s)	R^2	σ	$k*10^6$ (m/s)	P_m*10^6 (m/s)	R^2
5000	1.5	0.589	197.5	3.754	0.980	0.651	191.4	2.047	0.902	0.690	177.3	2.295	0.931
	3.0	0.617	231.2	4.505	0.987	0.665	216.9	2.392	0.923	0.717	203.2	2.100	0.939
	4.5	0.627	254.1	4.939	0.994	0.674	244.4	2.634	0.919	0.731	227.4	1.951	0.965
	6.0	0.641	269.7	5.329	0.989	0.693	262.4	3.069	0.936	0.753	247.4	1.620	0.983
10000	1.5	0.499	184.0	2.910	0.974	0.599	181.6	1.411	0.883	0.677	171.8	1.124	0.881
	3.0	0.519	222.3	3.377	0.946	0.616	207.6	1.652	0.888	0.689	197.6	1.289	0.903
	4.5	0.567	242.8	3.941	0.989	0.632	227.5	1.944	0.909	0.701	218.8	1.426	0.934
	6.0	0.592	262.2	4.504	0.981	0.647	251.5	2.188	0.943	0.711	234.8	1.614	0.964
15000	1.5	0.482	175.1	2.381	0.969	0.538	173.3	1.007	0.906	0.644	151.6	0.627	0.934
	3.0	0.497	198.1	2.728	0.985	0.557	197.9	1.137	0.890	0.665	176.5	0.919	0.916
	4.5	0.510	222.1	3.210	0.993	0.572	216.5	1.381	0.892	0.662	196.7	1.063	0.896
	6.0	0.523	249.8	3.648	0.998	0.590	239.6	1.672	0.928	0.674	223.1	1.241	0.964

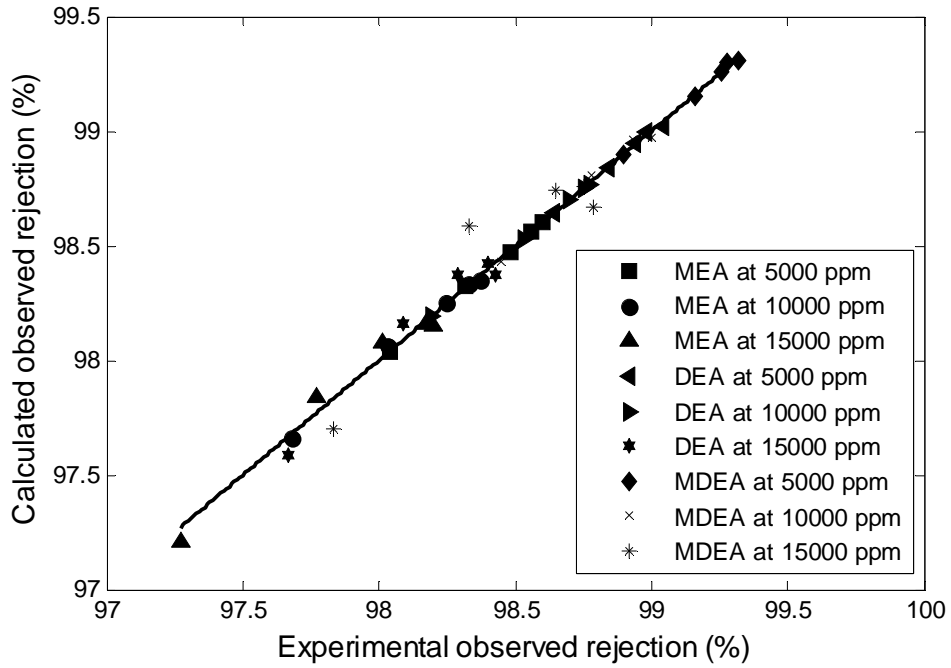


Fig. 5.32: Comparison of experimental and calculated observed rejection for AFC99 membrane using CFSD model.

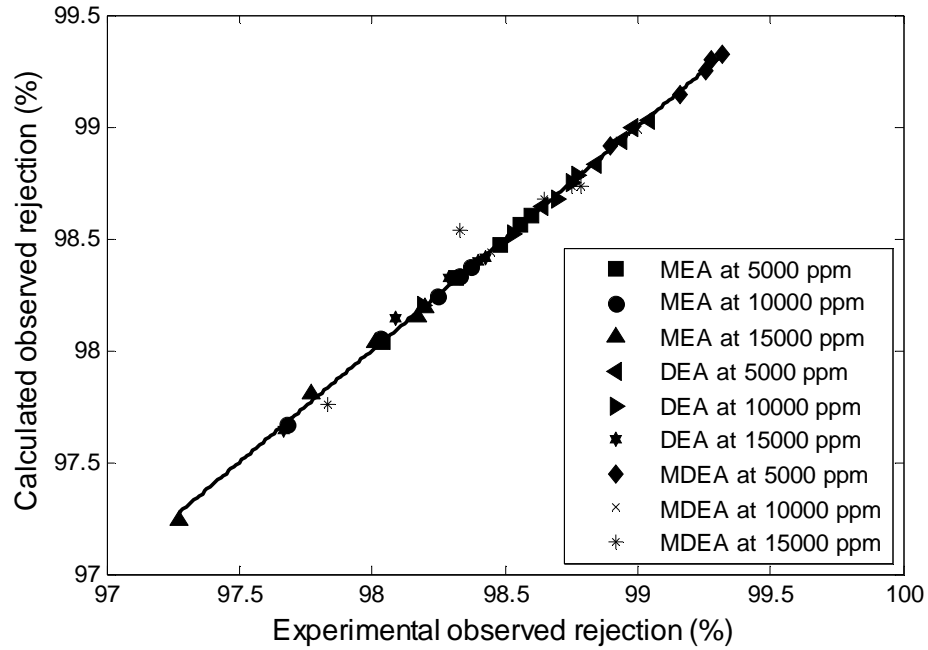


Fig. 5.33: Comparison of experimental and calculated observed rejection for AFC99 membrane using CFSK model.

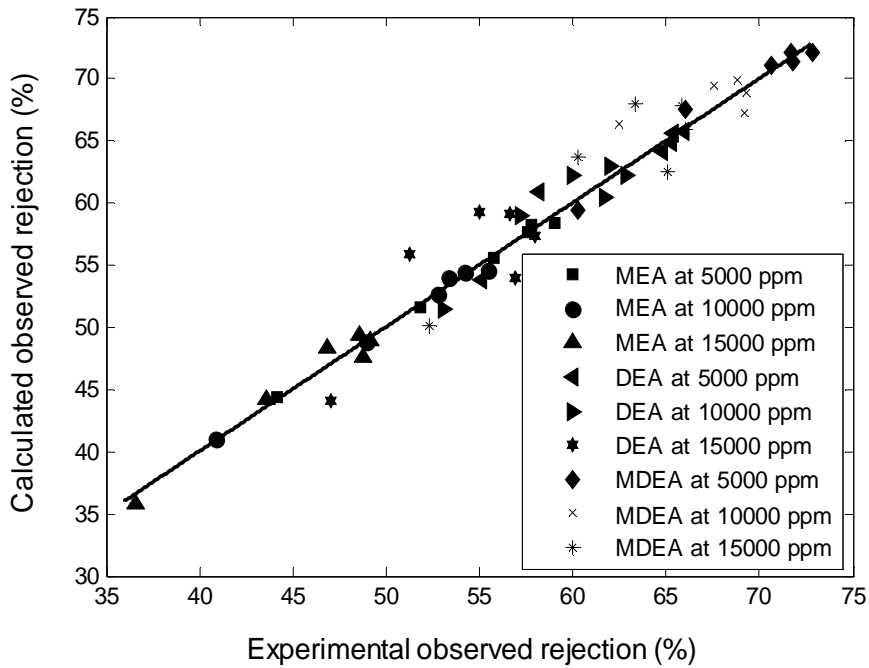


Fig. 5.34: Comparison of experimental and calculated observed rejection for AFC40 membrane using CFSM model.

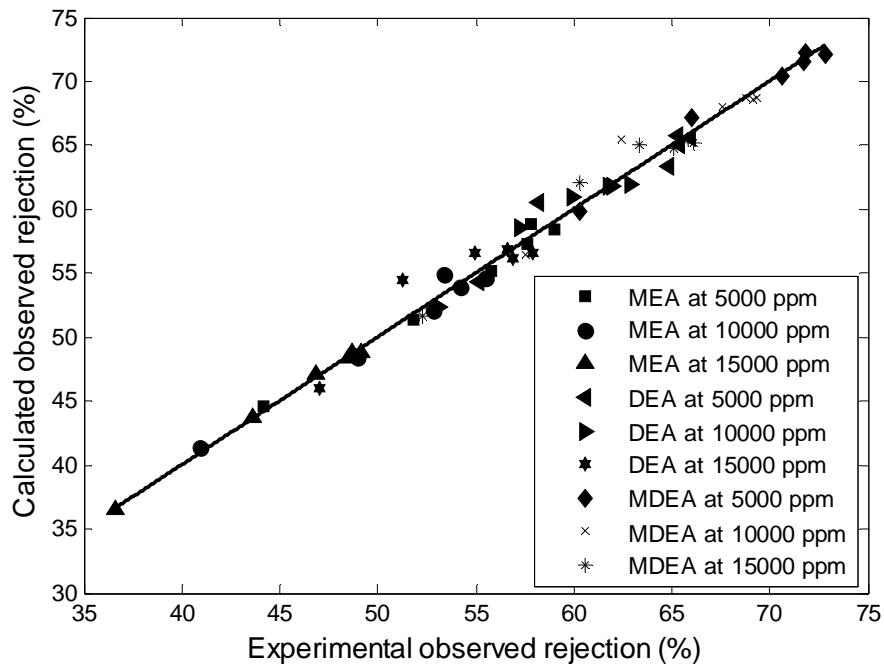


Fig. 5.35: Comparison of experimental and calculated observed rejection for AFC40 membrane using CFSK model.

5.2.3 Model Validation

The models validation was performed by comparing the observed rejection values predicted from the CFSD and CFSK models with a new set of data obtained experimentally at 5 l/min and 5000 mg/l for all amines under the study. It is assumed that there will be a linear correlation between the transport parameters, i.e, the mass transfer coefficient, k , the solute transport parameter, P_s or P_m and the reflection coefficient, σ , for both models obtained from Section 5.2.2 against the cross-flow velocity. Figures 5.36 to 5.38 show this correlation of k , P_s , P_m and σ versus cross-flow velocity, respectively in MEA solution for AFC99 membrane. The figures show that the linear assumptions of the correlations are very good as can be seen from the R^2 values; 0.99 for k , 0.93 for P_s , 0.96 for P_m and 0.93 for σ . Similarly, the same procedures were used to correlate the transport parameters of DEA and MDEA solutions with the cross-flow velocity and the final equations for both CFSD and CFSK models are given in Table 5.7 and 5.8, respectively.

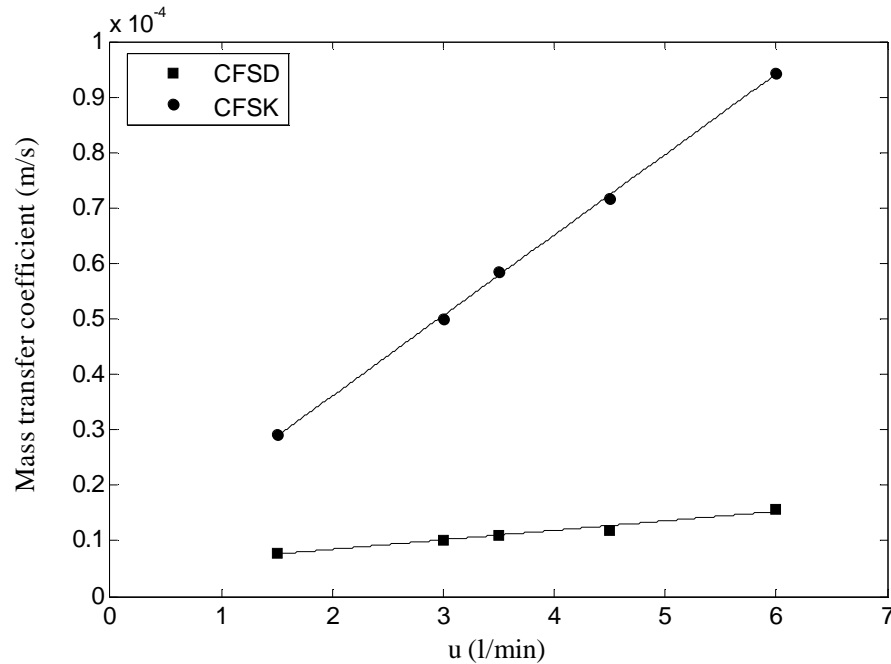


Fig. 5.36: Estimation of k for AFC99 membrane using CFSD and CFSK models for MEA-water system ($C_b=5000$ mg/l, pH 8).

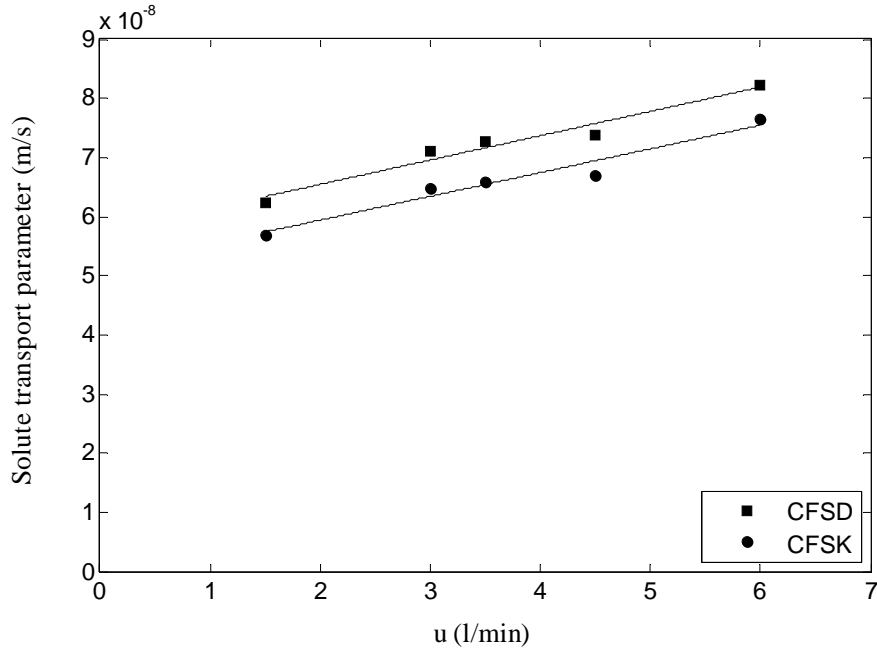


Fig. 5.37: Estimation of P_s and P_m for AFC99 membrane using CFSD and CFSK models for MEA-water system ($C_b=5000$ mg/l, pH 8).

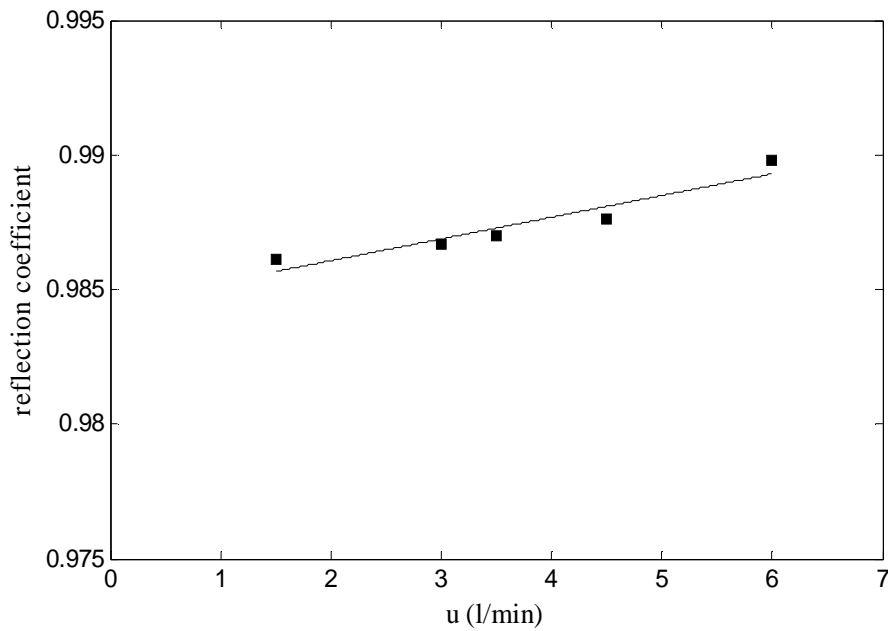


Fig. 5.38: Estimation of reflection coefficient (σ) for AFC99 membrane using CFSK model for MEA-water system ($C_b=5000$ mg/l, pH 8).

Table 5.7: Transport parameters correlation with cross-flow velocity for CFSD model across AFC99 membrane.

MEA solution	DEA solution	MDEA solution
$k = 1.7 \times 10^{-6} u + 5.0 \times 10^{-6}$	$k = 1.8 \times 10^{-6} u + 3.2 \times 10^{-6}$	$k = 1.6 \times 10^{-6} u + 3.0 \times 10^{-6}$
$P_s = 4.1 \times 10^{-9} u + 5.7 \times 10^{-8}$	$P_s = 3.4 \times 10^{-9} u + 3.4 \times 10^{-8}$	$P_s = 1.8 \times 10^{-9} u + 2.3 \times 10^{-8}$

Table 5.8: Transport parameters correlation with cross-flow velocity for CFSK model across AFC99 membrane.

MEA solution	DEA solution	MDEA solution
$k = 1.5 \times 10^{-5} u + 7.0 \times 10^{-6}$	$k = 1.4 \times 10^{-5} u + 5.9 \times 10^{-6}$	$k = 1.2 \times 10^{-5} u + 9.7 \times 10^{-7}$
$P_m = 4.0 \times 10^{-9} u + 5.1 \times 10^{-8}$	$P_m = 3.0 \times 10^{-9} u + 3.1 \times 10^{-8}$	$P_m = 1.9 \times 10^{-9} u + 2.0 \times 10^{-8}$
$\sigma = 8.1 \times 10^{-4} u + 0.9850$	$\sigma = 8.5 \times 10^{-4} u + 0.9871$	$\sigma = 6.6 \times 10^{-4} u + 0.9910$

Equations tabulated in Tables 5.7 and 5.8 were used to determine the respective new transport parameters for these amines in 5000 mg/l and cross-flow velocity of 5 l/min. The estimated parameters at these conditions are tabulated in Table 5.9.

Data tabulated in Table 5.9 were used to estimate the predicted observed rejection using CFSD and CFSK models. The observed predicted data was then compared with the experimental data as shown in Figures 5.39 and 5.40. The figures show that the calculated observed rejection is in good agreement with the experimental values and the errors are less than 3%. The findings show that both CFSD and CFSK models can provide excellent prediction of observed rejection.

Table 5.9: Estimated transport parameters for AFC99 membrane using CFSD and CFSK models ($C_b=5000$ mg/l, $u= 5$ l/min, pH 8).

Transport parameters	MEA solution		DEA solution		MDEA solution	
	CFSD	CFSK	CFSD	CFSK	CFSD	CFSK
$k*10^6$ (m/s)	13.50	82.00	12.20	75.90	11.00	60.97
P_m*10^8 (m/s)	7.750	7.100	5.10	4.600	3.200	2.950
σ	-	0.9885	-	0.9915	-	0.9939

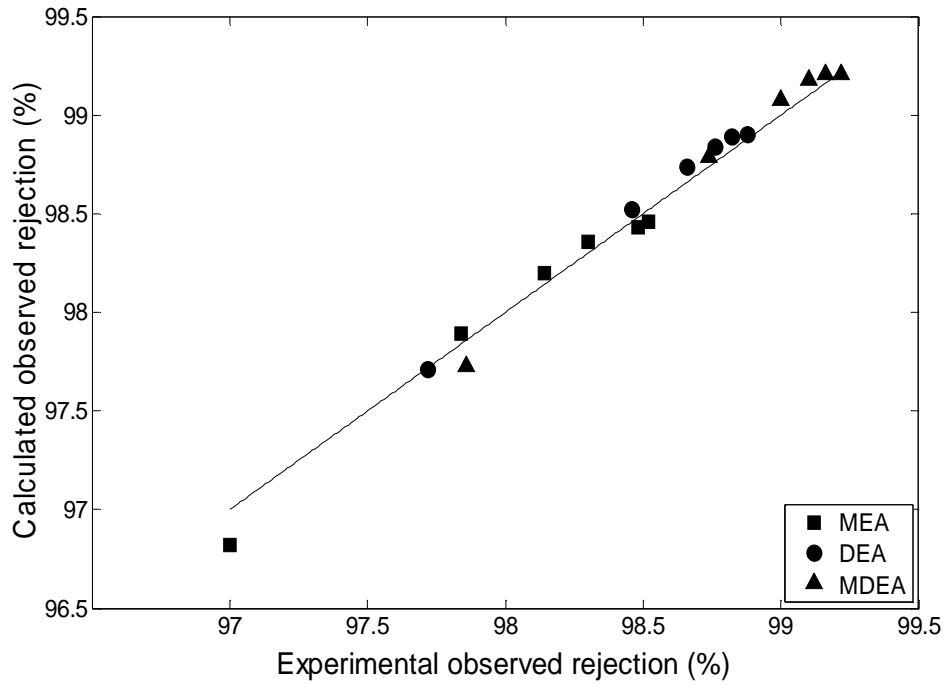


Fig. 5.39: Comparison of experimental and calculated observed rejection for AFC99 membrane using CFSD model.

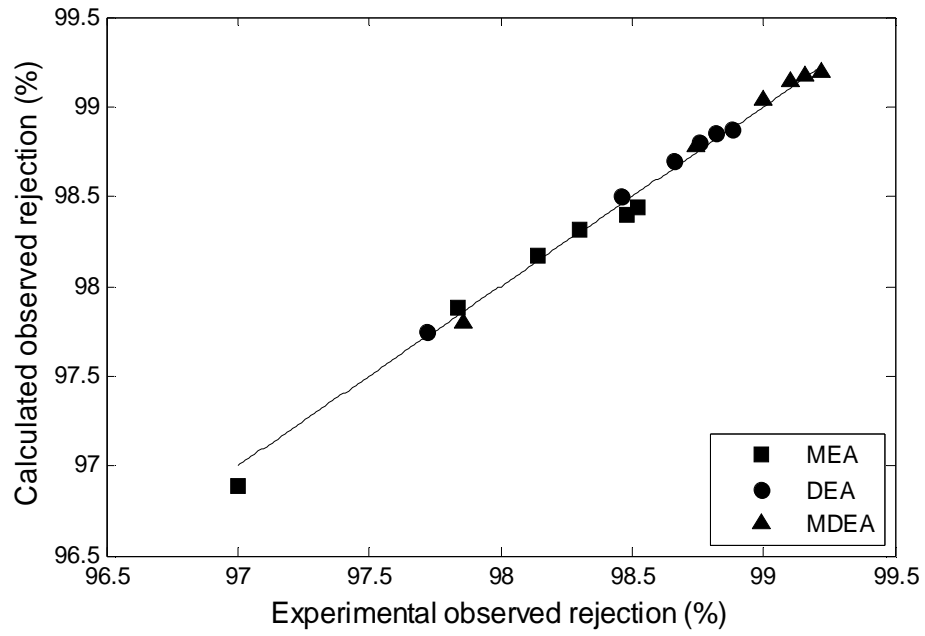


Fig. 5.40: Comparison of experimental and calculated observed rejection for AFC99 membrane using CFSK model.

CHAPTER 6

CONCLUSIONS AND RECOMMENDATIONS

6.1 Conclusions

The flux study shows that the permeate flux of the membranes increased linearly with increasing in operating pressure. In addition, the permeate flux of CA202 membrane was found to be the highest followed by AFC40 and AFC99 membranes, respectively. Moreover, the permeate flux was found to be decreasing as the feed concentration increased due to the effect of concentration polarization and osmotic pressure. On the other hand, increasing cross-flow velocity can reduce the concentration polarization effect, and subsequently increase the permeate flux. The rejection study by the membranes shows that, the observed rejection of the amines has generally increased with an increase in operating pressure and cross-flow velocity, whereas it decreased with an increase in feed concentration. It was found that the rejection efficiency of AFC99 membrane was the highest followed by AFC40 and CA202 membranes, respectively. The findings show that, AFC99 membrane was able to reject more than 96% of the amines under the present study. The AFC40 and CA202 membranes exhibited the highest rejection efficiency up to 59% and 26%, respectively at pH8 for the range of operating pressure in MEA solution. The highest rejection of DEA and MDEA by AFC40 was found to be 65.9 % and 72.8 %, respectively. However, the rejection of DEA and MDEA by CA202 was found to be significantly lower, which were 33.3% and 35.3%, respectively. It was also found that the observed rejection of the amines increased with the increment in their molecular weight. The rejection of MDEA by all membranes was

found to be the highest followed by DEA and MEA, respectively. The study also showed the permeate flux and observed rejection were affected by feed pH. When the feed pH decreased from 8 to 3, the permeate fluxes of AFC40 and CA202 membranes decreased, whereby the permeate flux of AFC99 membrane increased in contrary. On the other hand, the findings showed that the observed rejection increased when the feed pH decreased from 8 to 3 for all the three membranes under the present study. The investigation of the study showed that the observed rejection of the membranes increased on average by 0.50%, 21% and 11% for AFC99, AFC40 and CA202, respectively when the pH decreased from 8 to 3. The findings showed that for AFC40 and CA202 membranes, the rejection mechanism depends not only on molecular sieving but also on the charge interaction between the feed solution and the membranes.

The estimated transport parameters obtained from CFSD and CFSK models, including the solute transport parameter, reflection coefficient and mass transfer coefficients are dependent on feed concentration and cross-flow velocity. The solute transport parameter was found to be increasing with the cross-flow velocity and feed concentration for both models. Similarly, the mass transfer coefficient and reflection coefficients also increased with increasing in cross-flow velocity, but both were found to be decreasing with the increment in feed concentration. The validation study also shows that the models predictions are in excellent agreement with the experimental results.

The overall results show that membrane separation process, especially AFC99 membrane, has excellent observed rejection behavior for removal of amines from artificial wastewater. Similarly, nanofiltration and ultrafiltration membranes such as AFC40 and CA202 can also be selected for the same purpose but both are more suitable to be employed for complementing the existing biological treatment.

6.2 Recommendations

- i. In amine sweetening process, the use of mixed amines for acid gas removal is a common phenomenon. In addition, the wastewater from the sweetening process may contain other impurities beside amines. Therefore, it is recommended to test the membranes performance for binary and tertiary mixtures as well as for industrial wastewater.
- ii. Membrane performance is also sensitive to changes in feed water temperature due to morphological and structural changes of membranes, ionization of functional groups, and variation of activation energy of the solutes associated with temperature change. Therefore, it is recommended to study the effect of temperature on membrane performance in future work.
- iii. The effect of pH on membrane performance is quite interesting, especially for nanofiltration membrane. However, only 2 pH values are considered under the study. It would be more interesting if the membranes performances were studied at various pH values including at the isoelectric point. Therefore, it is recommended to conduct extensive pH study in the future study.

REFERENCES

- Abry, R.G.F. and DuPart, R.S. (1995). *Hydrocarbon Processing: Amine plant troubleshooting and optimization*. GAS/SPEC Technology Group, Gulf Publishing Co., Houston, Texas, 1-11.
- Ahmad, A.L. and Chan, C.Y. (2009). Sustainability of Palm Oil Industries: An Innovative Treatment Via Membrane Technology. *Journal of Applied Science*, 9 (17), 3074-3079.
- Ahmad, A.L. Ismail, S. Bhatia, S. (2005). Ultrafiltration behavior in the treatment of agro-industry effluent: Pilot scale studies. *Chemical Engineering Science*, 60, 5385-5394.
- Ahmadun, F-R., Pendashteha, A., Abdullaha, L.C., Biak, D.R.A., Madaenic, S.S., and Abidin. (2009). Review of technologies for oil and gas produced water treatment. *Journal of Hazardous Materials*, 170, 530–551.
- Ahmed, M. T., Taha, S., Chaabane, T., Akretche, D., Maachi, R., and Dorange, G. (2006). Nanofiltration process applied to the tannery solutions. *Desalination*, 200, 419-420.
- Arkhangelsky, E., Goren, U. and Gitis, V. (2008). Retention of organic matter by cellulose acetate membranes. *Desalination*, 223, 97-105.
- Asan, T. and Levine, A.D. (1996). Wastewater Reclamation and Reuse: Past, Present, and Future. *Water Science and Technology*, 33, 1-14.
- Baker, R.W. (2004). *Membrane Technology and Applications*, 2nd edition, Membrane Technology and Research, Inc. Menlo Park, California, 15-66.
- Ballet, G.T., Gzara, L., Hafiane, A., and Dhahbi, M. (2004). Transport coefficients and cadmium salt rejection in nanofiltration membrane. *Desalination*, 167, 369 -376.

- Banat, I.M., Nigam, P., Singh, D., and Marchant, R. (1996). Microbial decolorization of textile dye containing effluents: a review. *Bioresource Technology*, 58, 217-227.
- Baruth, E.E. (2005). *Water Treatment Plant Design*, American Water Works Association, 4th edition, McGraw-Hill, Inc. NY, USA.
- Bes-Piá, A., Mendoza-Roca, J.A., Alcaina-Miranda, M.I., Iborra-Clar, A., and Iborra-Clar, M.I. (2002). Reuse of wastewater of the textile industry after its treatment with a combination of physico-chemical treatment. *Desalination*, 149, 169 -174.
- Bowen, W.R. and Mukhtar, H. (1996). Characterization and prediction of separation performance of nanofiltration membranes. *Journal of Membrane Science*, 112, 263-274.
- Cakmakci, M. Kayaalp, N., and Koyuncu, I. (2008). Desalination of produced water from oil production fields by membrane processes. *Desalination*, 222, 176 -186.
- Casey, T.J. (1997). *Unit Treatment Processes in water and Wastewater Engineering*. John Wiley and Sons Ltd. England, 113-114.
- Cassano, A., Adzet J., Molinari, R., Buonomenna, M. G., Roig, J., and Drioli, E. (2003). Membrane treatment by nanofiltration of exhausted vegetable tannin liquors from the leather industry. *Water Research.*, 37, 2426.
- Cassano, A., Molinari, R., Romano, M., and Drioli, E. (2001). Treatment of aqueous effluents of the leather industry by membrane processes: a review. *Journal of Membrane Science*, 181, 111-126.
- Chaci, X., Chen, G., Yue, P.L., and Mi, Y. (1997). Pilot scale membrane separation of electroplating wastewater by reverse osmosis. *Journal of Membrane Science*, 123, 235-242
- Chandra, V., (2006). *Fundamental of Natural Gas: An International Perspective*, PennWell, Tulsa, Oklahoma, USA.
- Chen, X., Shen, Z., Zhu, X., Fan, Y., and Wang, W. (2005). Advanced treatment of textile wastewater for reuse using electrochemical oxidation and membrane filtration. *Water SA*, 31: 127-132.

- Childress, A.E. and Elimelech, M. (1996). Effect of solution chemistry on the surface charge of polymeric reverse osmosis and nanofiltration membranes. *Journal of Membrane Science* 119, 253-268.
- Chung, C.V., Buu, N.Q. and Chau, N.K. (2005). Influence of surface charge and solution pH on the performance characteristics of a nanofiltration membrane. *Science and Technology of Advanced Materials*, 6, 246–250.
- Clair, N.S., Perry L.M., and Gene F.P. 2003. *Chemistry for Environmental Engineering and Science*, 5th ed., New York, McGraw-Hill.
- Corbitt, R.A. (1999). *Standard Handbook of Environmental Engineering*, McGraw Hill, New York CRC Press, Boca Raton. 175-186.
- Damak, K., Ayadi, A., Zeghamati, B., and Schmitz, P. (2004). Concentration polarization in tubular membranes-a numerical approach. *Desalination*, 171, 139-153.
- Das, C., Patel, P., De, S., and DasGupta, S. (2006). Treatment of tanning effluent using nanofiltration followed by reverse osmosis. *Separation and Purification Technology*, 50, 291-299.
- DeLaat, J., Truong, L.G., and Legube, B. (2004). A comparative study of the effects of chloride, sulfate and nitrate ions on the rates of decomposition of H₂O₂ and organic compounds by Fe (II)/ H₂O₂ and Fe (III)/ H₂O₂. *Chemosphere*, 55, 715-723.
- Driscoll, T.P. (2008). *Industrial Wastewater Management, Treatment, and Disposal*, 3rd edition, Water Environment Federation, WEF Press, Alexandria, VA, USA.
- DuPart, M.S., Bacon, T.R., and Edwards, D.J. (1993). Understanding Corrosion in Alkanolamine Gas Treating Plants; Parts 1&2. *Hydrocarbon Process*, 72(4), 75-80.
- Duranceau, S.J. (2001). *Membrane Practices for Water Treatment*, American Water Works Association, Denver, Colorado, USA.
- Environmental Quality Act (EQA) [Act 127]. (1974). *Environmental Quality (Sewage and Industrial Effluents) Amendment Regulations*. Minister of Science, Technology and the Environment of Malaysia, 1-34.

- Faksness, L G., Grini P.G., and Daling P.S. (2004). Partitioning of semisoluble organic compounds between the water phase and oil droplets in produced water. *Marine Pollution Bulletin*, 48, 731– 742.
- Fox, CR. (1985). *Industrial wastewater control and recovery of organic chemicals* - in FL Slejko (Ed.), Adsorption Technology, Marcel Dekker, New York, 167-185.
- Freger, V., Pihlajamaki, A., Shabtai, Y., and Gilron, J. (2002). *Distribution of fixed charge functional groups in the polyamide composite membranes*, in: Supplementary Book of Abstracts, ICOM'02, Toulouse, France, 144.
- Freger, V. and Srebnik, S. (2003). Mathematical model of charge and density distributions in interfacial polymerization of thin films. *Journal of Applied Polymer Science*, 88, 1162–1169.
- Fritz, W. and Schluender, E.U. (1974). Simultaneous adsorption equilibria of organic solutes in dilute aqueous solutions on activated carbon. *Chemical Engineering Science*, 29, 1279-1282.
- Fürhacker, M., Pressl, A., and Allabashi, R. (2003). Aerobic biodegradability of Methyl-diethanolamine (MDEA) used in natural gas sweetening plants in batch test and continuous flow experiments. *Chemosphere*, 52, 1743-1748.
- Gogate, P.R. and Pandit, A.B. (2004). A review of imperative technologies for wastewater treatment I: oxidation technologies at ambient conditions. *Advances in Environmental Resource*, 8, 501-551.
- Ghosh, A.K., Jeong, B-H., Huang, X., and Hoek, E.M.V. (2008). Impacts of reaction and curing conditions on polyamide composite reverse osmosis membrane properties. *Journal of Membrane Science*, 311, 34–45.
- Gijzen, H.J. (2000). Cyanide toxicity and cyanide degradation in anaerobic wastewater treatment. *Water Research*, 34, 2447-2454.
- Granite, E.J. and O'Brien, T. (2005). Review of Novel Methods for Carbon Dioxide Separation from Flue and Fuel Gases. *Fuel Processing Technology*, 86, 1423-1434.

- Guangli, L., Yangsheng, L., Jinren, N., Hanchang S., and Qian, Y. (2004). Treatability of kraft spent liquor by microfiltration and ultrafiltration. *Desalination*, 160,131-141.
- Hawthorne, S.B., Kubaätová, A., Gallagher, J.R., Sorensen, J.A., and Miller, D.J. (2005). Persistence and biodegradation of monoethanolamine and 2-propanolamine at an abandoned industrial site. *Environmental Science & Technology*, 39, 3639-3645.
- Hilal, N., Ogunbiyi, O.O., Miles N.J., and Nigmatullin, R. (2005). Methods employed for control of fouling in MF and UF membranes: A comprehensive review. *Separation Science Technology*, 40, 1957-2005.
- Hurwitz, G., Guillen, G.R., and Hoek, E.M.V. (2010). Probing polyamide membrane surface charge, zeta potential, wettability, and hydrophilicity with contact angle measurements. *Journal of Membrane Science*, 349, 349–357.
- Imasu, K. (1985). Wastewater Recycle in the Plating Industry using Brackish Water Reverse Osmosis Elements. *Desalination* 56,137-142.
- Isa, A.A., Hassan, B., and Shafawi, A. (2005). Treatment of Amine contaminated effluent water via membrane application, *In proceedings of the 18th symposium of Malaysian Chemical Engineers*, 368-380.
- Jain, S.K., Purkait, M.K., De, S., and Battacharya, P. K. (2006). Treatment of leather plant effluent by membrane separation processes. *Separation Science Technology*, 41, 3329-3348.
- Jian-Jun, Q., Maung-Htun, O., Maung-Nyunt, W., C-M, A., and Fook-Sin, W. (2003). A dual membrane UF/RO process for reclamation of spent rinses from a nickel-plating operation - A case study. *Journal of Water Research*, 37, 3269-3278.
- Jou, F.Y., Otto, F.D., and Mather, A.E. (1997). The Solubility of Mixtures of H₂S and CO₂ in an MDEA Solution. *The Canadian Journal of Chemical Engineering*, 75, 1138-1141.
- Ju, H., McCloskey, B.D., Sagle, A.C., Wu, Y.H., Kusuma V. A., and Freeman, B.D. (2008). Cross linked poly (ethylene oxide) fouling resistant coating materials for oil/water separation. *Journal of Membrane Science*, 307, 260-267.

- Jude, S. and Jefferson, B. (2003). *Membrane for Industrial Wastewater Recovery and Re-use*, Elsevier Science Ltd, Oxford, UK.
- Kelkar, M. (2007). *Natural Gas Production Engineering*, PennWell, Tulsa, OK, USA.
- Kidnay, A.J, and Parrish, W.R. (2006). *Fundamentals of Natural Gas Processing*, Taylor and Francis Group, CRC Press, 91-133.
- Kohl, A. and Nielsen, R. (1997). *Gas Purification, 5th ed.*, Gulf Publishing, Houston, Texas.
- Koltuniewicz A.B. and Drioli E. (2008). *Membranes in Clean Technologies, 2nd ed.*, Wiley VCH, Verlag GmbH & Co. KGaA, Weinheim.
- Koyuncu, I., Yalcin, F., and Ozturk, I. (1999). Color removal of high strength paper and fermentation industry effluents with membrane technology. *Water Science Technology*, 40(11-12), 241-248.
- Koyuncu, I, Kural, E. and Topacik. D. (2001). Pilot scale nanofiltration membrane separation for waste management in textile industry. *Water Science & Technology*, 43 (10), 233-240.
- Greenlee, L.F., Lawler, D.F., Freeman, B.D., Marrot, B. and Moulinc, P. (2009). Reverse osmosis desalination: Water sources, technology, and today's challenges. *Water Research*, 43, 2317-2348.
- Lee, W., Ahn, C.H., Hong, S., Kim, S., Lee, S., Baek, W., and Yoon, W. (2010). Evaluation of surface properties of reverse osmosis membranes on the initial biofouling stages under no filtration condition. *Journal of Membrane Science*, 351, 112–122.
- Liu, L.-F., Yu, S.-C., Wu, L.-G., Gaob, C.-J. (2008). Study on a novel antifouling polyamide–urea reverse osmosis composite membrane (ICIC–MPD): III. Analysis of membrane electrical properties. *Journal of Membrane Science*, 310, 119–128
- Lonsdale, H.K., Merten, U. and Riley, R.L. (1965). Transport properties of cellulose acetate Osmotic Membranes. *Journal of Applied Polymer Science*, 9, 1341-1362.

- Malik P.K. (2004). Dye removal from wastewater using activated carbon developed from sawdust: adsorption equilibrium and kinetics. *Journal of Hazardous Materials*, 113(1), 81-88.
- Manttari, M., Pihlajamaki, A. and Nystrom, M. (2006). Effect of pH on hydrophilicity and charge and their effect on the filtration efficiency of NF membranes at different pH. *Journal of Membrane Science*, 280, 311-320.
- Martin, M.J., Artola, A., Dolors M.B. and Rigola, M. (2003). Activated carbons developed from surplus sewage sludge for the removal of dyes from dilute aqueous solutions. *Chemical Engineering Journal*, 94(33), 231-239.
- Meisen, A., Abedinzadegan, M., Abry, R.G., and Millard, M.G. (1996). Degraded Amine Solutions; Nature, Problems and Distillative Reclamation. Proc. 45th Annual Laurance Reid Gas Conditioning Conference, Norman, Oklahoma, 168-189.
- Metcalf and Eddy. (2003). *Wastewater Engineering: Treatment and Reuse*, 4th edition, McGraw-Hill Companies Inc. 1221 Avenue of Americas, New York, NY 10020.
- Mitarai, K., Fujii, M., Inoue, I., Kumoi, S., and Hikari. (1991). Method for Treating an Amine containing wastewater. *United States patent*, 5039424, 1-11.
- Monser, L. and Adhoum, N. (2002). Modified activated carbon for the removal of copper, zinc, chromium and cyanide from wastewater, *Separation and Purification Technology*, 26, 137-146.
- Murthy, Z.V.P. and Chaudhari, L.B. (2009). Rejection behavior of nickel ions from synthetic wastewater containing Na₂SO₄, NiSO₄, MgCl₂ and CaCl₂ salts by nanofiltration and characterization of the membrane. *Desalination*, 247, 610-622.
- Murthy, Z.V.P. and Gupta, S.K. (1997). Estimation of mass transfer coefficient using a combined nonlinear membrane transport and film theory model. *Desalination*, 109, 39-49.
- Murthy, Z.V.P. and Gupta, S.K. (1999). Sodium cyanide separation and parameter estimation for reverse osmosis thin film composite polyamide membrane. *Journal of Membrane Science*, 154, 89-103.
- Noronha, F.B., Schmal, M. and Sousa-Aguiar, E.F. (2007). *Natural Gas Conversion VIII: Studies in Surface Science and Catalysis*, Elsevier, Amsterdam, The Netherlands.

- Omar, A.A., Ramil, R.M. and Putri, N.F. (2010). Fenton Oxidation of Natural Gas Plant Wastewater. *Canadian Journal on Chemical Engineering & Technology*, 1, 1-6.
- Paul, D.R. (2004). Reformulation of the solution-diffusion theory of reverse osmosis, *Journal of Membrane Science*, 241, 371-386.
- PCI membranes. (2000). *Membranes and Modules: A user manual*, ITT PCI Membrane Ltd, United Kingdom.
- Pignatello, J., Oliveros E., and Mackay, A. (2006). Advanced Oxidation processes for organic contaminant destruction based on the Fenton reaction and related chemistry. *Critical Reviews in Environmental Science and Technology*, 36, 1-84.
- Rooney, P.C., Dupart, M.S., and Bacon, T.R. (1998). Oxygen's role in alkanolamine degradation, *Hydrocarbon Process.* 77, 109 -113.
- Robinson, T., McMullan, G., Marchant, R., and Nigam, P. (2001). Remediation of dyes in textile effluent: a critical review on current treatment technologies with a proposed alternative. *Bioresour. Technol.*, 77, 247-255.
- Rodriguez, M., Sarria, V., Esplugas., and Pulgarin, C. (2002). Photo-Fenton treatment of a biorecalcitrant wastewater generated in textile activities: biodegradability of the photo-treated solution. *Journal of Photochemistry and Photobiology*, 151, 129-135.
- Schafer, A.I., Fane, A.G., and Waite, T.D. (2005). *Nanofiltration – Principles and Applications*, Elsevier Ltd., Oxford, UK, 169-240.
- Scholz, W. and Lucas, M. (2003). Techno-economic evaluation of membrane filtration for the recovery and reuse of tanning chemicals, *Water Research* 37: 1859–1867
- Seidel, A., Waypa, J.J., and Elimelech, M. (2001). Role of charge (Donnan) exclusion in removal of arsenic from water by a negatively charged porous NF membrane. *Environmental Engineering Science*, 18, 105-113.
- Singh, R. (2006). *Hybrid Membrane Systems for Water Purification*, Technology, Systems Design and Operation, Elsevier, Amsterdam, The Netherlands.
- Slater C., Ferrari A., and Wisniewski P. (1987). Removal of Cadmium from Metal Processing Wastewaters by Reverse Osmosis. *Journal of Environmental Science and Health*, 22 (8), 707-728.

- Sohbi, B., Meakaff, M., Emtir, M., and Elgarni, M. (2007). The Using of Mixing Amines in an Industrial Gas Sweetening Plant, *In proceedings of the 25th world academy of science, engineering and technology*, 301-305.
- Soltanieh, M. and Gill, W. (1981). Review of Reverse Osmosis Membranes and Transport Models. *Chemical Engineering Communications*, 12, 279-363.
- Spiegler, K.S. and Kedem, O. (1966). Thermodynamics of hyperfiltration (reverse osmosis): criteria for efficient membranes. *Desalination*, 1, 311-326.
- Teodosiu, C.C., Kennedy, M.D., Van Straten, H.A., and Schippers J.C. (1999). Evaluation of secondary refinery effluent treatment using ultrafiltration membranes. *Water Research*, 33, 2172-2180.
- Van der Bruggen, D., Braeken, L., and Vandecasteele, C. (2002). Flux decline in nanofiltration due to adsorption of organic compounds. *Separation and Purification Technology*, 29, 23-31.
- Vandevivera, P.C., Bianchi, R., and Verstraete, W. (1998). Treatment and Reuse of Wastewater from the Textile Wet-Processing Industry: Review of Emerging Technologies. *Journal of Chemical Technology and Biotechnology*, 72, 289-302.
- Veroba, R. and Stewart, E. (2003). Fundamentals of Gas Sweetening, *Proceeding of the Laurance Reid Gas Conditioning Conference, Norman, OK*, 1.
- Vlasopoulos, N., Memon, F.A., Butler, D., Murphy, R. (2006). Life cycle assessment of wastewater treatment technologies treating petroleum process waters. *Science of Total Environment*, 367, 58-70.
- Wallberg, A.S., Jonsson, and Wickstrom, P. (2001). Membrane cleaning - a case study in a sulphite pulp mill bleach plant. *Desalination*, 141, 259-268.
- Wallberg, A.S., Jonsson, and Wimmerstedt, R. (2003). Fractionation and concentration of kraft black liquor lignin with ultrafiltration. *Desalination*, 154, 187-199.
- Waalkes, M.P. 2000. Cadmium carcinogenesis in review, *Journal of Inorganic Biochemistry*, 79, 241-244.
- Wenzel, H., Knudsen, H.H., Kristensen, G.H, and Hanser, J. (1996). Reclamation and reuse of process water from reactive dyeing of cotton. *Desalination*, 106, 195-203.

- William C.L and Gary J.P. (2004). *Standard Handbook of Petroleum and Natural Gas Engineering*, 2nd Edition, 1-447.
- Wilson, J.L. and Yuvancic, J. (2004). Process Selection for Dehydrating Gulf of Mexico Offshore Platform gas, *Proceeding of the Laurance Reid Gas Conditioning Conference, Norman OK*, 125.
- Winston Ho, W. S. and Poddar, T.K. (2001). New membrane technology for removal and recovery of chromium from waste waters. *Environmental Program*, 20, 44-49.
- Wong, P.W., Sulaiman, N.M., Nachiappan, M. and Varadaraj, B. (2003). Pre-treatment and membrane ultrafiltration using treated palm oil mill effluent (POME). *Songklanakarin Journal Science Technology*, 24, 891-898.
- Wu, T.Y., Mohammada, A.W., Jahim, J. Md. and Anuar, N. (2007). Palm oil mill effluent (POME) treatment and bioresources recovery using ultrafiltration membrane: Effect of pressure on membrane fouling. *Biochemical Engineering Journal*, 35, 309-317.
- Wu, T.Y., Mohammada, A.W., Jahim, J. Md. and Anuar, N. (2010). Pollution control technologies for the treatment of palm oil mill effluent (POME) through end-of-pipe processes. *Journal of Environmental Management*, 91, 1467-1490.
- Zhanga, Y., Maa, C., Yeb, F., Konga, Y., and Li, H. (2009). The treatment of wastewater of paper mill with integrated membrane process. *Desalination*, 236, 349-356.
- Zydney, A.L. and Zeman, L.J. (1996). *Microfiltration and ultrafiltration: principles and applications*, New York: CRC.

APPENDICES

Appendix A: Effect of amine solution on permeate flux

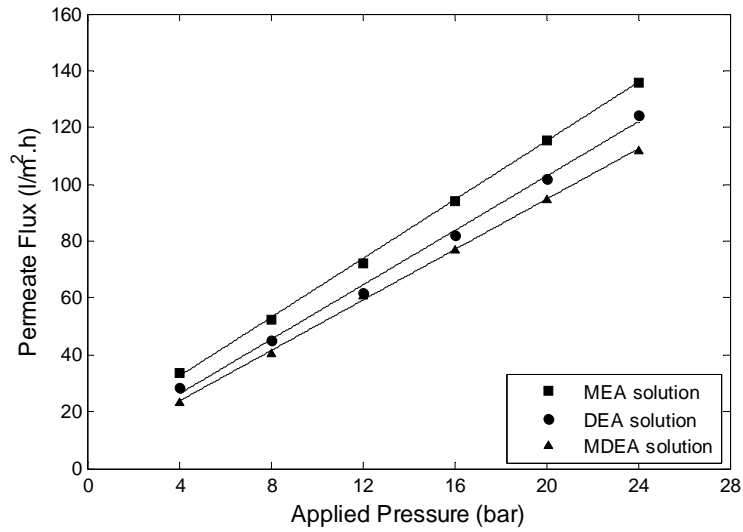


Figure A.1: Effect of amine types on permeate flux across AFC40 membrane ($C_b=5000$ mg/l, $u=6$ l/min and pH= 8).

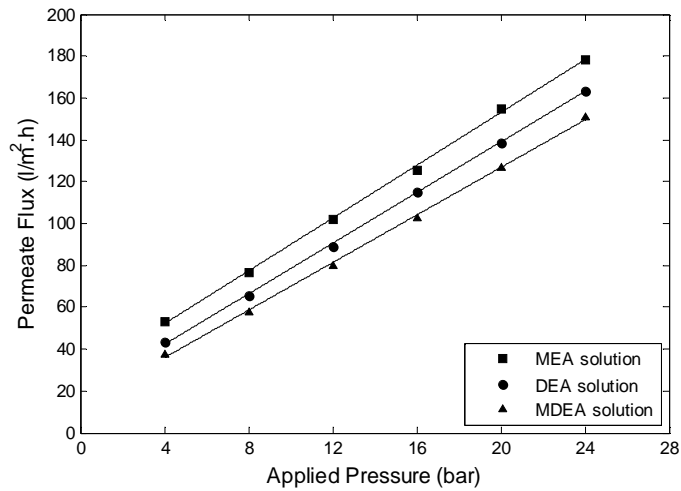


Figure A.2: Effect of amine types on permeate flux across CA202 membrane ($C_b=5000$ mg/l, $u=6$ l/min and pH= 8).

Appendix B: Effect of cross-flow velocity on permeate flux

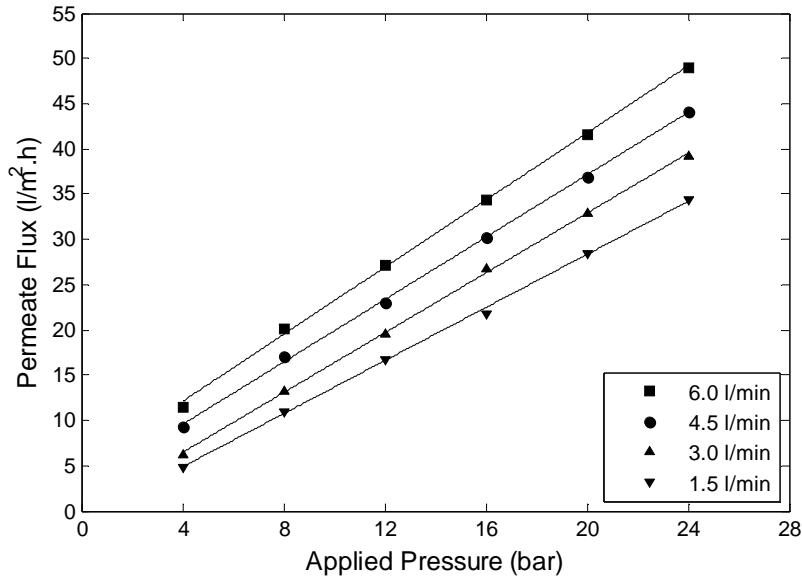


Figure B.1: Effect of cross flow velocity on DEA permeate flux across AFC99 membrane ($C_b=5000$ mg/l and pH=8).

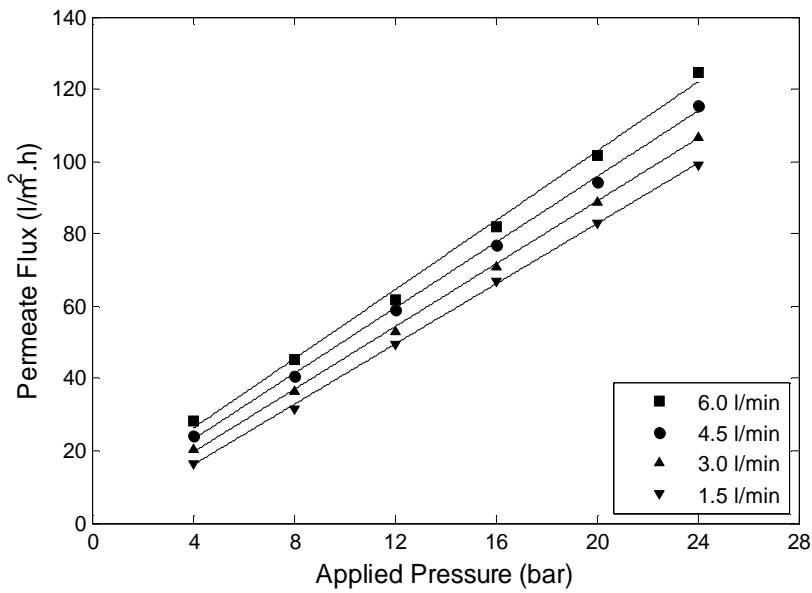


Figure B.2: Effect of cross flow velocity on DEA permeate flux across AFC40 membrane ($C_b=5000$ mg/l and pH=8).

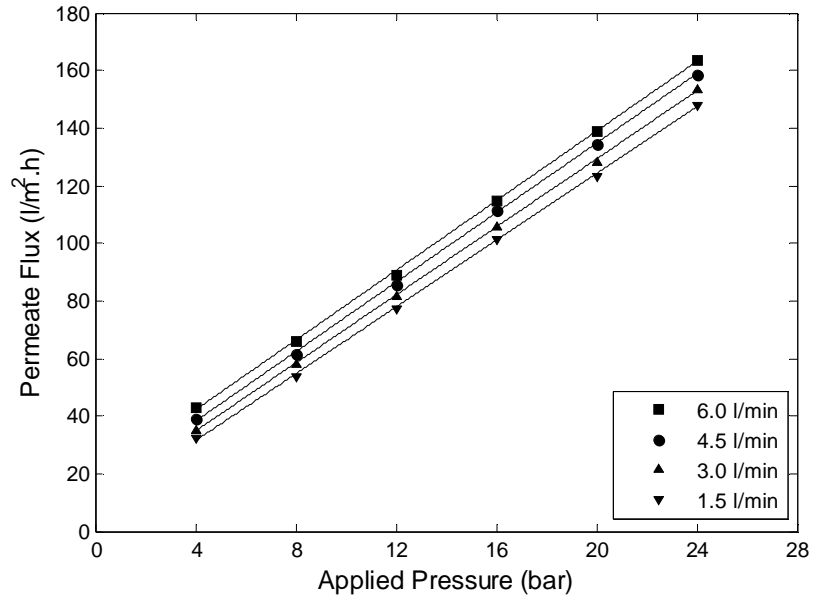


Figure B.3: Effect of cross flow velocity on DEA permeate flux across CA202 membrane ($C_b=5000$ mg/l and pH=8).

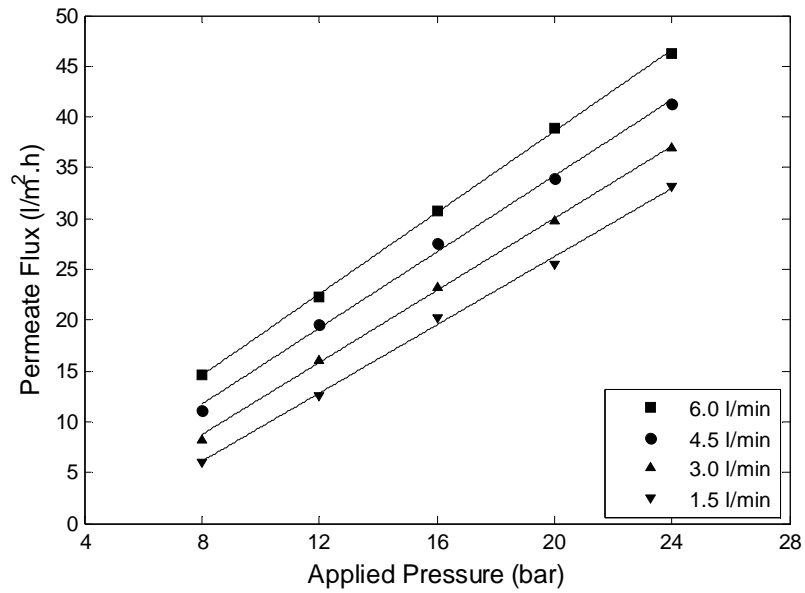


Figure B.4: Effect of cross flow velocity on MDEA permeate flux across AFC99 membrane ($C_b=5000$ mg/l and pH=8).

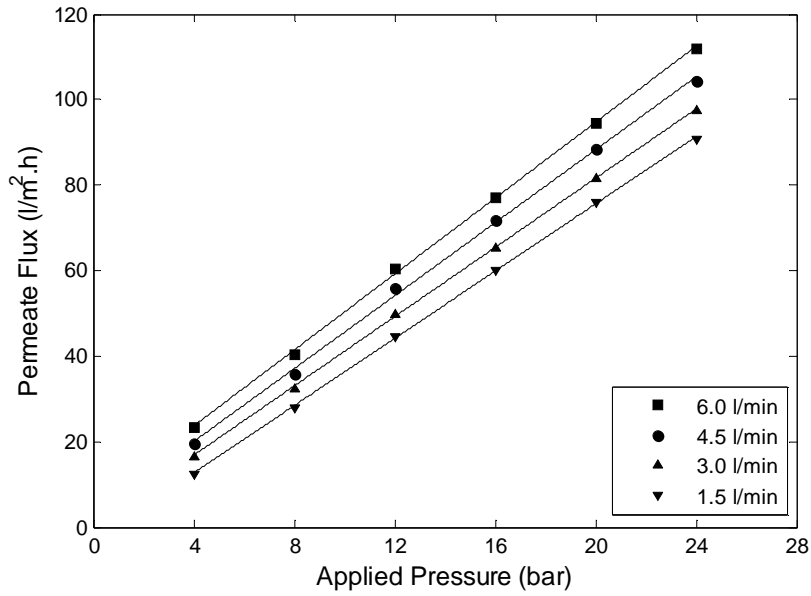


Figure B.5: Effect of cross flow velocity on MDEA permeate flux across AFC40 membrane ($C_b=5000$ ppm and pH=8).

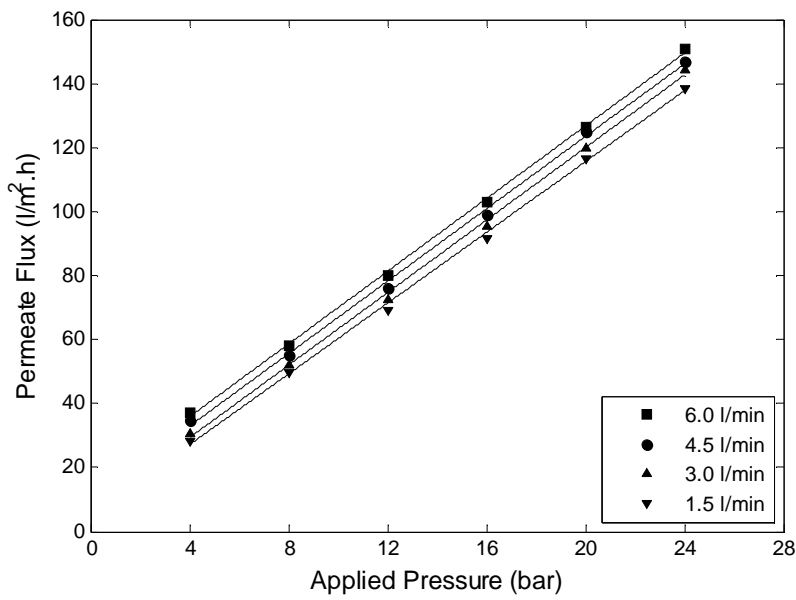


Figure B.6: Effect of cross flow velocity on MDEA permeate flux across CA202 membrane ($C_b=5000$ ppm and pH=8).

Appendix C: Physical properties of amines

Table C.1: Physical properties of amines.

	Monoethanolamine	Diethanolamine	Methyldiethanoamine
Structural Formula	$\text{H}_2\text{NCH}_2\text{CH}_2\text{OH}$	$\text{HN}(\text{CH}_2\text{CH}_2\text{OH})_2$	$\text{CH}_3\text{N}(\text{CH}_2\text{CH}_2\text{OH})_2$
Molecular Weight	61.08	105.14	119.16
Apparent Sp.Gr at 20/4 °C	1.017	1.092	1.040
Sp. Gr./ Δt at 10 to 80 °C	0.0008	0.00065	0.00059
Boiling point at 1 atm, °C	170.4	268	247
Vapor pressure at 20°C, mm Hg	0.36	<0.01	<0.01
Freezing point, °C	10.5	28.0	-21.0
Absolute viscosity at 20°C, cP	24.1	380(30°C)	101
Solubility at 20 °C, % by wt			
In water	Complete	Complete	Complete
Water in	complete	-	Complete
Solubility in organic liquids at 25 °C, % by wt			
Acetone	Complete	Complete	Complete
Benzene	0.6	0.03	-
Carbon	0.1	0.01	-
Tetrachloride	complete	Complete	Complete
Flash Point, °C	96	191	138

Appendix D: Experimental data for removal of amines from artificial wastewater across AFC99, AFC40 and CA202 membranes

Table D.1: Experimental data for MEA solution ($C_b=5000$ mg/l and pH=8).

Pressure (bar)	AFC99		AFC40		CA202	
1.5 l/min						
	J_v (l/m ² .h)	Ro	J_v (l/m ² .h)	Ro	J_v (l/m ² .h)	Ro
4	5.2116	0.9618	20.8858	0.4000	41.7234	0.1540
8	10.7928	0.9714	37.1543	0.4650	64.7094	0.1980
12	16.8144	0.9752	54.1443	0.5220	88.8778	0.2270
16	21.7854	0.9776	75.4148	0.5320	110.3006	0.2380
20	27.7432	0.9788	93.5471	0.5520	138.8778	0.2440
24	34.7844	0.9792	108.4569	0.5400	161.1824	0.2300
3.0 l/min						
4	7.4345	0.9662	24.8657	0.4140	45.9118	0.1650
8	14.3687	0.9748	41.4830	0.4760	68.4369	0.2030
12	19.5788	0.9778	60.3246	0.5360	92.6253	0.2350
16	27.4353	0.9804	81.4990	0.5560	115.4309	0.2510
20	32.7451	0.9814	99.3788	0.5680	144.4289	0.2490
24	40.2806	0.9816	118.7976	0.5660	165.7315	0.2380
4.5 l/min						
4	9.6192	0.9696	28.5571	0.4220	49.3387	0.1770
8	16.8337	0.9776	46.4525	0.4980	73.0461	0.2110
12	24.1082	0.9808	66.1719	0.5480	96.5331	0.2430
16	32.2244	0.9824	88.3768	0.5640	120.2806	0.2540
20	38.5972	0.9834	107.8160	0.5780	149.1182	0.2580
24	45.6914	0.9840	127.8517	0.5680	171.9238	0.2440
6.0 l/min						
4	13.8018	0.9752	33.4845	0.4420	52.9589	0.1920
8	21.6445	0.9804	52.2969	0.5180	76.6700	0.2200
12	28.6700	0.9832	72.2528	0.5580	101.9218	0.2470
16	35.7111	0.9848	94.2668	0.5760	125.6329	0.2560
20	44.0160	0.9856	115.5226	0.5900	154.5436	0.2600
24	51.1535	0.9860	136.0080	0.5780	178.1344	0.2480

Table D.2 : Experimental data for MEA solution ($C_b=10000$ mg/l and pH=8).

Pressure (bar)	AFC99		AFC40		CA202	
1.5 l/min						
	J_v (l/m ² .h)	Ro	J_v (l/m ² .h)	Ro	J_v (l/m ² .h)	Ro
4	-	-	15.3908	0.3375	37.1343	0.1420
8	6.4128	0.9689	31.1663	0.4100	58.5170	0.1830
12	12.2244	0.9739	46.9299	0.4550	82.1643	0.2010
16	19.1984	0.9771	64.6653	0.4740	106.6934	0.2110
20	24.4489	0.9786	81.7275	0.4700	133.3467	0.2195
24	30.0802	0.9788	98.1523	0.4475	155.5912	0.212
3.0 l/min						
4	-	-	18.6733	0.3620	41.1623	0.1540
8	10.1603	0.9711	35.8677	0.4200	62.5050	0.1910
12	16.1924	0.9759	53.9038	0.4600	86.2525	0.2100
16	22.5852	0.9793	70.7856	0.4850	111.7234	0.2160
20	28.5972	0.9804	88.5571	0.5020	138.5371	0.2240
24	34.1082	0.9807	105.5471	0.4775	162.0641	0.22
4.5 l/min						
4	6.0120	0.9691	22.1242	0.3850	43.7074	0.1600
8	13.7475	0.9737	39.7395	0.4660	66.5331	0.1960
12	20.9619	0.9779	58.4970	0.5030	90.2405	0.2170
16	26.6132	0.9808	76.1519	0.5260	116.4930	0.2215
20	32.6253	0.9817	94.1687	0.5370	143.9479	0.2300
24	40.1202	0.9821	112.6052	0.5150	166.9940	0.228
6.0 l/min						
4	8.4253	0.9736	27.4628	0.4090	47.5025	0.1650
8	16.9308	0.9768	45.2353	0.4895	70.8526	0.2025
12	24.1123	0.9803	64.0526	0.5280	95.4263	0.2205
16	31.7352	0.9825	83.8917	0.5420	120.1805	0.2290
20	38.6359	0.9833	101.0828	0.5550	147.5426	0.2340
24	44.6339	0.9837	120.0602	0.5340	171.8154	0.2325

Table D.3 : Experimental data for MEA solution ($C_b=15000$ mg/l and pH=8).

Pressure (bar)	AFC99		AFC40		CA202	
1.5 l/min						
	J_v (l/m ² .h)	Ro	J_v (l/m ² .h)	Ro	J_v (l/m ² .h)	Ro
4	-	-	10.3611	0.3040	31.4830	0.1140
8	2.1643	0.9642	24.7094	0.3907	52.5050	0.1413
12	6.3932	0.9716	39.9198	0.4287	76.2124	0.1693
16	11.5034	0.9743	55.5872	0.4473	100.3206	0.1793
20	17.3747	0.9762	70.1002	0.4533	126.5731	0.1907
24	23.6273	0.9765	85.5752	0.4607	150.7214	0.1820
3.0 l/min						
4	-	-	13.4068	0.3280	35.7114	0.1200
8	3.8874	0.9653	28.4369	0.4077	56.1723	0.1500
12	9.0782	0.9734	46.7375	0.4487	81.6633	0.1740
16	15.5110	0.9771	61.4068	0.4660	104.8898	0.1853
20	21.4870	0.9779	78.8537	0.4713	131.9238	0.1973
24	27.0541	0.9785	94.5090	0.4603	155.8918	0.1900
4.5 l/min						
4	-	-	16.9142	0.3453	38.4970	0.1300
8	6.7936	0.9703	31.3623	0.4187	60.4409	0.1600
12	12.6253	0.9753	50.9218	0.4547	86.3126	0.1820
16	18.5772	0.9783	66.7731	0.4747	110.4409	0.1900
20	25.1904	0.9795	84.8501	0.4800	136.6333	0.2013
24	31.5631	0.9800	101.4228	0.4770	160.1202	0.1987
6.0 l/min						
4	4.2126	0.9668	21.1836	0.3660	42.4273	0.1387
8	10.6724	0.9727	36.9906	0.4360	65.2156	0.1667
12	16.7904	0.9777	55.5671	0.4687	90.0502	0.1900
16	22.9685	0.9801	73.1591	0.4853	115.1856	0.1980
20	29.6293	0.9817	91.6947	0.4913	141.8054	0.2067
24	36.2287	0.9820	109.9101	0.4873	166.1585	0.2013

Table D.4: Experimental data for DEA solution ($C_b=5000$ mg/l and pH=8).

Pressure (bar)	AFC99		AFC40		CA202	
1.5 l/min						
	J_v (l/m ² .h)	Ro	J_v (l/m ² .h)	Ro	J_v (l/m ² .h)	Ro
4	4.7940	0.9686	16.3768	0.5060	32.0236	0.2120
8	10.8927	0.9760	31.4429	0.5590	53.6477	0.2430
12	16.7543	0.9810	49.2745	0.5880	77.2545	0.2610
16	21.7854	0.9834	66.9980	0.6200	101.3627	0.3000
20	28.3450	0.9844	82.8697	0.6300	123.3267	0.3090
24	34.3872	0.9846	98.8016	0.6220	147.7154	0.3120
3.0 l/min						
4	6.1323	0.9728	20.4048	0.5240	35.2701	0.2250
8	13.2265	0.9798	36.4329	0.5650	57.8357	0.2590
12	19.4994	0.9836	53.1703	0.6130	81.3222	0.2780
16	26.6934	0.9856	71.1222	0.6360	105.9319	0.3080
20	32.8858	0.9864	88.7735	0.6380	128.1162	0.3230
24	39.1780	0.9866	106.9299	0.6300	153.5070	0.3180
4.5 l/min						
4	9.1984	0.9756	24.1683	0.5420	38.7776	0.2380
8	16.9936	0.9830	40.6016	0.5760	61.3226	0.2700
12	23.0056	0.9854	58.8373	0.6200	85.4705	0.2900
16	30.2609	0.9876	76.7531	0.6440	111.5832	0.3190
20	36.9343	0.9884	94.4886	0.6480	134.4289	0.3300
24	44.0477	0.9888	115.3912	0.6410	158.5972	0.3230
6.0 l/min						
4	11.3982	0.9792	28.2849	0.5510	43.1254	0.2590
8	20.0401	0.9854	45.2317	0.5820	65.7773	0.2830
12	27.1174	0.9878	61.8415	0.6480	88.8506	0.2990
16	34.3631	0.9894	81.9057	0.6540	114.8847	0.3260
20	41.6449	0.9902	101.8255	0.6590	138.6961	0.3330
24	48.8907	0.9904	124.4534	0.6530	163.5105	0.3280

Table D.5: Experimental data for DEA solution ($C_b=10000$ mg/l and pH=8).

Pressure (bar)	AFC99		AFC40		CA202	
1.5 l/min						
	J_v (l/m ² .h)	Ro	J_v (l/m ² .h)	Ro	J_v (l/m ² .h)	Ro
4	-	-	9.9595	0.4540	26.4529	0.1975
8	6.4725	0.9764	24.6253	0.5200	48.0962	0.2285
12	9.7395	0.9810	38.3928	0.5535	69.1583	0.2660
16	16.1964	0.9839	53.7475	0.5765	93.3467	0.3020
20	20.9579	0.9844	68.6934	0.5875	119.8998	0.3140
24	26.4168	0.9850	81.7395	0.5755	141.6032	0.3070
3.0 l/min						
4			13.2625	0.4860	30.6212	0.2120
8	8.6369	0.9787	28.7976	0.5355	53.3667	0.2420
12	12.5050	0.9823	42.6613	0.5715	74.5090	0.2770
16	18.6373	0.9852	58.6413	0.5985	98.7575	0.3100
20	24.7936	0.9860	73.5042	0.6020	124.2485	0.3180
24	30.6974	0.9862	88.7735	0.5910	147.6954	0.3110
4.5 l/min						
4	5.0501	0.9721	17.1547	0.5090	34.1483	0.2295
8	11.2425	0.9803	31.8240	0.5535	56.2525	0.2555
12	16.0762	0.9836	47.4553	0.5825	79.3387	0.2835
16	22.4008	0.9860	63.4473	0.6075	103.6473	0.3160
20	28.2325	0.9869	79.2589	0.6145	129.0180	0.3215
24	34.2926	0.9872	95.7920	0.6065	153.2064	0.3180
6.0 l/min						
4	7.7031	0.9754	21.2835	0.5310	37.2718	0.2425
8	13.7813	0.9819	35.9675	0.5725	61.0832	0.2700
12	19.9402	0.9847	52.8181	0.5995	83.6710	0.2910
16	26.9609	0.9869	67.5021	0.6200	109.3882	0.3200
20	32.6179	0.9877	85.5563	0.6290	133.3200	0.3270
24	39.4387	0.9879	103.0086	0.6175	158.4554	0.3205

Table D.6: Experimental data for DEA solution ($C_b=15000$ mg/l and pH=8).

Pressure (bar)	AFC99		AFC40		CA202	
1.5 l/min						
	J_v (l/m ² .h)	Ro	J_v (l/m ² .h)	Ro	J_v (l/m ² .h)	Ro
4	-	-	5.4505	0.3760	19.3186	0.1807
8	1.8433	0.9673	18.3006	0.4343	42.6653	0.2187
12	5.3110	0.9732	33.3066	0.4997	63.2265	0.2420
16	10.0605	0.9761	49.9359	0.5193	87.1142	0.2850
20	15.7154	0.9775	64.2685	0.5330	109.4790	0.2970
24	20.8377	0.9777	78.7575	0.5160	134.0281	0.2860
3.0 l/min						
4	-	-	7.6148	0.4213	22.8257	0.1913
8	3.7671	0.9707	22.3407	0.4683	45.8317	0.2263
12	7.4549	0.9773	36.8297	0.5130	67.2545	0.2517
16	13.3106	0.9791	53.8918	0.5360	91.5431	0.2920
20	19.5752	0.9802	68.0561	0.5470	115.2906	0.3003
24	24.4449	0.9805	83.9519	0.5433	139.0782	0.2950
4.5 l/min						
4	-	-	10.1808	0.4447	26.2926	0.2083
8	5.6513	0.9747	26.0116	0.4990	49.8798	0.2450
12	10.4008	0.9802	41.2028	0.5267	71.8637	0.2590
16	16.8337	0.9810	58.3166	0.5483	96.6934	0.3047
20	22.9058	0.9822	73.1267	0.5640	120.3006	0.3100
24	27.8357	0.9827	89.0585	0.5567	144.6693	0.3043
6.0 l/min						
4	-	-	13.5009	0.4703	30.0301	0.2223
8	8.3651	0.9767	29.0913	0.5130	53.4604	0.2533
12	13.6610	0.9809	45.6566	0.5497	76.5095	0.2707
16	19.2578	0.9829	63.5302	0.5663	101.6650	0.3017
20	25.6369	0.9840	78.4550	0.5793	126.3591	0.3193
24	31.9161	0.9843	96.3093	0.5690	149.9097	0.3107

Table D.7: Experimental data for MDEA solution ($C_b=5000$ mg/l and pH=8).

Pressure (bar)	AFC99		AFC40		CA202	
1.5 l/min						
	J_v (l/m ² .h)	Ro	J_v (l/m ² .h)	Ro	J_v (l/m ² .h)	Ro
4	-	-	12.3848	0.5220	28.0561	0.2410
8	5.9783	0.9814	27.9559	0.5950	49.8196	0.2840
12	12.6138	0.9866	44.4649	0.6400	69.1583	0.3140
16	20.2568	0.9874	60.0000	0.6560	91.5030	0.3240
20	25.4925	0.9878	75.7154	0.6770	116.4529	0.3280
24	33.1354	0.9884	90.7575	0.6610	138.3968	0.3260
3.0 l/min						
4	-	-	16.5126	0.5560	30.6012	0.2520
8	8.2966	0.9842	32.3447	0.6140	52.1443	0.2900
12	16.0725	0.9880	49.8758	0.6640	72.5852	0.3210
16	23.3062	0.9886	65.4349	0.6800	95.5511	0.3320
20	29.7992	0.9892	81.4990	0.6980	119.7194	0.3330
24	36.9343	0.9896	97.3587	0.6890	144.1283	0.3310
4.5 l/min						
4	4.8096	0.9768	19.3383	0.5760	34.5291	0.2620
8	11.0621	0.9866	35.9519	0.6350	55.2906	0.2960
12	19.5186	0.9900	55.7711	0.6840	75.8717	0.3240
16	27.4954	0.9910	71.6032	0.6940	98.8978	0.3470
20	33.9679	0.9914	88.2168	0.7110	124.6693	0.3490
24	41.3026	0.9918	104.2882	0.7000	146.7335	0.3460
6.0 l/min						
4	7.6826	0.9804	23.3741	0.6030	37.2758	0.2710
8	14.5878	0.9890	40.2849	0.6600	57.9298	0.3030
12	22.2066	0.9916	60.5176	0.7060	79.7633	0.3270
16	30.7523	0.9926	76.9709	0.7170	102.8847	0.3520
20	38.8526	0.9928	94.4835	0.7280	126.4995	0.3530
24	46.3149	0.9932	111.8997	0.7180	150.5717	0.3510

Table D.8: Experimental data for MDEA solution ($C_b=10000$ mg/l and pH=8).

Pressure (bar)	AFC99		AFC40		CA202	
1.5 l/min						
	J_v (l/m ² .h)	Ro	J_v (l/m ² .h)	Ro	J_v (l/m ² .h)	Ro
4	-	-	7.7555	0.5000	19.8998	0.2220
8	2.9856	0.9787	20.6573	0.5735	40.7615	0.2595
12	6.4533	0.9843	35.5551	0.6360	61.3828	0.2795
16	12.7455	0.9870	51.0180	0.6540	84.8898	0.2970
20	18.0721	0.9874	65.1463	0.6640	107.5752	0.3075
24	24.0721	0.9877	77.6152	0.6600	129.5992	0.3045
3.0 l/min						
4	-	-	10.2601	0.5310	24.5291	0.2320
8	4.0485	0.9812	24.1683	0.5980	44.4890	0.2705
12	9.0577	0.9857	40.6413	0.6450	67.0541	0.2955
16	16.2565	0.9872	55.9960	0.6665	89.9800	0.3110
20	22.0882	0.9882	69.2345	0.6765	111.5230	0.3225
24	28.4369	0.9884	82.4489	0.6725	135.1703	0.3165
4.5 l/min						
4	-	-	12.5651	0.5560	28.8377	0.2440
8	6.8741	0.9825	27.7960	0.6100	49.7996	0.2790
12	12.4244	0.9866	45.1299	0.6665	71.4830	0.3145
16	19.0220	0.9883	60.7010	0.6775	93.5671	0.3290
20	25.7675	0.9890	75.4906	0.6860	115.9719	0.3380
24	31.5391	0.9893	88.6569	0.6840	140.4609	0.3350
6.0 l/min						
4	-	-	15.4869	0.5750	32.9388	0.2495
8	9.3280	0.9845	32.0967	0.6245	53.5807	0.2825
12	15.2859	0.9878	49.0869	0.6760	75.9478	0.3055
16	22.6881	0.9893	66.4189	0.6880	97.9137	0.3370
20	29.5486	0.9898	82.3065	0.6930	121.4845	0.3445
24	36.0277	0.9900	96.3093	0.5690	145.5567	0.3420

Table D.9: Experimental data for MDEA solution ($C_b=15000$ mg/l and pH=8).

Pressure (bar)	AFC99		AFC40		CA202	
1.5 l/min						
	J_v (l/m ² .h)	Ro	J_v (l/m ² .h)	Ro	J_v (l/m ² .h)	Ro
4	-	-	3.6469	0.4473	16.5531	0.1947
8	-	-	12.7214	0.5540	33.0661	0.2173
12	5.3507	0.9759	28.1723	0.5913	58.6974	0.2437
16	10.0798	0.9815	43.8637	0.6313	78.8978	0.2673
20	15.0541	0.9826	58.8577	0.6317	99.7395	0.2823
24	19.8156	0.9831	71.6874	0.6240	123.6273	0.2787
3.0 l/min						
4	-	-	6.0926	0.4780	18.5772	0.2107
8	-	-	16.3527	0.5667	39.0782	0.2313
12	7.1543	0.9777	31.3587	0.6093	63.1263	0.2527
16	12.8657	0.9827	48.7936	0.6413	83.5271	0.2913
20	18.0361	0.9845	63.4629	0.6447	104.6493	0.2967
24	23.5671	0.9847	76.3287	0.6333	129.3587	0.2920
4.5 l/min						
4	-	-	7.8156	0.4987	22.1443	0.2213
8	2.8858	0.9747	19.6990	0.5853	44.0080	0.2493
12	9.1383	0.9807	35.4313	0.6193	66.6733	0.2633
16	14.4890	0.9848	52.5655	0.6490	87.9359	0.3040
20	20.7415	0.9855	67.9154	0.6500	111.2024	0.3147
24	26.9940	0.9858	82.4044	0.6393	134.0080	0.3127
6.0 l/min						
4	-	-	10.1705	0.5227	27.0812	0.2340
8	5.2959	0.9783	23.4307	0.6027	48.7061	0.2633
12	11.9759	0.9833	40.5412	0.6333	71.2337	0.2800
16	17.0311	0.9865	57.5531	0.6587	91.9960	0.3260
20	23.4102	0.9875	73.0796	0.6607	116.2889	0.3303
24	29.9097	0.9879	89.8098	0.6510	138.9769	0.3267

Table D.10: Experimental data for MEA solution ($C_b=5000$ mg/l and pH=3).

Pressure (bar)	AFC99		AFC40		CA202	
6.0 l/min						
	J_v (l/m ² .h)	Ro	J_v (l/m ² .h)	Ro	J_v (l/m ² .h)	Ro
4	16.9107	0.9849	25.3757	0.5960	37.8134	0.2400
8	26.6600	0.9898	45.7168	0.6580	64.8546	0.2680
12	33.7216	0.9920	65.0949	0.6840	89.0471	0.2880
16	41.2634	0.9927	86.2784	0.6940	116.7904	0.3030
20	49.8499	0.9933	104.4530	0.7020	144.0321	0.3040
24	57.7934	0.9939	122.3711	0.6890	167.2618	0.2980

Table D.11: Experimental data for DEA solution ($C_b=5000$ mg/l and pH=3).

Pressure (bar)	AFC99		AFC40		CA202	
6.0 l/min						
	J_v (l/m ² .h)	Ro	J_v (l/m ² .h)	Ro	J_v (l/m ² .h)	Ro
4	17.5727	0.9876	20.7021	0.7330	35.9073	0.2660
8	26.4193	0.9912	35.7075	0.7800	57.4122	0.2940
12	34.3631	0.9932	56.0281	0.8200	81.6650	0.3320
16	45.2558	0.9944	74.3434	0.8340	106.7398	0.3480
20	54.8040	0.9950	93.4399	0.8480	130.9288	0.3570
24	64.8144	0.9952	116.6696	0.8440	154.9649	0.3490

Table D.12: Experimental data for MDEA solution ($C_b=5000$ mg/l and pH=3).

Pressure (bar)	AFC99		AFC40		CA202	
6.0 l/min						
	J_v (l/m ² .h)	Ro	J_v (l/m ² .h)	Ro	J_v (l/m ² .h)	Ro
4	11.3741	0.9880	18.5375	0.8620	29.1478	0.3260
8	20.0401	0.9926	33.4870	0.9030	49.6694	0.3530
12	29.7894	0.9944	50.9423	0.9260	73.1591	0.3770
16	38.2748	0.9952	68.5166	0.9370	95.9278	0.3820
20	47.4223	0.9958	85.2301	0.9420	118.6760	0.3900
24	55.5466	0.9962	103.5667	0.9360	141.6048	0.3830

Table D.13: Experimental data for water permeability.

Pressure (bar)	AFC99 membrane	AFC40 membrane	CA202 membrane
	J_v (l/m ² .h)	J_v (l/m ² .h)	J_v (l/m ² .h)
4	17.9940	38.3109	56.5697
8	28.4052	60.8425	82.4473
12	42.9689	84.2528	108.6259
16	55.8475	110.3952	135.1294
20	70.9168	134.8044	165.4965
24	82.2066	160.1284	193.0351

Table D.14: Experimental data for AFC99 ($C_b=5000$ mg/l, $u=3.5$ l/min and pH=8).

Pressure (bar)	MEA solution		DEA solution		MDEA solution	
	J_v (l/m ² .h)	Ro	J_v (l/m ² .h)	Ro	J_v (l/m ² .h)	Ro
4	8.4253	0.9680	7.8636	0.9738		
8	15.6469	0.9762	14.9248	0.9812	9.5085	0.9850
12	21.3039	0.9792	20.7021	0.9844	17.5326	0.9882
16	28.5657	0.9808	28.1645	0.9862	24.7543	0.9892
20	34.9448	0.9820	33.9418	0.9868	31.3340	0.9898
24	42.2467	0.9828	41.1635	0.9872	38.9168	0.9904

Table D.15: Experimental data for validation for AFC membrane ($C_b=5000$ mg/l, $u=3.5$ l/min and pH=8).

Pressure (bar)	MEA solution		DEA solution		MDEA solution	
	J_v (l/m ² .h)	Ro	J_v (l/m ² .h)	Ro	J_v (l/m ² .h)	Ro
4	10.5918	0.9700	9.6289	0.9772	5.6570	0.9786
8	19.2578	0.9784	18.2949	0.9846	12.9990	0.9874
12	26.2387	0.9814	25.0351	0.9866	20.8225	0.9900
16	32.9789	0.9830	31.8957	0.9876	29.0070	0.9910
20	39.8395	0.9848	38.1545	0.9882	34.9047	0.9916
24	46.5797	0.9852	44.6540	0.9888	42.9689	0.9922